MUTATION, EXOME SEQUENCING AND LINKAGE ANALYSES IN TURKISH CMT FAMILIES

by

Alperen Erdoğan

B.S., Molecular Biology and Genetics, Middle East Technical University, 2010

Submitted to the Institute for Graduate Studies in
Science and Engineering in partial fulfillment of
the requirements for the degree of
Master of Science

Graduate Program in Molecular Biology and Genetics
Boğaziçi University

2012

MUTATION, EXOME SEQUENCING AND LINKAGE ANALYSES IN TURKISH CMT FAMILIES

APPROVED BY:

Assoc. Prof. Esra Battaloğlu (Thesis Supervisor)	.....
Prof. S. Hande Çağlayan	.....
Prof. Uğur Özbek	.....

DATE OF APPROVAL: 05.09.2012

To my mother…

ACKNOWLEDGEMENTS

I would like to express my special thanks to my supervisor Assoc. Prof. Esra Battaloğlu for her guidance, valuable critics and encouragement during this study. I would like to thank other members of the thesis committee, Prof. S. Hande Çağlayan and Prof. Uğur Özbek for evaluating my thesis. I also would like to express my appreciation to Prof. Albena Jordanova for her great help, guidance and hospitality during my stay in Antwerp and to Assoc. Prof. Marina Kennerson who helped to perform exome sequencing analysis.

I appreciate Prof. Yeşim Parman, Assist. Prof. Vildan Çakmak Altunayoğlu and all other clinicians for providing blood samples and clinical data of the patients. I am also grateful to patients for participating in this study.

I would like to thank Yıldız Koca for her great friendship and endless support whenever I needed. I would like to express my special thanks to my lab members Merve Kılınç, Kaya Akyüz, Burçak Özeş, Kerem Yıldırım, Duygu Dağlıkoca and Merve Sıvacı. I feel really lucky to have such great friends. I could not finish this master without them.

I would like to thank Gönenç Çobanoğlu for his candid friendship and to Selen Zülbahar for her support and friendship. I also would like to thank other members of Lab 204; Aslı Uğurlu, Özden Akay, Neslihan Zöhrap and Mahmut Can Hız for their friendships.

Last but not least, I would like to express my appreciation to my beloved family and my wonderful sister, Elif Erdoğan. I could not have a better family.

Finally, I am grateful to TUBITAK-BIDEB 2210 for awarding and supporting me during my master.

ABSTRACT

MUTATION, EXOME SEQUENCING AND LINKAGE ANALYSES IN TURKISH CMT FAMILIES

Charcot-Marie-Tooth disease (CMT) also known as hereditary motor and sensory neuropathy (HMSN) is the most frequent inherited neuropathy. The patients with CMT generally have distal muscle weakness and atrophy in the peroneal muscles. In the first part of this study, *GJB1, PRPS1*, *GDAP1* and *SH3TC2* were screened for mutations in a total of 34 Turkish CMT patients. Four variations have been identified for *GJB1,* including two mutations in its 5'UTR. Two other variations identified were in *GDAP1* and *SH3TC2*. Exome sequencing was performed for two families for which mutation analysis in the known CMT genes did not give a positive result. A novel variation was observed in the 5'UTR of *GJB1* in one of these families. For the second family, whole genome linkage analysis was conducted since exome sequencing was not informative by itself. Combination of these two analyses helped to identify three candidate genes in the family. In the third part of the study, X chromosome linkage analysis was performed for four families. For three them, the analysis did not give any conclusive results. For the forth family, the locus linked to the disease was about 102 Mb that harbor about 1100 genes. Additional analysis should be performed for those families to identify the causative gene. This study contributed to the genetics of CMT with two major findings. First, the variations that were identified in the 5'UTR of *GJB1* have been shown to cause the disease with a higher incidence than expected. Besides, known CMT genes were excluded in one family and consequently three candidate genes have been identified. Determination of the causative gene among these candidates with future studies is crucial in understanding the genetic basis and will help molecular diagnosis of the disease.

ÖZET

TÜRK CMT AİLELERİNDE MUTASYON, EKZOM DİZİLEME VE BAĞLANTI ANALİZLERİ

Charcot-Marie-Tooth hastalığı (CMT) diğer bir adıyla herediter motor ve duysal nöropati en sık görülen kalıtsal nöropatidir. CMT hastalarında genellikle distal kas zaafı ve peroneal kaslarda atrofi vardır. Bu çalışmanın ilk bölümünde, *GJB1, PRPS1, GDAP1* ve *SH3TC2* genlerinde toplam 34 Türk CMT hastasında mutasyon taraması gerçekleştirildi. *GJB1*'in kodlayan bölgesinde iki varyasyon belirlenirken genin 5'UTR'ında iki mutasyon daha saptandı. *GDAP1* ve *SH3TC2* genlerinde ise birer mutasyon tanımlandı. CMT genlerinde mutasyon taşımayan iki ailede sorumlu genin belirlenmesi amacıyla ekzom dizilemesi gerçekleştirildi. Bu ailelerden birinde, *GJB1*'in 5'UTR bölgesinde yeni bir varyasyon gözlendi. İkinci ailede ise ekzom dizileme sonuçlarından tek başına bilgi edinilememesi nedeni ile tüm genom bazında bağlantı analizi yapıldı. Bu iki analizden elde edilen bulguların karşılaştırılması ile üç aday gen tanımlandı. Çalışmanın son bölümünde, dört CMT ailesinde X kromozomuna bağlantı analizi uygulandı. Analiz üç aile için sonuç vermezken dördüncü ailede 102 Mb uzunluğunda bir bölgeye bağlantı gösterdi. Bağlantı veren bölgenin çok büyük olması ve yaklaşık 1100 gen içermesi nedeniyle hastalığa yol açan gen tanımlanamadı. Genin belirlenmesi amacıyla farklı yöntemler kullanılması gerekmektedir. Bu çalışma sonucunda özellikle iki önemli sonuca varılmıştır. Birincisi, *GJB1*'in 5'UTR bölgesinde bulunan varyasyonların beklenenden daha sık hastalığa yol açabileceğinin gösterilmesidir. İkincisi, bir ailede bilinen tüm CMT genlerinin dışlanması sonrasında üç aday gen tanımlanmasıdır. İleride gerçekleştirilecek olan araştırmalarda bu aday genlerden hangisinin hastalığa yol açtığı belirlenebilecektir. CMT genlerinin ve mutasyonların tanımlanması hastalığın genetik alt yapısının anlaşılması ve hastalara moleküler tanı ile yardımcı olunması açısından son derece önemlidir.

TABLE OF CONTENTS

LIST OF FIGURES

LIST OF TABLES

LIST OF SYMBOLS

A	Adenine
C	Cytosine
D	Aspartic acid
F	Phenylalanine
G	Guanine
H	Histidine
I	Isoleucine
L	Leucine
M	Methionine
N	Asparagine
Q	Glutamine
R	Arginine
S	Serine
T	Thymine
V	Valine
W	Tryptophan
X	Stop codon
Y	Tyrosine

LIST OF ACRONYMS / ABBREVIATIONS

AD	Autosomal dominant
$AgNO_3$	Silver nitrate
alt	Alternative
APS	Ammonium peroxodisulphate
AR	Autosomal recessive
ARAP1	ArfGAP with RhoGAP domain, ankyrin repeat and PH domain 1
bp	Basepair
BTBD18	BTB (POZ) domain containing 18
Ca	Calcium
cAMP	Cyclic adenosine monophospate
CCDS	Consensus CDS
CDS	Coding sequences
chr	Chromosome
cM	Centimorgan
CMAP	Compound muscle action potentials
CMT	Charcot-Marie-Tooth
CNS	Central nervous system
Cx32	Connexin 32
Cx43	Connexin 43
dbSNP	SNP database
DI	Dominant Intermediate
DNA	Deoxyribonucleic acid
DNM2	Dynamin 2
dNTP	Deoxyribonucleotide Triphosphate
DTCS	Dye Terminator Cycle Sequencing
DYNC1H1	Cytoplasmic dynein 1 heavy chain 1
EGFR	Epidermal growth factor receptor
EGR2	Early growth response protein 2
ESE	Exonic splicing enhancer

GDAP1	Ganglioside-induced differentiation-associated-protein 1
GJB1	Gap junction protein, beta 1
GST	Glutathione-S-transferases
GTP	Guanosine triphosphate
HCl	Hydrochloric acid
het	Heterozygous
HMSN	Hereditary motor and sensory neuropathy
HNPP	Hereditary Neuropathy with Liability to Pressure Palsy
hom	Homozygous
ID1	Inhibitor of DNA binding 1, dominant negative helix-loop-helix protein
IGV	Integrative Genomics Viewer
IP_3	Inositol trisphosphate
IRES	Internal ribosome entry site
KCl	Potassium chloride
KD	Knockdown
kDa	Kilodalton
$KHCO_3$	Potassium bicarbonate
KLHL3	Kelch like 3
LOD	Logarithm (base 10) of odds
m	Meter
Mb	Megabase
MBP	Myelin basic protein
mg	Milligram
$MgCl_2$	Magnesium chloride
min	Minute
ml	Milliliter
mM	Millimolar
MPZ	Myelin protein zero
MYO7A	Myosin VIIA
NA	Not available
Na_2EDTA	Disodium ethylenediamine tetraacetate
$NaBH_4$	Sodium borohydride
NaCl	Sodium chloride

NaOH	Sodium hydroxide
NCBI	National center for biotechnology information
NCV	Nerve conduction velocity
NEFL	Neurofilament light polypeptide
ng	Nanogram
NH_4Cl	Ammonium chloride
NHLBI	National Heart, Lung, and Blood Institute
P0	Protein zero
PAGE	Polyacrylamide Gel Electrophoresis
PCR	Polymerase chain reaction
PH	Pleckstrin homology
PIP_3	Phosphatidylinositol (3,4,5)-triphosphate
PLP	Proteolipid protein
PM	Plasma membrane
pmol	Picomole
PMP-22	Peripheral myelin protein-22
PNS	Peripheral nervous system
PRPS1	Phosphoribosyl pyrophosphate synthetase 1
RBC	Red blood cell
rcf	Relative centrifugal force
ref	Reference
RNA	Ribonucleic acid
ROS	Reactive oxygen species
s	Second
SC	Schwann cell
SDS	Sodium dodecyl sulfate
SERPINA3	Serpin peptidase inhibitor, clade A, member 3
SH3TC2	Src homology 3 domain and tetratricopeptide repeats-containing protein 2
SLC35F2	Solute carrier family 35, member F2
SNP	Single nucleotide polymorphism
SOX10	SRY (sex determining region Y) box 10
SSCP	Single strand conformation polymorphism
STR	Short tandem repeat

TBE	Tris-Borate-EDTA
TE	Tris-EDTA
TEMED	Tetramethylethylenediamine
temp	Temperature
TF	Transcription factor
TMD	Transmembrane domain
UTR	Untranslated region
v	Volume
w	Weight
µg	Microgram

1. INTRODUCTION

Charcot-Marie-Tooth disease (CMT) is the most common inherited neuropathy also known as hereditary motor and sensory neuropathy (HMSN) (Timmerman *et al.,* 1992). The disease was first described by French neurologists Jean-Martin Charcot and Pierre Marie (Charcot and Marie, 1886) and independently by English neurologist Howard Henry Tooth (Tooth, 1886). It was described later as a peripheral nervous system (PNS) disorder by Hoffmann (Hoffmann, 1889).The prevalence of CMT is about 36 per 100000 people (Krajewski *et al.,* 2000). Up to now, approximately 45 different causative CMT genes or loci have been identified implicating its genetic heterogeneity (Murphy *et al.,* 2012).

The typical clinical features of CMT are slowly progressive distal muscle weakness and atrophy, which first affects the peroneal and small foot muscles and afterwards affects the hands and forearms. Moreover, deformity in foot, such as *pes cavus,* gait impairments, distal sensory loss, loss of tendon jerks and claw toes are observed in the affected individuals (Figure 1.1). Although CMT has typical features, different clinical symptoms may be seen in different subtypes of the disease (Sivakumar *et al.,* 2005; Young and Suter, 2003; Kuhlenbäumer *et al.,* 2002).

Figure 1.1. CMT phenotype with wasting of thenar, peroneal atrophy, pes cavus and hammerhead toes (Sivakumar *et al.,* 2005).

CMT can be classified into three main subtypes according to clinical, electrophysiological and histopathological features: CMT1 (demyelinating), CMT2 (axonal degeneration) and intermediate CMT (Berciano *et al.,* 2011). If the myelin or myelinating Schwann cells are defected, nerve conduction velocities (NCV) are slower than 38m/s, the neuropathy can be classified as CMT1. When degeneration starts in the axons compound muscle action is reduced, the NCV value remains above 38 m/s and the neuropathy is classified as CMT2 (Thomas and Calne, 1974). Intermediate CMT is characterized by presence of both axonal degeneration and demyelinating features and the NCV value is between 25-45 m/s (Jordanova *et al.,* 2006).

CMT can also be classified according to the inheritance pattern, that can be autosomal dominant (AD), autosomal recessive (AR), X-linked dominant or X-linked recessive. Thus for the categorization of CMT types, both the clinical characteristics and the inheritance pattern are considered. Some causative genes are known to be responsible for both demyelination and axonal degeneration while different mutations in the same gene may show dominant and recessive traits (Reilly *et al.,* 2011) (Figure 1.2).

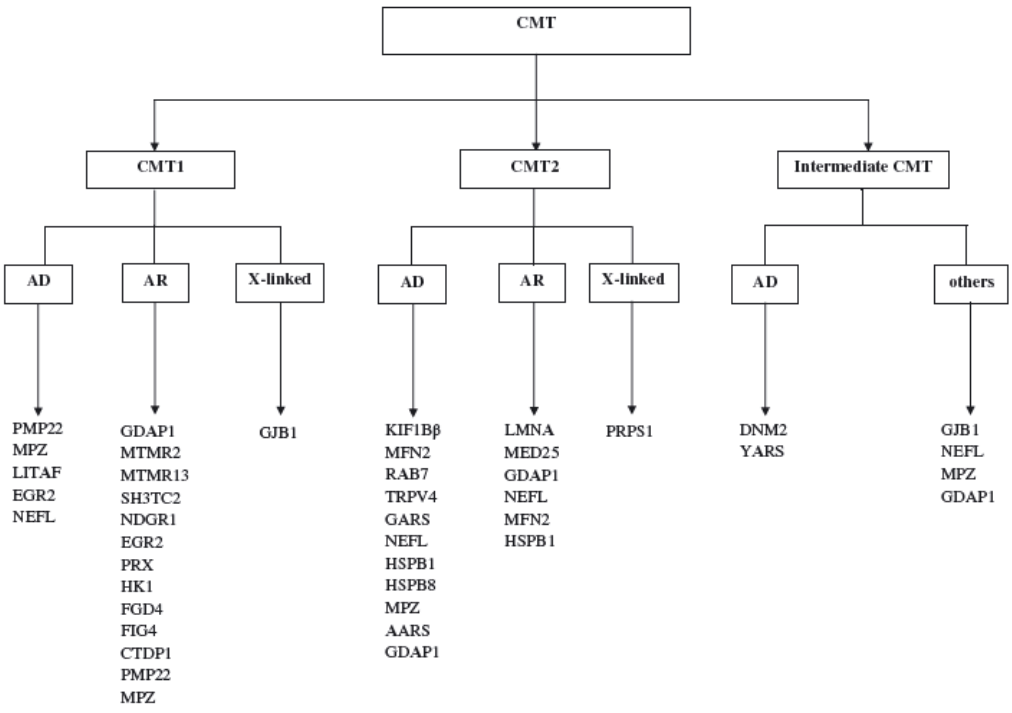

Figure 1.2. Classification of causative genes of CMT (Reilly *et al.,* 2011).

As mentioned earlier, more than 40 causative genes are responsible for CMT. Most of the CMT proteins are localized at either the Schwann cells (SCs) and myelin or the neurons (Figure 1.3) (Juarez and Palau, 2012).

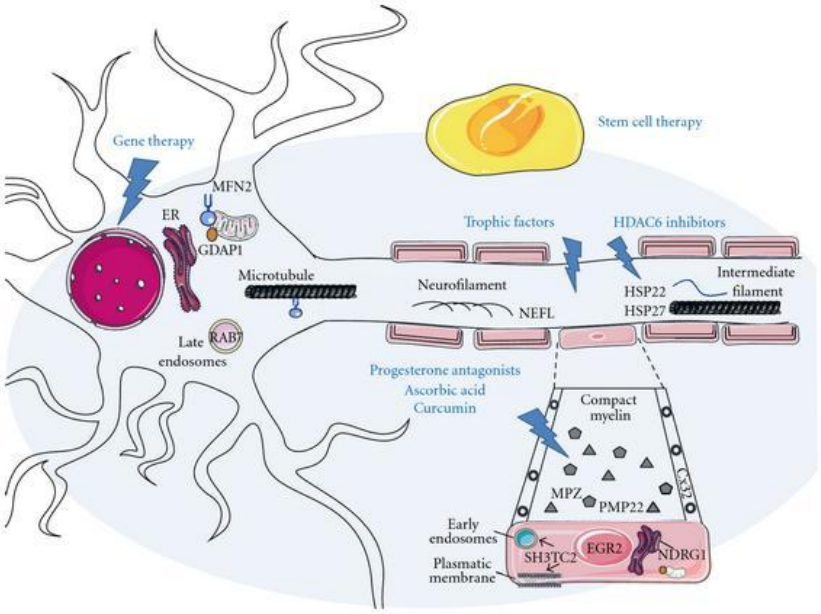

Figure 1.3. Peripheral nerve structure and the location of some CMT proteins (Juarez and Palau, 2012).

Myelin, which has a lipid and protein rich structure, is a highly specialized extension of the plasma membrane of SCs in the peripheral nervous system (PNS) (Bronstein, 2000). Its function in the neurons is to reduce the dispersion of the electrical current. So, axonal conduction velocity in the neurons is fastened during the transmission through the axon (Snipes *et al.,* 1992). In the CNS, proteolipid protein (PLP), myelin basic protein (MBP) and myelin-associated proteins are the major structural myelin proteins and they are protein zero (P0), MBP and peripheral myelin protein-22 kD (PMP-22) in the case of PNS (Campagnoni, 1988; Lemke, 1989).

Schwann cells (SCs) are the glial cells of the PNS, which has important roles during development and axonal maintenance. Moreover, they take role after nerve injury during the process of regeneration (Bray and Aguayo, 1974). SCs that are migrating from neural crest cells can be differentiating into two groups: myelinating and non-myelinating SCs

(Figure 1.4). This differentiation is directed by cell extrinsic signals that mostly come from axons (Mirsky and Jessen, 1999). After the formation of myelin sheath around SCs with the nodes of Ranvier, an efficient and fastened action potential transmission is obtained (Niemann *et al.*, 2006). Non-myelinating SCs are also important for neurons since they are very rich in voltage-gated sodium channels and essential for rapid conduction change. Thus, SCs also determine the ion-channel distribution and neuronal survival during development and regeneration after the defect (Edgar and Garbern, 2004; Poliak and Peles, 2003).

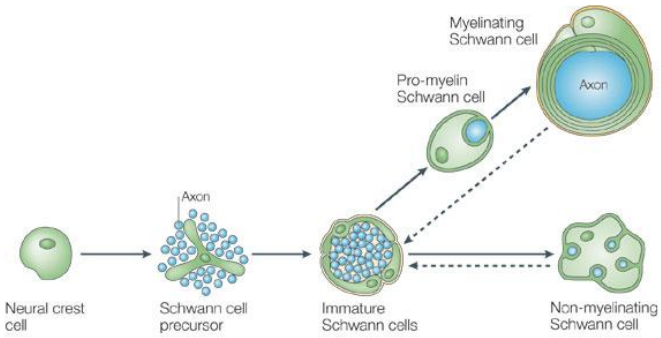

Figure 1.4. Main cell types and differentiation pattern involved in Schwann cell development (Jessen and Mirsky, 2005).

SCs and neurons are functionally tightly connected and they regulate the activities of each other closely. In order to match the numbers of SCs and axons, survival and proliferation of SC-precursors at early developmental stages depend on axonal signals (Niemann *et al.*, 2006). In CMT, the defective genes that are expressed in either SCs or neurons are probably responsible for the disruption of Schwann cell-axon interactions. Mutations in axonal transport genes are associated with primary SCs defects. These mutations may hinder Schwann cell-axon interaction and therefore, cause axonal atrophy and disability (Sahenk, 1999; Suter and Scherer, 2003).

1.1. Charcot-Marie-Tooth Disease Type 1 (CMT1) and Type 4 (CMT4)

The most common type of CMT is CMT1 that accounts for about 70% of all CMT cases. The patients suffering from CMT1 have demyelination that results in severely slow

NCVs (lower than 38m/s) with almost 100% penetrant phenotype independent of age. Other features of the disease are apparent enlarged nerves and onion bulb formation in biopsy samples (Wise *et al.,* 1993; Baxter *et al*., 2002). While dominant form of demyelinating CMT is designated as CMT1, demyelinating recessive form of it is called CMT type 4 (CMT4) (Dubourg *et al.*, 2006).

CMT1A is a subgroup of CMT1 that is associated with a 1.5 Mb duplication on chromosome 17p11.2 that contains the peripheral myelin protein (PMP22) gene. (Lupski *et al.,* 1991; Raeymeakers *et al.,* 1991, Matsunami *et al.,* 1992; Patel *et al.,* 1992; Timmerman *et al.,* 1992; Valentijn *et al.,* 1992a). Approximately 50% of the patients, suffering from CMT, carry this duplication. CMT1A patients may also have point mutations in the transmembrane region of PMP22 (Valentijn *et al.,* 1992b; Roa *et al.,* 1993). On the other hand, the most frequently mutated genes in CMT4 are ganglioside-induced differentiation-associated-protein 1 gene (*GDAP1*) and Src homology 3 domain and tetratricopeptide repeats-containing protein 2 (*SH3TC2)* (Inherited peripheral neuropathies mutation database, 2007). Mutations in *GDAP1* and *SH3TC2* are classified as CMT4A and CMT4C, respectively.

1.1.1. CMT4A

The locus for CMT4A was first mapped in a Tunisian family to chromosome 8q13-q21. The family had hypomyelination with slow motor NCV values (Ben Othmane *et al.,* 1993). *GDAP1*, found on that locus, was identified to be responsible for the disease (Baxter *et al.,* 2002), designated as CMT4A, and turned out to be the most frequently mutated gene among recessive demyelinating neuropathy patients (Cassereau *et al.* 2011). The mutations in this gene may also cause intermediate recessive CMT, autosomal recessive and dominant CMT2 (Senderek *et al.,* 2003a; Cuesta *et al.,* 2002; Claramunt *et al.,* 2005).

GDAP1 is a member of a subfamily of glutathione-S-transferases (GSTs). The protein has five domains, of which two are typical GST domains found on both N- and C-terminals of the protein. GSTs are important molecules since they have roles in detoxification and reduction of reactive oxygen species (ROS) (Cuesta *et al.,* 2002). The

transmembrane domain (TMD) is found at the C-terminus of GDAP1 and responsible for insertion to mitochondrial outer membrane. Hydrophobic domain is in the flanking C-terminal region of the protein (Marco *et al.*, 2004). Two helices, α4 and α5, are found between amino acids 152–164 and 169–195 that form α4–α5 loop (Figure 1.5).

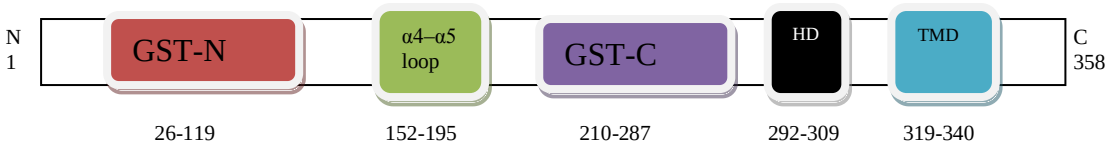

Figure 1.5. Positions of estimated structural domains of GDAP1 protein. Start and end of the amino acid positions for each domain is indicated under the figure (Modified from Cassereau *et al.* 2011).

This gene encodes a mitochondrial protein that is found on outer membrane of mitochondria. The role of protein is not fully understood yet but it is shown that it promotes fission events in mitochondria and may regulate the mitochondrial dynamics (Niemann *et al.*, 2005). The protein is ubiquitously expressed in nervous tissues (Cuesta *et al.*, 2002). Since GDAP1 is expressed by both myelinating Schwann cells and motor and sensory neurons (Niemann *et al.*, 2005), defects in GDAP1 may affect either Schwann cells or neurons, or both.

1.1.2 CMT4C

The locus for CMT4C was first mapped in two consanguineous Algerian families to chromosome 5q23-33. The patients were reported to have scoliosis as an additional feature and their motor NCV were between 20-32 m/s, suggesting demyelination (LeGuern *et al.*, 1996). The gene, SH3TC2, was identified in 12 families with CMT4C from Turkey, Germany, Italy, Greece and Iran (Senderek *et al.*, 2003).

The gene is encoding a 144kDa protein that has seven domains. Two of these domains are N-terminal SH3 and five of them are C-terminal tetratricopeptide repeat (TPR) motifs (Roberts *et al.*, 2009) (Figure 1.6).

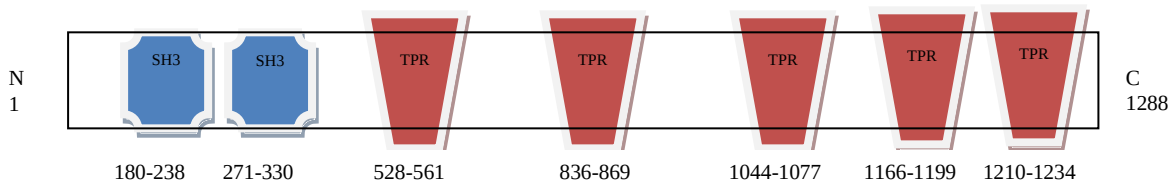

Figure 1.6. Predicted domains of SH3TC2 protein. Numbers under the domains indicate the start and end of the amino acid positions for each (Modified from Roberts *et al.*, 2009).

The protein is highly conserved among vertebrates and expressed in brain, spinal cord and sciatic nerve. The role of the protein is still unknown but since it has SH3 and TPR domains it is speculated that it has interactions with other proteins and forms multiprotein complexes (Senderek *et al.*, 2003b). On the other hand, more recent studies show that, the protein is co-localized with endocytic components suggesting that the protein may have a role in endocytic pathway and therefore defects in the protein may cause neuropathy with demyelination (Lupo *et al.*, 2009).

1.2. Charcot-Marie-Tooth Disease Type 2 (CMT2)

Another subgroup of CMT is CMT type 2 (CMT2), the axonal degeneration form of the disease. The clinical features of the subtype are loss of large myelinated fibers and a relatively normal NCV value (around 38 m/s or higher) but reduced compound muscle action potentials (CMAP) (Dyck *et al.*, 1993; De Sandre-Giovannoli *et al.*, 2002). The inheritance of this subtype can be dominant, recessive or X-linked (Figure 1.2).

1.3. Dominant Intermediate Charcot-Marie-Tooth Disease (DI-CMT)

Symptoms of the disease in intermediate CMT cases show similarity to that of both demyelinating and axonal degeneration. NCV value for this subtype can vary from 25 to 45 m/s. *DNM2* (Zuchner *et al.*, 2005) and *YARS* (Jordanova *et al.*, 2006) are the causative genes that are related to DI-CMT. However, mutations in some other genes such as *GJB1*, *NEFL*, *MPZ* and *GDAP1* can also result in DI-CMT with NCV values between 25 to 45 m/s with different modes of inheritance (Figure 1.2). Therefore, the usefulness of including DI-CMT to CMT classification is still under discussion (Reilly *et al.*, 2011).

1.4. X-Linked Charcot-Marie-Tooth Disease (CMTX)

X-linked CMT is the second most common form of the disease (Kleopa and Scherer, 2002). Up to now, two causative genes were identified on the X chromosome, which are *GJB1* (CMTX1) and *PRPS1* (CMTX5). In addition, three more loci, CMTX2, CMTX3, CMTX4, have been identified that show linkage to the disease, but no causative genes were identified for these loci. Among these subtypes only CMTX1 is dominantly inherited while the other forms are inherited recessively. Due to X-inactivation, in the case of CMTX1, females are mildly affected. On the other hand, in the recessive cases, females are mostly asymptomatic (Bone *et al.,* 1997). Most cases are demyelinating in CMTX but motor NCV values are moderately higher when compared to that of other demyelinating types (England and Garcia, 1996). In some cases, both axonal degeneration and demyelination can be observed (Senderek *et al*, 1999).

1.4.1. CMTX1

The locus for CMTX1 was first mapped in four families to a region adjacent to the centromere of X chromosome (Xq13.1) (Fischbeck *et al.,* 1986). The causative gene, *GJB1,* was first identified in eight families (Bergoffen *et al.,* 1993). Up to date, more than 300 mutations have been identified in the coding region of *GJB1* (Szigeti and Lupski, 2009). Mutations have also been identified in the 5'UTR, promoter or splice site region, of its nerve specific transcript. Mutations in the 5'UTR may affect the transcription level by disrupting the binding of transcription factors (TFs) to the promoter of *GJB1*, altering the splicing process or changing the internal ribosome entry site (IRES) before translation (Ionasescu *et al.*, 1996; Houlden *et al.,* 2004; Wang *et al.,* 2000; Li *et al.,* 2009).

GJB1 encodes for a connexin protein whose molecular mass is 32 kDa (Cx32). Cx32 is expressed in myelinating SCs and oligodendrocytes (Ri *et al.,* 1999). Although the mutations in *GJB1* mainly affect the peripheral nervous system, in some cases patients may also have some defects in their CNS, since the protein is also expressed in oligodendrocytes (Nicholson and Corbett, 1996; Parman *et al.,* 2007).

Cx32 is a gap junction protein that forms channels to allow the permeation of molecules such as secondary messengers, cAMP and Ca^{+2} (Bevans *et al.*, 1998). Connexons are composed of six connexins that form two opposite hemichannels. These hemichannels are found in each adjacent plasma membrane to form complete cell-cell channel (Stauffer, 1995). Connexin proteins can also be found in the membrane of endoplasmic reticulum and/or Golgi apparatus (Figure 1.7) that shows the importance of Cx32 in membrane trafficking. Some of the mutations in *GJB1* are thought to cause abnormalities in membrane trafficking and still some are responsible for defective radial pathway between SCs (Niemann *et al.*, 2006; Kleopa and Scherer, 2006).

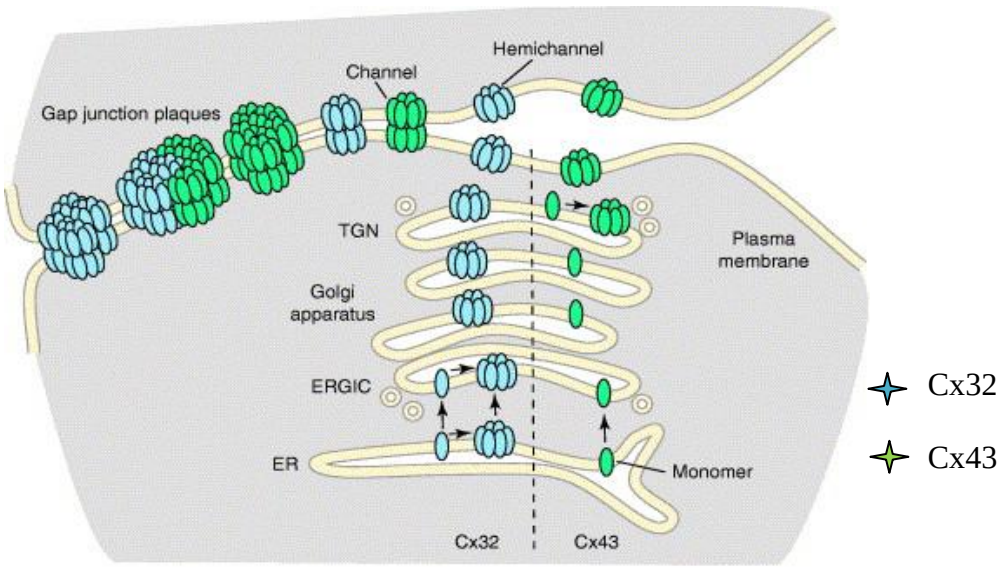

Figure 1.7. Channel formation on the plasma membrane of adjacent cells for Cx32 and Cx43. Connexins can also be observed in the membrane of ER and Golgi apparatus (Koval, 2006).

1.4.2. CMTX5

The locus for CMTX5 was first identified in a Korean family, which mapped to chromosome Xq21.32-q24. Beside peripheral neuropathy, the symptoms were deafness and optic atrophy for the family (Kim *et al.*, 2005). Later on, *PRPS1*, was identified to be responsible for the disorder in the same family and in another family, who had Rosenberg-

Chutorian syndrome suggesting that these are allelic disorders caused by the same gene (Kim *et al.,* 2007).

PRPS1 encodes for an enzyme, which is ubiquitously expressed in human tissues. The role of the enzyme is crucial since it mediates the purine metabolism and nucleotide biosynthesis (Taira *et al.,* 1989). This gene is the first one that is known to have a role in metabolic activity among the causative genes for CMT. Therefore, this gene was thought to bring a new approach to understanding the peripheral nerve specific metabolism (Kim *et al.,* 2007). However, Korean family is the only reported CMT case with a *PRPS1* mutation.

1.5. Genetic Analyses to Identify Genetic Background of CMT

1.5.1. Exome Sequencing

In recent years, next generation DNA sequencing technology has been improved and the cost has decreased. As a result of this improvement, read depth and output for the sequencing is increased. In the light of these advances, whole exome sequencing has become an important and efficient technique to identify the genetic background of the inherited diseases (Ng *et al.,* 2009; Choi *et al.,* 2009; Robinson *et al.,* 2011).

In the human genome, there are approximately 180000 exons that are found in about 22000 genes. The total of these protein-coding regions is named as an exome, which comprises 30 Mb in length and only 1% of the whole genome. Since the exome constitutes approximately 85% of the functional variations, exome sequencing is a very helpful and important analysis in order to understand the causes of genetic diseases (Botstein and Risch, 2003).

Whole genome sequencing is another technique to unravel the genetic cause of the disease; however, the cost is around 10000$ per patient. Both exome and whole genome sequencing are efficient analyses, especially, to identify mutations in an inherited disease with high genetic heterogeneity. On the other hand, when comparing exome and whole genome sequencing, exome sequencing is more feasible as 85% of the functional variations are found in the exome (Lupski *et al.,* 2010).

The CMT disease is a good candidate to test the efficiency of exome sequencing especially for genetic diagnosis since it is a relatively rare and genetically heterogeneous (Montenegro *et al.,* 2011). In a recent study, three members from a large family with CMT were exome sequenced and mutations in *DYNC1H1* were found in all affected members. Mutations were excluded for frequently mutated CMT genes previously by conventional methods and exome sequencing revealed the mutation in a less frequently mutated gene (Weedon *et al.,* 2011). In another recent study, 25 individuals with CMT phenotype were exome sequenced and only eight of them were found to have mutations in CMT genes. The reason for the low rate of mutation detection may be the limitations in exome sequencing like presence of mutations in non-exonic regions, low depth of coverage or presence of the causative mutation in a novel, unidentified gene (Choi *et al.,* 2012). Therefore, if the cause of the disease cannot be identified by a single analysis, another analysis, like linkage analysis, can be performed. In a very recent paper, it is indicated that, a novel gene, *KLHL3*, was identified by combining exome sequencing and whole genome linkage analysis, responsible for a Mendelian disorder, familial hyperkalemic hypertension (Louis-Dit-Picard *et al.,* 2012).

1.5.2. Linkage Analysis

Linkage analysis is an efficient tool to determine the loci that can be segregating with the inherited disease phenotype for an affected family. Different methods for linkage analysis include the use of SNP arrays or STR panels. Two-point LOD score method is generally used in order to find the candidate locus responsible for the corresponding disease. However, linkage analysis only determines the loci that may have a variation and sequencing is necessary to identify the causative variants (Bailey-Wilson and Wilson, 2011). In the case of CMT, many causative genes have been identified by linkage analysis up to date, as in the case for other inherited diseases. In a recent study, whole genome linkage analysis was performed by using SNP array for a family with CMT phenotype and 35 regions were found with the highest LOD score. Five already identified causative genes were found on these regions and they were sequenced to identify the variation. A variant was observed in all patients in *EGR2* (Safka Brozkova *et al,* 2012). This study was a proof for the usefulness of whole genome linkage analysis for the molecular diagnosis of inherited diseases such as CMT.

When the linkage analysis results in a region that is relatively large, direct sequencing of candidate genes in this region may not be feasible. Therefore, a secondary analysis like exome sequencing could be of use in determining the candidate genes and delineating the causative gene.

In the light of this information, due to inconclusive results with only exome sequencing, we have used a combination of exome sequencing and whole genome linkage analyses for one of our CMT families in the scope of this thesis.

2. AIM OF THE STUDY

In this study, we aim to investigate the genetic basis of the CMT disease using three different approaches; mutation, exome sequencing and linkage analyses. By screening known causative CMT genes for mutations we aim to help the patients with molecular diagnosis of the disease. The families that do not present mutations in the known CMT genes will then be analyzed by linkage and exome sequencing analyses to unravel the causative genes. Our specific aim is to identify novel CMT genes by performing exome sequencing and linkage analyses.

3. MATERIALS

3.1. Subjects

Peripheral blood samples of Turkish CMT patients and their family members were provided by various neurology departments around Turkey. Detailed electrophysiological and histopathological features of patients and pedigrees were obtained from clinicians.

3.2. Chemicals

All solid and liquid chemicals used in this study were bought from Merck (Germany), Sigma (USA) and Riedel de-Häen (Germany) unless stated otherwise in the text.

3.3. Fine Chemicals

In the following sections, fine chemicals that were used in this study are given in detail.

3.3.1. Enzymes

Taq DNA Polymerase used in the experiments performed in our department was purchased from Fermentas (MBI Fermentas, Lithuania).

Titanium Taq DNA Polymerase used in amplification of coding sequences (CDS) of *GDAP1, SH3TC2* and 5'UTR of *GJB1* genes and short tandem repeats (STR) markers in the X chromosome were purchased from Clontech Laboratories (Clontech, France) and these experiments were performed in University of Antwerp.

3.3.2. Oligonucleotide Primers

The primers used in the PCR-SSCP for *PRPS1* gene and PCR-direct sequencing analysis for *GJB1, SH3TC2* and *GDAP1* genes were synthesized by Integrated DNA technologies (Leuven, Belgium). Direct sequencing was performed by using the same primers as for the amplification or with additional primers if required. The primers designed for X chromosome scan were also synthesized by Integrated DNA technologies (Leuven, Belgium). All the forward primers were 5' FAM or HEX labeled. The primers were designed using Primer 3 software (Rozen and Skaletsky, 2000).

The primer sequence sets used for amplification and direct sequencing of different genes and PCR conditions are given in Table 3.1 through Table 3.9.

Table 3.1. Sequences of the primers used for exon amplification of *PRPS1* for PCR-SSCP analysis.

Exon	Primer (F/R)*	Primer Sequence (5'→3')	Product Size (bp)	Annealing Temp. (°C)
Exon 1	PRPS1-1F	ATTGAGTCTGTGGCCGACTT	244	63
	PRPS1-1R	GGGCAGGTGAGGTCTAGTCA		
Exon 2	PRPS1-2F	ATGGATATGGAGGGCTGACA	299	65
	PRPS1-2R	CAAGTGCTCCTGCTTCCTCT		
Exon 3	PRPS1-3F	TTCTTTCCTCCCCTCCATTT	164	56
	PRPS1-3R	TCCTCCCACCTTTCAAACAC		
Exon 4	PRPS1-4F	TGAAGCAAAACTGATCCAGC	195	59
	PRPS1-4R	TCCCAGTACATTGGGAACAA		
Exon 5	PRPS1-5F	GAACACGCTCTGTTTTGCAG	286	62
	PRPS1-5R	GGTTCCAAAAGGAATCAGCA		
Exon 6	PRPS1-6F	TGGAAGCCTAAGCAGGCTAAT	273	64
	PRPS1-6R	TTTGCACAAATCTCATCCTCA		
Exon 7	PRPS1-7F	GGCCAGTCATCTCTGACCAT	257	65
	PRPS1-7R	AAGCTACACTGGAGCAAGCC		

Table 3.2. Sequences of the primers used for exon amplification of *GJB1* for PCR-Direct sequencing analysis.

Region	Primer (F/R)*	Primer sequence (5'→3')	Product Size (bp)	Annealing Temp. (°C)
Exon 1	Cx32-1F	TGAGGCAGGATGAACTGGACAGGT	306	59
	Cx32-1R	TTGCTGGTGAGCCACGTGCATGGC		
	Cx32-2F	ATCTCCCATGTGCGGCTGTGGTCC	432	63
	Cx32-2R	GATGATGAGGTACACCACCT		
	Cx32-3F	CGTCTTCATGCTAGCTGCCTCTGG	304	60
	Cx32-3R	TGGCAGGTTGCCTGGTATGT		

Table 3.3. Sequences of the primers used for 5'UTR amplification of *GJB1* for PCR-Direct sequencing analysis.

Region	Primer (F/R)*	Amplified Region	Primer sequence (5'→3')	Product Size (bp)	Annealing Temp. (°C)
5'UTR	5'UTR-GJB1-F	from -849 to +120	CTCAGGGAAAATCCTGGTGA	989	67.5
	5'UTR-GJB1-R		TCATCACCCCACACACTCTC		

Table 3.4. Sequences of the internal primers used for direct sequencing of 5'UTR of *GJB1*.

Region	Primer (F/R)*	Sequenced region	Primer sequence (5'→3')
5'UTR	5'UTR-GJB1-IF	from -424 to +120	TGAGACCATAGGGGACCTGT
	5'UTR-GJB1-IR	from -849 to -314	CCCTGTCCCCTAGCTCCTTA

Table 3.5. Sequences of the primers used for exon amplification of *GDAP1* for PCR-Direct sequencing analysis.

Exon	Primer (F/R)*	Primer sequence (5'→3')	Product Size (bp)	Annealing Temp. (°C)
Exon 1	GDAP1-1F	GCCCTTCATAACCAGGGTCTC	605	68
	GDAP1-1R	TCATCTCCGATCGATTCTCC		
Exon 2	GDAP1-2F	GGCTGCTTAGCGGTGTCCAGGG	330	62
	GDAP1-2R	GGGAACACATAGTTGTGTTG		
Exon 3	GDAP1-3F	GCTTTTGAGTGTAACAACTCATG	317	65
	GDAP1-3R	GACCATGAGACATGCTAGGTC		
Exon 4	GDAP1-4F	CAGGGTAAGCCCAAGGCAGAG	288	66
	GDAP1-4R	GTAGAACATTTACTCCGTGCAG		
Exon 5	GDAP1-5F	GGCTGAACTCTGTAAGAGTTTG	281	62
	GDAP1-5R	GACCTAAGAATGTTCCCATG		
Exon6	GDAP1-6F	GAGACCACTGATACCAGCTGG	530	65
	GDAP1-6R	CAGAGAGCCACGGGCAATCAC		

Table 3.6. Sequences of additional primers used for direct sequencing of *GDAP1*.

Exon	Primer (F/R)*	Primer sequence (5'→3')
Exon 1	GDAP1-1F-Seq.	CCGGCGAAACTACATTTCC
Exon 6	GDAP1-6F-Seq.	TGATACCAGCTGGAGTCTGTCTG
	GDAP1-6R-Seq.	GGGCAATCACAGGGTCTAGC

Table 3.7. Sequences of the primers used for exon amplification of *SH3TC2* for PCR-Direct sequencing analysis.

Exon	Primer (F/R)*	Primer sequence (5'→3')	Product Size (bp)	Annealing Temp. (°C)
Exon 1	SH3TC2-ex01F	AGGAGCCCTGTTCCCCAGGC	581	69
	SH3TC2-ex01R	TGGGAGTGGCAGCCAGGAGC		
Exon 2	SH3TC2-ex02F	CTGCTGGATTGAGATGGCATGTA	518	68
	SH3TC2-ex02R	TGCCAGATTGTGAAGAGCTTTGAG		

Table 3.7. Sequences of the primers used for exon amplification of *SH3TC2* for PCR-Direct sequencing analysis (cont.).

Exon	Primer (F/R)*	Primer sequence (5'→3')	Product Size (bp)	Annealing Temp. (°C)
Exon 3	SH3TC2-ex03F	CAGAGCCCTCCTGGGTTCAGTAT	538	70
	SH3TC2-ex03R	TCATTCAGAGTTCCTGCCCACTC		
Exon 4	SH3TC2-ex04F	TCTTTTGCTGCTGCCGCTGT	491	68
	SH3TC2-ex04R	ACCAGAGCCAGGCCAATTCCTT		
Exon 5	SH3TC2-ex05F	TGGCAGGTTGGGGCTTGTGG	525	70
	SH3TC2-ex05R	GTGGAGCCCTGGCTTGGGTATC		
Exon 6	SH3TC2-ex06F	TGAATTCCCTCTCAATGGCTTTTT	535	62
	SH3TC2-ex06R	GACCCACCCAGAATCTGTTCTCTC		
Exon 7	SH3TC2-ex07F	AAGTTCTCAATAAACTTTTGCCATCA	459	62
	SH3TC2-ex07R	CCCCTAGCATCTGTGTGTCCT		
Exon 8	SH3TC2-ex08F	TCCTGTGTCATTCCTGCCAATTT	541	68
	SH3TC2-ex08R	TGAACTGACGCATTCTCTCCTTTC		
Exon 9	SH3TC2-ex09F	ACTGGACAACCACACCCCTCAGTTC	623	68
	SH3TC2-ex09R	CCAGTACAGCCAGTCACCCACGG		
Exon 10-11	SH3TC2-ex10-11F	GGGTACACCTGGAGGCATGGGC	394	70
	SH3TC2-ex10-11R	TCAGGCTCCGGCAGGCGATAG		
Exon11	SH3TC2-ex11bF	AGAGCCTGGGAGGAGCATCAG	552	71
	SH3TC2-ex11bR	GGAGCCTTTATGTCTCAGCCTCTG		
	SH3TC2-ex11cF	GCCAGGGTGTACTTCGAGGAGG	569	68
	SH3TC2-ex11cR	GCCAAGGCAGAAACTTCACCCC		
	SH3TC2-ex11dF	TGCAGTGGCCTCTGTCCAGC	660	68
	SH3TC2-ex11dR	TCACAATAGAGTCGTACAGCCTGC		
	SH3TC2-ex11eF	AGCTATCTTCGGGCCTTGAACAG	548	68
	SH3TC2-ex11eR	CAGCAGCCTCCCTTCCATCTC		
Exon 12	SH3TC2-ex12F	CCCATGCTGCTGGGAAGCTA	461	68
	SH3TC2-ex12R	GCTTGCCCAAGGCTACACCA		
Exon 13	SH3TC2-ex13F	TTCCTGCTCAGAGCTTCTGTTTCA	531	68
	SH3TC2-ex13R	CGGGACAAGTGACGTTACAGATG		
Exon 14	SH3TC2-ex14F	CACCACCAAAAGCAATCTCTCAT	534	68
	SH3TC2-ex14R	AAGTTTATCAGAACCTTCCCTGAGC		
Exon 15	SH3TC2-ex15F	CCACTGCCGTTCCCCAACCC	342	70
	SH3TC2-ex15R	CAGGGCCTGCGGTGTTATTGC		

Table 3.7. Sequences of the primers used for exon amplification of *SH3TC2* for PCR-Direct sequencing analysis (cont.).

Exon	Primer (F/R)*	Primer sequence (5'→3')	Product Size (bp)	Annealing Temp. (°C)
Exon 16	SH3TC2-ex16F	GCCCCAGCACAGTCCCTGAC	586	70
	SH3TC2-ex16R	AGCCACAGACATGGTGGCAAGG		
Exon 17	SH3TC2-ex17F	GAGTGGCCAGCACAGCCTCC	384	71
	SH3TC2-ex17R	GGGGGCTAGGCCAGGTAAGGAC		

Table 3.8. Sequences of the primers used for multiplex PCR for X chromosome analysis.

Marker	Plex #	Primer (F/R)*	Primer sequence (5'→3')	Label	Product Size (bp)
DXS7104	1	DXS7104-F	AAGCCAAGGTCCCTCTCG	FAM	280
		DXS7104-R	GTTTCTTCTTCTGCTCCTCTCCTGGTC	-	
DXS1073	1	DXS1073-F	CATCTCACTCCCTGAAGATGACT	HEX	417
		DXS1073-R	GTTTCTTCCCTAGAGATGGCATAGGTCTG	-	
DXS1036	1	DXS1036-F	GCAAATCCATTTCAATCTCCA	FAM	454
		DXS1036-R	GTTTCTTATTGCCTTCAAACACTTCCTTT	-	
DXS8009	1	DXS8009-F	GCTTCTGAATTCTTCATTGCTTT	HEX	486
		DXS8009-R	GTTTCTTTTTCCCATTTCTGTGTATGTGG	-	
DXS6809	2	DXS6809-F	CCACTTGCCGTCATATAGACACT	FAM	432
		DXS6809-R	GTTTCTTTGTTAGTCTCCTTGGCCTCACT	-	
DXS8096	2	DXS8096-F	CCAAGGTTCAGATCCCAGATT	HEX	451
		DXS8096-R	GTTTCTTATTGAATACAACAGAGCCCTTACA	-	
DXS8103	2	DXS8103-F	AAGCTGTCTGGCTTTCACCTA	FAM	471
		DXS8103-R	GTTTCTTTCAGAGAACTGAGCCTAATGGA	-	
DXS8014	2	DXS8014-F	ATTGGCCTGTCATCTTCTCTTT	HEX	490
		DXS8014-R	GTTTCTTGAGCAACAGCTGGGCACT	-	
DXS1227	3	DXS1227-F	TGATCTGTCCCAGGAGGTG	FAM	374
		DXS1227-R	GTTTCTTCAATGTGCTTTCCAGAGGTG	-	
DXS8022	3	DXS8022-F	TTGAAGTGCGTTGGAAACC	HEX	453
		DXS8022-R	GTTTCTTCACAGTGATGAATTGTACTTTGGTG	-	
DXS8051	3	DXS8051-F	GAGATGGGTATGCTTAGTGCTTAAAT	FAM	479
		DXS8051-R	GTTTCTTTTCTTAAATAAGCGGAGATGCTTT	-	
DXS8110	4	DXS8110-F	CCTTAATCCAGGGCAGCAG	FAM	401
		DXS8110-R	GTTTCTTTGATATTGTTGGGCCAGTCTC	-	
DXS8107	4	DXS8107-F	AAACCACTCACCAAATGCTTC	HEX	436
		DXS8107-R	GTTTCTTCCCAAGGTGTGTGAGGACA	-	
DXS1211	4	DXS1211-F	GCTTCCAACTTGTTCTAAGTGTAGG	FAM	483
		DXS1211-R	GTTTCTTTGACAGCTGGAAAGTGACTAGG	-	

Table 3.9. Sequences of the primers used for amplification of the selected regions identified during whole genome linkage, haplotype and exome sequencing analysis.

Gene	Primer (F/R)*	Primer sequence (5'→3')	Product size (bp)	Annealing Temp. (°C)
BTBD18	BTBD18-F	TCTGGCACTCTTCTGCTCAA	405	68
	BTBD18-R	CCTGCTCCCACCTGTCTTT		
ARAP1	ARAP1-F	CCCAAGTTCTGACCACTTCC	580	68
	ARAP1-R	GCAGCACAGGGGAGAGTAAG		
MYO7A	MYO7A-F	GAATGAGAAAGGTGGGGACA	516	67.5
	MYO7A-R	CCTGGCTCAAGACGTTTCC		
SLC35F2	SLC35F2-F	CTGCTGTTCGTGGCATTTG	448	68
	SLC35F2-R	TGGGCCAGCTTGTTTATCAC		
SERPINA3	SERPINA3-F	CCCTCACCCCCAATAACTTT	499	67
	SERPINA3-R	CCTGGACATTGGTGAGACCT		
ID1	ID1-F	GGTGAGCAAGGTGGAGATTC	405	68
	ID1-R	CGCCTGTGAAAACGAGAAG		

* F: Forward primer, R: Reverse primer

3.3.3. DNA Size Markers

The size markers used in this study were 100-bp DNA ladder with a range of 100-1000 bp (Fermentas, Lithuania) or 100-bp DNA ladder with a range of 100-3000 bp (Solis Biodyne, Estonia).

3.3.4. Other Fine Chemicals

High Pure PCR Purification Kit was purchased from Roche (Switzerland).

3.4. Buffers and Solutions

3.4.1. DNA Extraction from Peripheral Blood

Table 3.10. Ingredients that are used for DNA extraction from peripheral blood.

Cell Lysis Buffer	155 mM NH_4Cl 10 mM $KHCO_3$ 1 mM Na_2EDTA (pH 7.4)
Nuclei Lysis Buffer	10 mM Tris-HCl (pH 8.0) 400 mM NaCl 2 mM Na_2EDTA (pH 7.4)
Sodiumdodecylsulphate	10% SDS (w/v) (pH 7.2)
Proteinase K	20 mg/ml
Tris-EDTA (TE) Buffer	20 mM Tris-HCl (pH 8.0) 0.1 mM Na_2EDTA (pH 8.0)
5 M NaCl solution	292.2 g NaCl in 1 L dH_2O

3.4.2. Polymerase Chain Reaction (PCR)

Table 3.11. Ingredients that are used for PCR.

10 X $MgCl_2$ Free Buffer	100 mM Tris-HCl 500 mM KCl (pH 9.1 at 20°C) (Fermentas, Lithuania)
Magnesium Chloride ($MgCl_2$)	25 mM $MgCl_2$ (Fermentas, Lithuania)
Deoxyribonucleotide Triphosphates (dNTPs)	100 mM of each dNTP (Fermentas, Lithuania)
Betaine	

3.4.3. Agarose Gel Electrophoresis

Table 3.12. Ingredients that are used for Agarose Gel Electrophoresis.

5 X Tris-Borate-EDTA (TBE) Buffer	0.89 M Tris-Base 0.89 M Boric Acid 20 mM Na_2EDTA (pH 8.3)
1 or 2% Agarose Gel	1 or 2% Agarose (w/v) (Peqlab, Germany) in 0.5 X TBE Buffer
Ethidium Bromide	10 mg/ml
6 X Loading Buffer	2.5 mg/ml Bromophenol Blue 1% SDS (w/v) in 2 ml glycerol

3.4.4. Polyacrylamide Gel Electrophoresis (PAGE)

Table 3.13. Ingredients that are used for PAGE.

5 X TBE Buffer	0.89 M Tris-Base 0.89 M Boric Acid 20 mM Na_2EDTA (pH 8.3)
30 % Acrylamide Stock (29:1)	29% Acrylamide (w/w) 1% N, N'-methylenebisacrylamide (w/w)
Ammoniumpersulfate	1% APS (w/v)
Tetramethylethylenediamine (TEMED)	
6 X Denaturing Loading Dye	95% Formamide (w/v) 20 mM EDTA 0.05% Xylene Cyanol (w/v) 0.05% Bromophenol Blue (w/v)

3.4.5. Silver Staining

Table 3.14. Ingredients that are used for Silver Staining.

Solution 1	0.1% $AgNO_3$ in dH_2O (w/v)
Solution 2	1.5% NaOH (w/v) 0.01% $NaBH_4$ (w/v) 0.015% Formaldehyde (v/v)

3.4.6. PCR and Ethanol Precipitation for Direct Sequencing

Table 3.15 Ingredients that are used for PCR and ethanol precipitation in DNA sequencing facility of Bogazici University.

3 M Sodium Acetate
0.5 M Sodium-EDTA
Glycogen
Dye Terminator Cycle Sequencing (DTCS) mix
Sample Loading Solution

3.5. Equipment

Automated DNA Sequencing, whole genome and X chromosome scan analysis using GeXP genetic analysis system (Beckman Coulter, USA) were conducted by core facilities of University of Antwerp (Belgium). Automated DNA sequencing was also performed in out department by using GeXP genetic analysis system (Beckman Coulter, USA).

The equipments used for the other experiments that were performed in our department are listed in Table 3.16.

Table 3.16. Equipments used during this study.

Autoclave	Model MAC-601 (Eyela, Japan)
Centrifuges	Centrifuge 5415C (Eppendorf, Germany) Allegra X-22R Centrifuge (Beckman Coulter, USA)

Table 3.16. Equipments used during this study (cont.).

Deep Freezers	-20°C (Bosch, Germany) -20°C (Arçelik, Turkey) -70°C (Thermo Forma, USA)
Documentation System	GelDoc Documentation System (Bio-Rad, USA)
Electrophoresis Equipments	Mini-Sub Cell (Bio-Rad, USA) PROTEAN Vertical Electrophoresis System (Bio-Rad, USA)
Genetic Analyzer	GeXP genetic analysis system (Beckman Coulter, USA)
Incubators	DRI Block DB-2A (Techne, UK) Shake'n'Stack (Hybaid, UK) Oven EN400 (Nuve, Turkey)
Magnetic Stirrer	Speed Safe (Hanna Instruments, USA) MK 418 (Nüve, Turkey)
Oven	Microwave Oven (Vestel, Turkey)
Power Supplies	Power Pac Model 3000 (Bio-Rad, USA) PS 304 (Apelex, France)
Refrigerator	+4°C (Arçelik, Turkey)
Shaker	SL 350 (Nüve, Turkey)
SpeedVac	SPD111V (Thermo Scientific, USA).
Spectrophotometer	NanoDrop ND-1000 (NanoDrop, USA)
Thermal Cyclers	Icycler (Bio-Rad, USA) Mycycler (Bio-Rad, USA) Runik Thermal Cycler (Sacem, Turkey) C 1000 Thermal Cycler (Bio-Rad, USA)
Vortex	Nuvemix (Nuve, Turkey)

4. METHODS

4.1. DNA Extraction from Peripheral Blood

Ten ml blood samples from patients and their family members were collected in K_3EDTA tubes. Before DNA extraction, the samples were stored at 4˚C. Blood samples were transferred into sterile 50 mL centrifuge tubes. To lyse the erythrocyte membranes, approximately 30 mL red blood cell (RBC) lysis buffer was added and left at 4˚C for 25 minutes. The lysed samples were centrifuged at 2576 relative centrifugal force (rcf), at 4˚C for 10 min. After discarding the supernatant, 10 mL RBC lysis buffer was added to the samples. By vortexing, the pellet was resuspended and centrifugation was repeated at 2576 rcf, at 4 ˚C for 10 minutes. The supernatant was discarded and 3 mL nuclei lysis buffer, 40 µl Proteinase K and 50 µl of 10% SDS were added to the pellet. Thereafter, the samples were incubated at 37˚C overnight in order to degrade cellular proteins. The next day, 2.5 M NaCl were added, the samples were vortexed and centrifuged at room temperature at 2576 rcf for 20 minutes. The supernatant was transferred into a new 50 mL centrifuge tube. After addition of 2 volume of absolute ethanol (-20˚C), the DNA was precipitated. The genomic DNA was taken into a 1.5 mL microcentrifuge tube and allowed to air-dry. Accordingly the DNA was dissolved in 100-300 µl of Tris-EDTA (TE) buffer.

4.2. Quantitative Analysis of Extracted DNA

Nanodrop ND-1000 spectrophotometer was used to measure the genomic DNA concentration at 260nm. The main principle of the measurement was based on the finding that absorbance of 50 µg of pure double stranded DNA has an absorbance of 1.0 at 260 nm. To ensure the purity of DNA A_{260}/A_{280} ratio should be between around 1.8.

4.3. Mutation Analysis

In this study 34 Turkish CMT patients were screened for mutations. They were previously found to be negative for CMT1A duplication and HNPP deletion. Eleven of these patients were screened for mutations in the coding sequence of *GJB1*. Out of

remaining 23 Turkish CMT patients, 15 patients, that were previously found to be negative for point mutations in the *GJB1* coding sequence, were screened for mutations in the 5'UTR of *GJB1* that harbors the putative transcription factor binding sites. Thirteen were screened for *PRPS1*, 18 were screened for *GDAP1* and 12 were screened for *SH3TC2* with overlap between the groups based on pedigree analyses.

4.3.1. Mutation Analysis of *PRPS1* by Using PCR-SSCP

PCR-SSCP method is used to identify the genetic variants by using polyacrylamide gel electrophoresis. After amplifying the region of interest, double stranded DNA is denaturated by heat and cooled on ice allowing it to fold on itself as a single stranded DNA resulting in a unique conformation depending on the primary sequence. By using this method, even a single nucleotide change can be determined (Orita *et al*., 1989).

4.3.1.1. Polymerase Chain Reaction (PCR). Seven exons of the *PRPS1* were amplified by using the primers for which the sequences and annealing temperatures are given in Table 3.1.

PCR was performed in a total volume of 25 µl for all exons of *PRPS1*, using the chemicals described below (Table 4.1).

Table 4.1 Ingredients for PCR of all exons of *PRPS1*.

Ingredients	**Volume (µl)**
DNA (100 ng)	1
10X polymerase buffer	2.5
$MgCl_2$ (2.0 mM)	1.5
dNTPs (0.1 mM)	0.2
Forward and Reverse Primers (10pmol/µl)	1 from each
Taq DNA Polymerase (1 Unit)	0.1
dH_2O	17.7

Conditions for PCR of all *PRPS1* exons are given in Table 4.2. To check the amplicon size, a mixture of 5 µl of PCR product and 1 µl of agarose loading buffer was

loaded on 2% (w/v) agarose gels and by the help of DNA size marker, size of the amplicon was confirmed.

Table 4.2 Conditions of PCR for all exons of *PRPS1*.

Conditions of PCR	
Initial denaturation	5 min at 95ºC
Denaturation (35 cycles)	30 s at 95ºC
Annealing (35 cycles)	30 s at annealing temperature
Extension (35 cycles)	45 s at 72ºC
Final Extension	7 min at 72ºC
Cooling	1 min at 4ºC

4.3.1.2. Single Strand Conformation Polymorphism (SSCP). The amplicons were loaded on 8% (v/v) acrylamide gels to detect whether there is a different migration pattern. In preparing the SSC gel, one mm spacers were used between two glasses whose sizes are 20 cm-20 cm and 22 cm-20 cm. They were fixed by using clamps.

Acrylamide gel (8% v/v) was prepared with the ingredients as described in Table 4.3. After the addition of last ingredient, TEMED, the solution was immediately poured between the two glasses. Plastic combs were placed in the upper part of the gel. The gel was left at least half an hour for polymerization. The amplicons that were mixed with loading buffer was denatured at 95˚C for 5 min and kept on ice for 5 min more. The samples were loaded to the gel and were run in 0.5 X TBE buffer at 120V for 16 hours.

Table 4.3. Ingredients used for Polyacrylamide Gel Preparation.

Ingredients	**Volume**
29:1 acrylamide- N, N'-methlene-bis-acrylamide (30%)	16 mL
5 X TBE buffer	7.2 mL
10% APS	600 µl
TEMED	60 µl
dH_2O	36 mL

4.3.1.3. Silver Staining. DNA fragments that were fractionated on polyacrylamide gel were visualized with the help of silver staining method. The gel was incubated with solution 1 (Table 3.13) for 10-15 min. Thereafter, the gel was washed with dH_2O and incubated with solution 2 on shaker until the bands were visible. Finally, the gel was sealed in a transparent folder. If there were a shift in the migration pattern of any of the exons compared to that of control samples, the patient's DNA was amplified again and directly sequenced with both forward and reverse primers.

4.3.2. Mutation Analysis of CDS of *GJB1*, 5' UTR of *GJB1, GDAP1* and *SH3TC2* by using PCR-Direct Sequencing

Direct sequencing was an efficient method to detect variants in the genomic DNA if the PCR product was specific and strong enough. PCR was repeated when non-specific or weak bands were obtained on the gels either by changing the cycle conditions or concentrations of the chemicals.

4.3.2.1. Polymerase Chain Reaction (PCR). CDS of *GJB1*, 5'UTR of *GJB1*, six exons of *GDAP1* and 17 exons of *SH3TC2* were amplified by using the primers for which sequences and annealing temperatures are given in Tables 3.2-3.7.

PCR was performed in a total volume of 20 µl with chemical concentrations described in Table 4.4. Since *Titanium Taq* DNA Polymerase Buffer contains Mg^{+2}, additional Mg^{+2} was not added in PCR for 5'UTR of *GJB1*, six exons of *GDAP1* and 17 exons of *SH3TC2*. Betaine was used to reduce the secondary structures in GC-rich regions that are present in the 5'UTR of *GJB1*, exons 2-6 of *GDAP1*, exon 1, exon 6, exon 7, exon 10-11, and exon 17 of *SH3TC2*.

Table 4.4. Ingredients for PCR of CDS of *GJB1*, 5'UTR of *GJB1*, six exons of *GDAP1* and 17 exons of *SH3TC2*.

Ingredients	**Volume (µl)**
DNA (20ng)	1
10X *Titanium Taq* DNA polymerase buffer	2.5
dNTPs (0.1 mM)	0.2

Table 4.4. Ingredients for PCR of CDS of *GJB1*, 5'UTR of *GJB1*, six exons of *GDAP1* and 17 exons of *SH3TC2* (cont.).

Forward and Reverse Primers (10pmol/µl)	1 from each	
Titanium Taq DNA Polymerase (1 Unit)	0.1	
Betaine	-	7.35
dH_2O	14.7	7.35

Titanium Taq DNA polymerase was used to amplify all the amplicons except for the CDS of *GJB1* that was performed by *Taq* DNA polymerase. Conditions of PCR are given in Table 4.5. For all exons of *GDAP1* extension temperature was 68ºC whereas for all other amplicons it was 72ºC. Another exception was the 7 min of final extension of PCR for CDS of *GJB1* since *Taq* DNA polymerase was used for amplification. To check the size of amplicons and to ensure absence of non-specific bands, a mixture of 5 µl of PCR product and 1 µl of agarose loading buffer was loaded on 2% (w/v) agarose gel. DNA size marker was used to confirm the size of the amplicon.

Table 4.5. Conditions of PCR for CDS of *GJB1*, 5'UTR of *GJB1*, six exons of *GDAP1* and 17 exons of *SH3TC2*.

Conditions of PCR		
Initial denaturation		5 min at 95ºC
Denaturation	35 cycles	30 s at 95ºC
Annealing		30 s at annealing temperature
Extension		45 s at 72ºC
Final Extension		3 min at 72ºC
Cooling		1 min at 4ºC

4.3.2.2. Direct Sequencing. PCR products of CDS of *GJB1* were purified by using the High Pure PCR purification kit (Roche). Sequencing reaction was performed with amplified DNA diluted to a concentration of 6.5 ng/µl. The size of the amplicons was between 300-500 bp. The conditions for sequencing reactions are given in Table 4.6-4.7.

Table 4.6. Ingredients for sequencing PCR of CDS of *GJB1*.

Ingredients	**Volume (µl)**
Primer (10pmol/µl)	0.5
DNA	1
Master Mix	4
High Pure H_2O	4.5

Table 4.7. Conditions for sequencing PCR of CDS of *GJB1*.

Conditions of PCR	
30 cycles	20 s at 96°C
	20 s at 50°C
	4 min at 60°C
cooling	1 min at 4°C

The sequencing products of coding sequence of *GJB1* were precipitated with ethanol. For this purpose, after addition of 5 µl of stop solution (2 µl 3M Na-acetate, 2 µl 100mM Na-EDTA, 1 µl of glycogen) 60 µl ice-cold 95% EtOH was added to all samples and mixed. Samples were centrifuged for 15 min at 14000 rpm at 4°C. After removal of the supernatant, samples were rinsed twice with ice-cold 200 µl 70% EtOH by centrifugation for 4 min at 14000 rpm. Ethanol was discarded carefully to prevent loss of the pellet. The pellet was completely dried by using SpeedVac SPD111V (Thermo Scientific, USA) until it becomes transparent (approximately 2 min). The samples were re-suspended in 40 µl sample loading solution. Finally, automated sequencing was performed for coding sequence of *GJB1* with GeXP genetic analysis system (Beckman Coulter, USA) in our department DNA core facility.

Purification of PCR products, sequencing reaction and automated sequencing for 5'UTR of *GJB1* and coding sequences of *SH3TC2* and *GDAP1* was performed by core facility of University of Antwerp using GeXP genetic analysis system (Beckman Coulter, USA). The outcomes of sequencing reactions were analyzed and aligned using Clustal X or SeqMan software (DNASTAR) and the NCBI genome browser.

4.4. Exome Sequencing

In this study, two families, namely, P158 and P444 were exome sequenced. The clinical data for the probands are given in Table 4.8. DNA samples were diluted to 80 ng/µl in a total volume of 50 µl for exome sequencing. The sequencing was performed by Axeq technologies (Axeq Technologies, Australia). Illumina Exome Enrichment protocol was followed for the enrichment of the target regions. The captured libraries were sequenced using Illumina HiSeq 2000 Sequencer. The target region size was over 62Mb that corresponds to almost 21000 genes. It covers 95% of the genes that were listed in CCDS database. About 81.5% of target region was sequenced/covered for more than 10 times.

Table 4.8. Clinical data for the probands.

	Affected Members	**Severity**		**Age of onset**	**Median motor NCV**	**Additional features**
		Mobility	**Upper limbs**			
P158	3 brothers, mother and mother's father	Abnormal	Normal	1st decade	31 m/s	Pes cavus Sensory ataxia
P444	2 siblings, mother, mother's 3 siblings and mother's mother	Abnormal	Distal weakness	1st decade	50 m/s	NA*

*Not Available

4.5. Whole Genome Linkage Analysis

For the eight members of family P444, whole genome linkage analysis was performed using the core facility of University of Antwerp. DNA samples were diluted to 20 ng/µl in a final volume 10 µl. Home-made MMP_10 panel was used that includes 436 STR markers chosen from all chromosomes (Appendix D). Distance between STR markers is roughly equally spread within each chromosome. However, average distance between markers differs from chromosome to chromosome (Table 4.9). Forward primers of STR

markers were FAM or HEX labeled. For size fractionation, GeneScan LIZ 600 size standard were used.

Table 4.9. Distance between STR markers in MMP_10 panel.

Chromosome	**Number of STR markers**	**Average distance between STR markers**	**Standard Deviation**
1	32	9.01	3.25
2	32	8.15	2.64
3	27	8.25	2.74
4	27	7.51	2.84
5	24	8.14	2.51
6	24	7.87	2.41
7	26	7.06	2.45
8	23	6.86	2.62
9	19	8.32	2.76
10	22	7.79	2.71
11	18	8.18	2.93
12	23	7.21	2.05
13	13	8.32	2.78
14	18	7.52	2.63
15	16	7.10	2.81
16	17	7.59	2.65
17	15	7.58	2.27
18	14	8.79	2.81
19	12	8.23	3.43
20	10	10.20	4.37
21	4	9.82	4.64
22	6	11.09	8.86
X	16	7.15	3.75

Integrative Genomics Viewer (IGV) software was used to determine the length of the amplicons for all STR markers. After determining the length of the amplicons, two-point LOD score analysis was performed by using EasyLinkage software. By using the Two-Point Pedigree Simulation Analysis of FastSLink v2.51, the power of family was calculated and STR markers that gave LOD score values higher than 1.0 were chosen with their adjacent markers to construct haplotypes.

4.6. X chromosome Linkage Analysis

Four families (P232, P381, P408, P636) whose clinical data are given in Table 4.10 were analyzed by X chromosome linkage analysis. The families were selected based on pedigree analysis and evaluation of their clinical data.

Table 4.10. Clinical data for the probands.

	Affected Members	**Severity**		**Age of onset**	**Median NCVs**	**Additional Features**
		Mobility	**Upper limbs**			
P232	2 siblings and mother	Normal	Normal	2nd decade	27.8 m/s	Pes cavus Tremor
P381	2 brothers	Confined to wheelchair	NA	NA	NA	NA
P408	2 brothers	Normal	Distal weakness	3rd decade	25 m/s	Pes cavus Tremor Deafness Bilateral cataract Cerebellar dysfunction
P636	2 brothers	NA	NA	1st decade	NA	NA

*Not available

In total, 30 STR markers were used for X chromosome linkage analysis. Sixteen STR markers that were already designed by core facility of University of Antwerp were used for the analysis (Appendix E). Multiplex PCR was performed for an additional 14 X-linked

STR markers using the primers that are given in Table 3.8. For each plex, primer mix was prepared by adding of 1.5 µl of each stock primer to a total volume of 500 µl water. Conditions for multiplex PCR are given in Table 4.11. For size fractionation, GeneScan LIZ 600 size standard was used. Integrative Genomics Viewer (IGV) software was used to determine the length of the amplicons for all STR markers. After determining the length of the amplicons, two-point LOD score analysis was performed by using EasyLinkage software. The STR markers have been selected to encompass the whole length of the chromosome with a similar distance between the markers. The average and standard deviation of the distance between STR markers are 3.39 and 2.05 cM, respectively.

Table 4.11. Ingredients and conditions for multiplex PCR.

<table>
<tr><th>Ingredients</th><th>Volume (µl)</th><th colspan="2">Conditions of PCR</th></tr>
<tr><td>DNA (20 ng/µl)</td><td>2</td><td>Initial denaturation</td><td>10 min at 98°C</td></tr>
<tr><td>Primer Mix</td><td>3</td><td rowspan="3">Denaturation
Annealing
Extension
} 23cycles</td><td rowspan="3">45 sec at 98°C
45 sec at 60°C
2 min at 68°C</td></tr>
<tr><td>10X Titanium Taq DNA polymerase buffer</td><td>1.5</td></tr>
<tr><td>dNTPs (0.1 mM)</td><td>0.375</td></tr>
<tr><td>Titanium Taq DNA polymerase (1 unit)</td><td>0.075</td><td rowspan="2">Final Extension</td><td rowspan="2">10 min 72°C</td></tr>
<tr><td>dH_2O</td><td>8.05</td></tr>
</table>

5. RESULTS

In this study, to understand the molecular genetic basis of CMT disease, three genetic approaches were used: mutation screening, exome sequencing and linkage analysis.

5.1. Mutation Analysis

All patients that were screened for mutations in this study were previously found to be negative for *PMP22* deletion/duplication. Mutations in two of the genes, namely *GJB1* and *PRPS1*, segregate as X-linked whereas *GDAP1* and *SH3TC2* mutations segregate as autosomal recessive traits. Detailed pedigree and clinical examination were performed before the analysis such that the patients that were screened for *GJB1* and *PRPS1* did not show male to male transmission and females in the family were either mildly affected or not affected at all. The patients that were screened for mutations in *PRPS1* were previously found to be negative for mutations in *GJB1* in our laboratory.

The patients that were screened for mutations in *GDAP1* and *SH3TC2* showed recessive segregation in their pedigrees. Parents were consanguineous and there were more than one affected sibling in these families. Electrophysiological findings were also considered and patients with NCV values below 38 m/s, suggesting demyelination were screened for mutations in *SH3TC2*. Since *GDAP1* recessive mutations may cause either axonal degeneration or demyelination, NCV values were not considered during patient selection for this gene.

For the variations' nomenclature, Human Genome Variation Society website was used as a reference (den Dunnen and Antonarakis, 2000). Adenine (A) in the ATG translation initiation site was designated as +1. The novelty of the identified mutations was checked using inherited peripheral neuropathies mutation database.

5.1.1. Mutation Analysis of CDS and 5'UTR of *GJB1*

Mutation analysis of coding sequences (CDS) and 5'UTR of *GJB1* were performed using PCR and subsequent direct sequencing techniques. Eleven patients were screened for mutations in the coding sequence of *GJB1* and two patients were found to have mutations.

The first variation was identified in two siblings, P824-1 (female) and P824-2 (male). The c.614A>G mutation leads to N205S change at amino acid level and was previously reported by Bone *et al.* in 1997. The affected sister was heterozygous and the brother was hemizygous for the mutation (Figure 5.1).

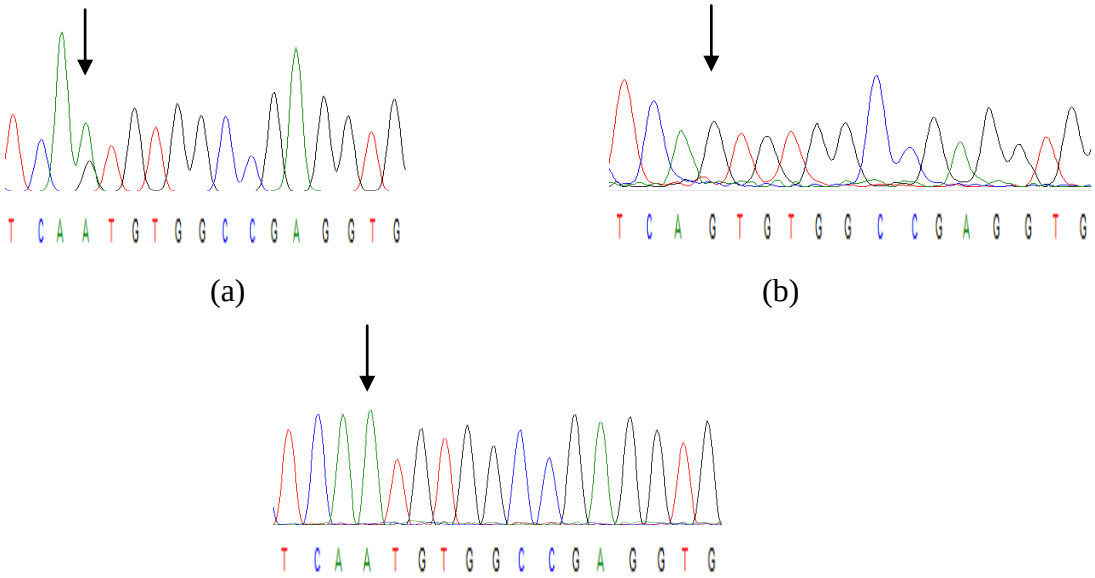

Figure 5.1. (a) Chromatograms showing the heterozygous c.614A>G change for the female patient (P824-1) (b) the hemizygous c.614A>G change for the male patient (P824-2) and (c) the sequence for the male control.

Second variant in the CDS of *GJB1* was observed in a male patient (P788). Patient was hemizygous for the c.204C>A variation that leads to F68L alteration at amino acid level (Figure 5.2). This variation is not found in dbSNP, 1000genome and NHLBI Exome Sequencing Project databases. Phenylalanine is highly conserved at that position among mammalian species (Figure 5.3). Therefore, this variation can be designated as a novel mutation.

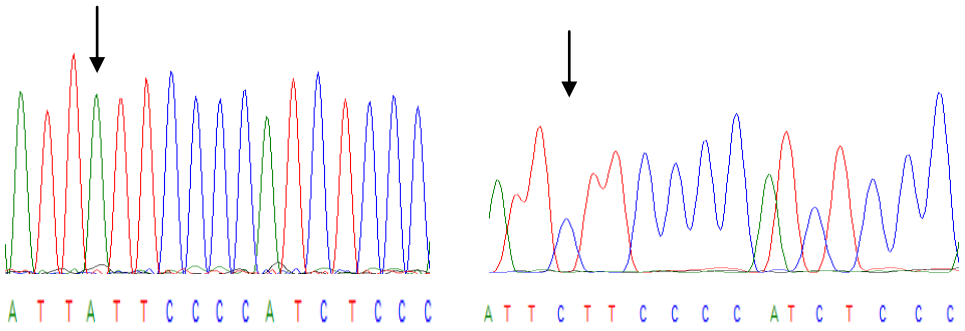

(a) (b)

Figure 5.2. (a) Chromatograms showing the hemizygous c.204C→A change for the male patient (P788) and (b) the sequence for the male control.

Macaca mulatta	CNTLQPGCNSVCYDQ**F**FPISHVRLWSLQ
Bos taurus	CNTLQPGCNSVCYDH**F**FPISHVRLWSLQ
Pan troglodytes	CNTLQPGCNSVCYDQ**F**FPISHVRLWSLQ
Mus musculus	CNTLQPGCNSVCYDH**F**FPISHVRLWSLQ
Rattus norvegicus	CNTLQPGCNSVCYDH**F**FPISHVRLWSLQ
Homo sapiens	CNTLQPGCNSVCYDQ**F**FPISHVRLWSLQ
P232	CNTLQPGCNSVCYDQ**L**FPISHVRLWSLQ

Figure 5.3. Conservation of phenylalanine at the position 68 among mammalian species, marked by black box.

For 5'UTR of *GJB1*, 15 patients were screened for mutations and three variants were found at the promoter region of transcript variant 2 that is a nerve specific transcript.

First variant c.-541 A>G, a novel variation, was found in a male patient (P232) (Figure 5.4). It was not reported in dbSNP, 1000genome database and NHLBI Exome Sequencing Project database. 95 Turkish and 92 non-Turkish unaffected individuals were sequenced but this variation was not observed in any of the controls. This nucleotide is highly conserved among mammalian species (Figure 5.5).

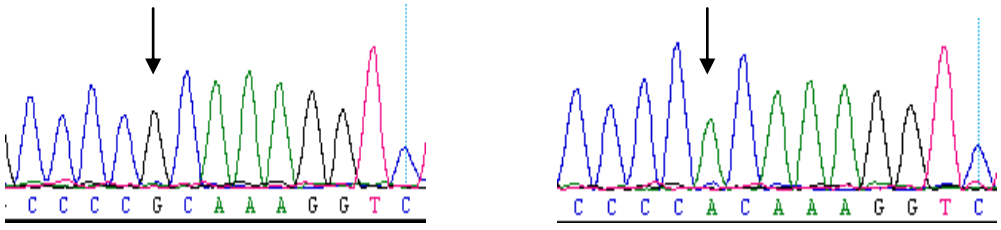

(a) (b)

Figure 5.4. (a) Chromatogram showing the hemizygous c.-541 A>G change for the male patient (P232) (b) Chromatogram for male control.

Macaca mulatta	AGAGCCCC**A**CAAAGGTCTCATTGTGCAG
Bos taurus	AGAGCCCC**A**CAAAGGTCCCATTGTGCAG
Canis lupus	AGAGCTCC**A**CAAAGGTCCCATTGTGCAG
Mus musculus	AGCGCCCC**A**CAAAGGTCCCATTGTACAG
Rattus norvegicus	AGCGCCCC**A**CAAAGGTCCCATTGTACAG
Homo sapiens	AGAGCCCC**A**CAAAGGTCTCATTGTGCAG
P232	AGAGCCCC**G**CAAAGGTCTCATTGTGCAG

Figure 5.5. Conservation of the nucleotide at position -541 among mammalian species, which is shown in black box.

Second variant for 5'UTR of *GJB1* was c.-528T>C; this novel variant was found in three affected members (P727.1-P727.2 and P727.3) of the family P727 (Figure 5.6). It was not present in dbSNP, 1000genome and NHLBI Exome Sequencing Project databases. It was also absent in 95 Turkish and 92 non-Turkish controls that were analysed by direct sequencing. This nucleotide is highly conserved among mammalian species (Figure 5.7).

The last variation c.-6G>A was observed in a male patient (P304) (Figure 5.8) and three further affected individuals in the same family were found to carry this allele. The variation was absent in 94 Turkish and 92 non-Turkish controls and also in dbSNP and 1000genome database, however it was reported as a polymorphism in NHLBI Exome Sequencing Project database.

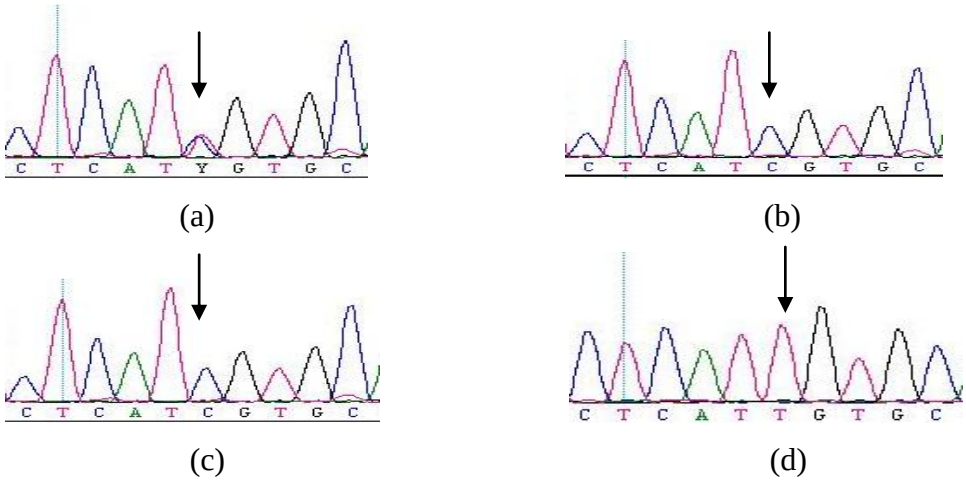

Figure 5.6. (a) Chromatogram showing the heterozygous change for the female patient P727-1 (b) and (c) Chromatograms showing the hemizygous change for the male patients P727-2 and P727-3 (d) Chromatogram for unaffected female in the same family (P727).

Macaca mulatta	AGAGCCCCACAAAGGTCTCATTGTGCAG
Bos taurus	AGAGCCCCACAAAGGTCCCATTGTGCAG
Canis lupus	AGAGCTCCACAAAGGTCCCATTGTGCAG
Mus musculus	AGCGCCCCACAAAGGTCCCATTGTACAG
Rattus norvegicus	AGCGCCCCACAAAGGTCCCATTGTACAG
Homo sapiens	AGAGCCCCACAAAGGTCTCATTGTGCAG
P727	AGAGCCCCACAAAGGTCTCATCGTGCAG

Figure 5.7. Conservation of the nucleotide at position -528 (shown in black box) among mammalian species.

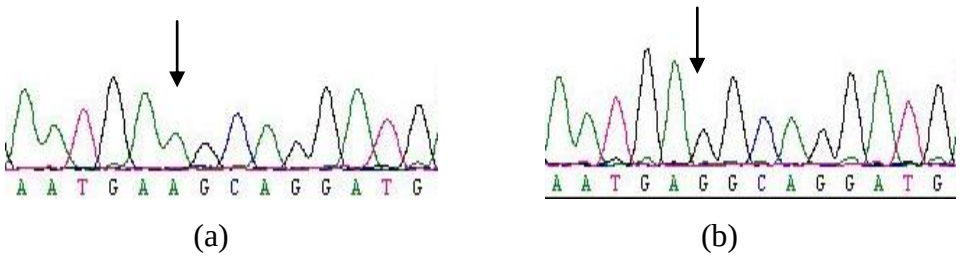

Figure 5.8. (a) Chromatogram showing the hemizygous c.-6G>A change for the male patient (P304) (b) Chromatogram for male control.

5.1.2. Mutation Analysis of *PRPS1*

Mutation analysis of CDS of *PRPS1* was performed by using PCR-SSCP technique. Thirteen patients that were previously found to be negative for mutations in *GJB1* were screened for mutations in *PRPS1*. Single strand conformation changes were not observed in any seven exons of this gene. SSCP results for exon 1, exon 6, and exon 7 of *PRPS1* were given in Figure 5.9.

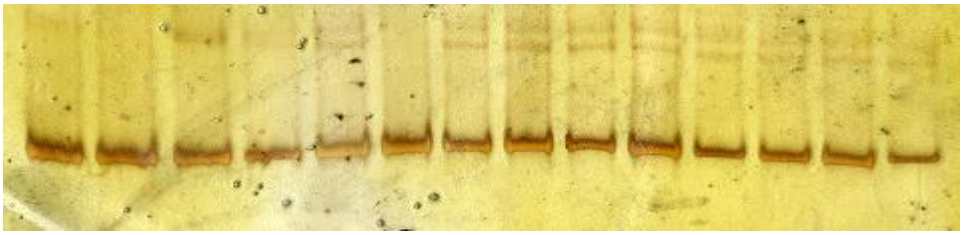

(a)

(b)

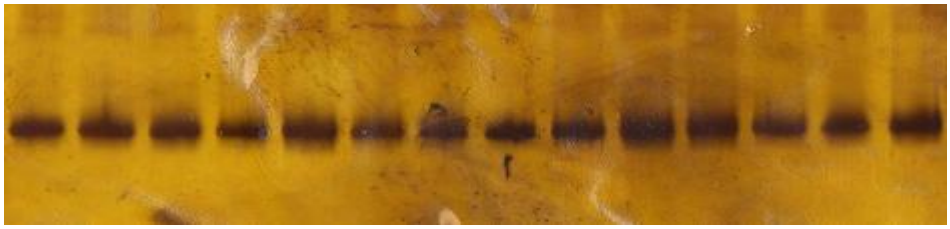

(c)

Figure 5.9. SSCP gels (8%) for (a) exon 1 (b) exon 6 (c) exon7 of *PRPS1*.

5.1.3. Mutation Analysis of *GDAP1*

Mutation analysis of *GDAP1* CDS was performed by using PCR-direct sequencing technique in 18 Turkish CMT patients.

A homozygous nonsense variation was observed in two sisters in family P950. The novel variation was c.112C>T that leads to Q38X change at amino acid level and hypothetically results in truncated protein translation. Parents were unaffected and heterozygous as expected and the unaffected sibling was homozygous for wild type allele (Figure 5.10). The variation was not observed in dbSNP, 1000genome database and NHLBI Exome Sequencing Project database.

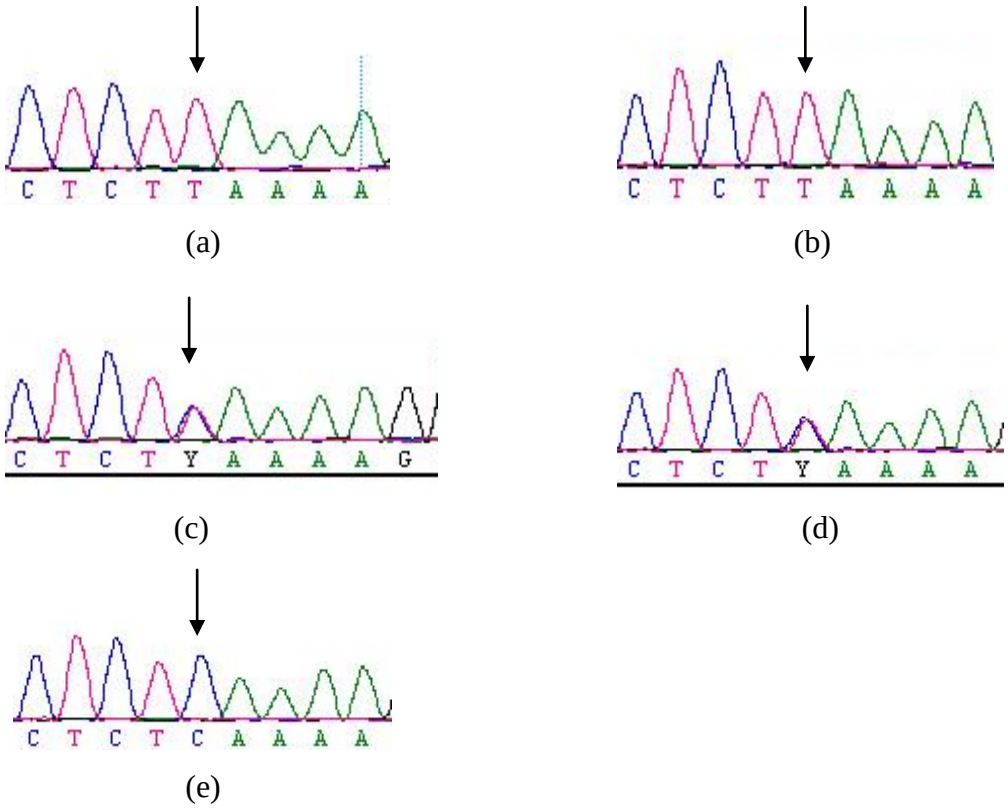

Figure 5.10. (a) and (b) Chromatograms showing the homozygous change for the affected sisters of family P950 (c) and (d) Chromatograms showing the heterozygosity for unaffected parents (e) Chromatogram for unaffected sister.

5.1.4. Mutation Analysis of *SH3TC2*

Mutation analysis of CDS of *SH3TC2* was performed by using PCR-direct sequencing technique in 12 Turkish CMT patients.

A homozygous nonsense variation c.2860C>T that leads to R954X probably results in production of a truncated protein. It was identified in two affected siblings of the family

P909. As expected, unaffected parents were heterozygous for this allele (Figure 5.11). This homozygous variation was reported by Azzedine *et al.* (2006).

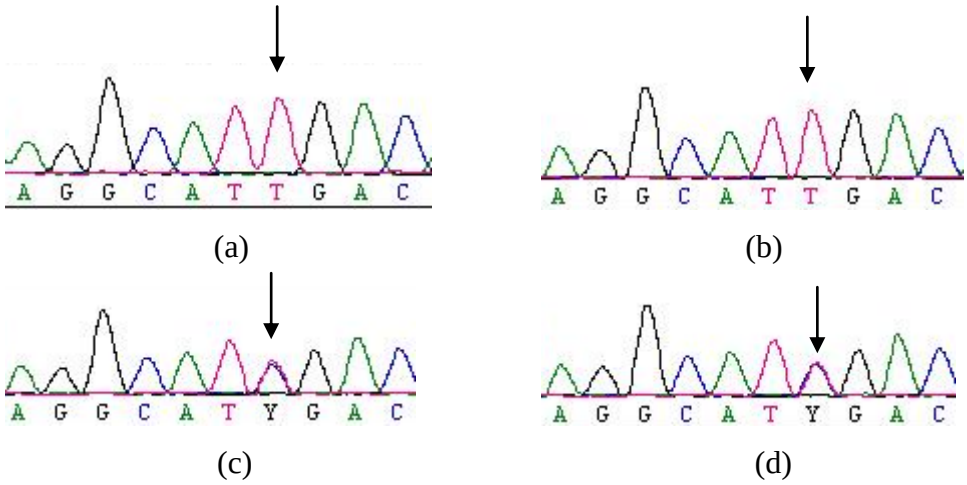

Figure 5.11. (a) and (b) Chromatograms showing the homozygous change for the affected sisters of family P909 (c) Chromatogram showing the heterozygosity for unaffected mother (d) Chromatogram showing the heterozygosity for unaffected father.

5.2. Exome Sequencing

Three individuals from each of the two families (P158 and P444) were exome sequenced. Among these three selected individuals two of them were affected and one of them was unaffected. The raw data was processed by the company (Axeq Technologies) using their pipeline for sequencing, alignment and variant analysis that yields a spreadsheet file, which includes all found variations. Most of the SNPs were previously reported in databases but still some were novel. As a first step for the analysis of this spreadsheet file, known causative CMT genes were checked for variations in splice sites, exons and 5'UTRs. Nonsynonymous and nonsense changes, frameshift insertions and deletions that were present in both patients but absent in the healthy control in the family were selected. The analysis was done through filtration of the processed data by the following categories: dbSNP (the variations found in this database were eliminated), presence of variation in affected and absence in unaffected member, heterozygous/homozygous state, region (3'UTR, non-coding RNA, intronic regions were discarded), ratio of alternative depth to total depth. Those with a ratio below 0.2 were eliminated.

The affected members of the family P158 (Figure 5.12) showed a variation at splice site of *GJB1* located on the X-chromosome.

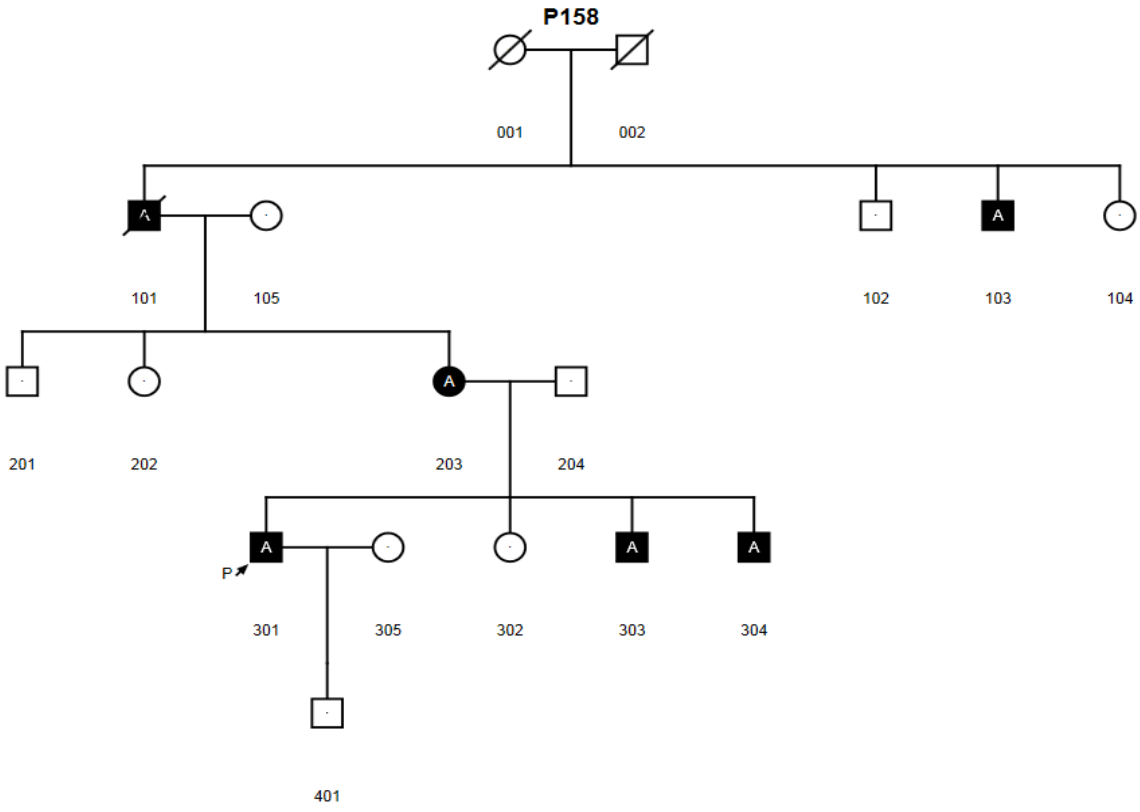

Figure 5.12 Pedigree of the family P158. Squares and circles represent males and females respectively. Black filled boxes with 'A' show affected individuals. 'P' indicates the proband.

The variation was c.-18A>G change that corresponds to the second last base of the intron 1 of *GJB1*. As expected the female patient (203) was heterozygous for the variation. The details regarding this mutation can be found in Table 5.1. It was found in affected individuals in the family but was not observed in the unaffected individual. This variation was predicted by online splice site predictor program (Desmet *et al.*, 2009) to affect splicing by abolishing binding of SRp40 protein (Figure 5.13). For exome sequencing analysis, depth of coverage is a very important indicator that shows the number of reads for that nucleotide. The depths of coverage for alternative reads were six and three for the affected male (103) and female individuals, respectively, for this nucleotide. The region was directly sequenced to confirm the variation and its inheritance using primers listed in

Table 3.10. Three additional affected members of the family were also sequenced directly. Same variation was observed in these patients (Figure 5.14). This variation was not observed in dbSNP, 1000genome database and NHLBI Exome Sequencing Project database. 95 Turkish and 92 non-Turkish controls were screened for this nucleotide and the variation was not observed. Among close mammalian species this nucleotide is highly conserved (Figure 5.15).

Table 5.1. Exome sequencing results for two affected members of family P158.

Patient #	**Chr. name**	**Chr.start**	**Chr.end**	**Ref. base**	**Alt. base**	**Hom./het. status**
103	X	70443540	70443540	A	G	Hom.
203	X	70443540	70443540	A	G	Hom.
Patient #	**Total depth**	**Alt. depth**	**dbSNP**		**region**	**Gene**
103	6	6	Not found		splicing	*GJB1*
203	3	3	Not found		splicing	*GJB1*

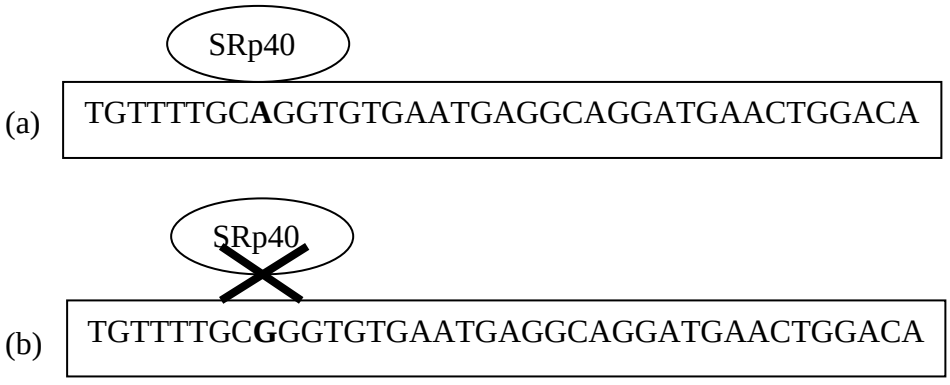

Figure 5.13. (a) Binding of SRp40 protein to splice site of *GJB1* in unaffected individual (b) Binding of SRp40 protein is completely abolished in affected individual according to online splice site predictor program (Desmet *et al.*, 2009). Position -18 is shown in bold.

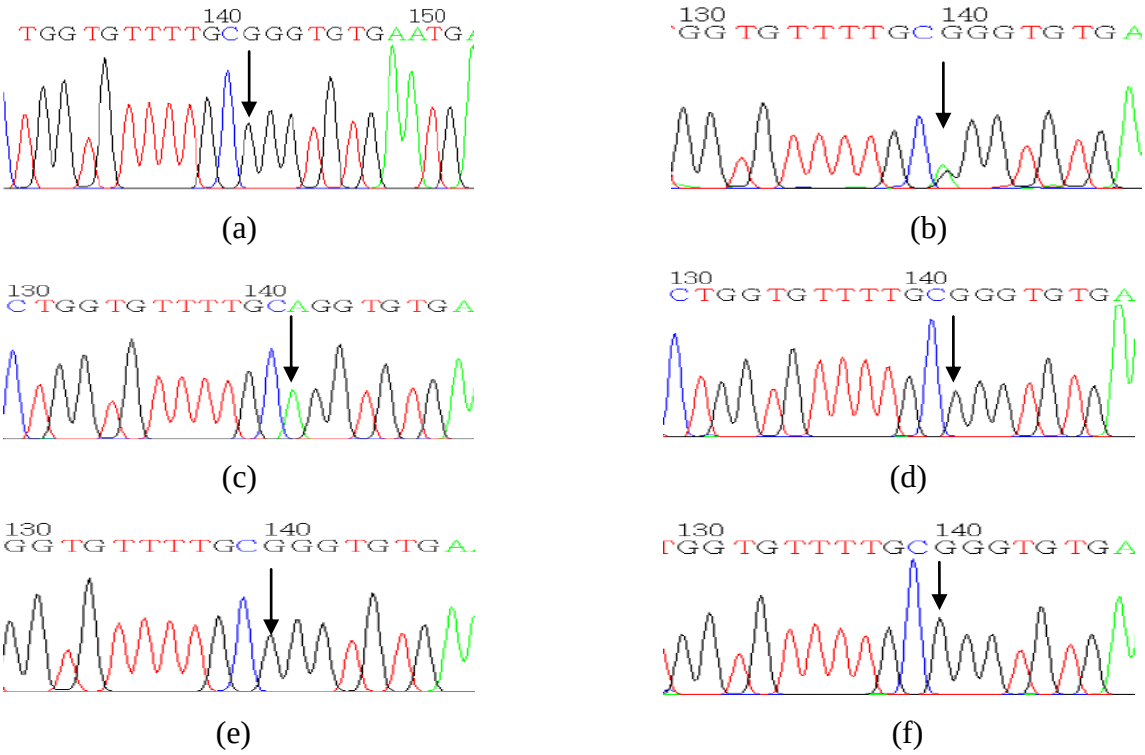

Figure 5.14. (a) and (b) Chromatograms showing that hemizygous and heterozygous change for male, 103, and female patient, 203, (exome sequenced) respectively (c) Chromatogram showing the sequence for unaffected male 204 (exome sequenced) (d) (e) and (f) Chromatograms showing the hemizygous change for other male patients (301, 303 and 304) respectively.

Bos taurus	TTTTGC**A**GGTGTGAATGAGGCAGGATG
Canis lupus	TTTTGC**A**GGTGTGAATGAGGCAGGATG
Macaca mulatta	TTTTGC**A**GGTGTGAATGAGGCAGGATG
Mus musculus	TTTCAC**A**GGTGTGAATGAGGCAGGATG
Pan troglodytes	TTTTGC**A**GGTGTGAATGAGGCAGGATG
Rattus norvegicus	TTTCCC**A**GGTGTGAATGAGGCAGGATG
Homo sapiens	TTTTGC**A**GGTGTGAATGAGGCAGGATG
P158	TTTTGC**G**GGTGTGAATGAGGCAGGATG

Figure 5.15. Conservation of the nucleotide at position -18 among species. Position -18 is shown in black box and +1 is shown in red box.

For the family 444, exome sequencing did not yield any meaningful results by itself. Since the family pedigree shows that the inheritance of the disease is dominant, only heterozygous variants were selected during filtration of the processed data. All known causative genes were checked and no published or novel mutation was identified. In order to delineate the region that bears the mutation causing the disease, whole genome linkage analysis was performed. Combination of whole genome linkage and the exome sequencing analyses is a very effective way in finding the causative gene.

5.3. Whole Genome Linkage Analysis

In addition to exome sequencing, whole genome linkage analysis was performed to identify the causative gene for family P444. Genomic DNA samples from four affected and four unaffected members of the family were used for the linkage analysis. It was performed using 436 highly polymorphic STR markers covering all chromosomes. Two point LOD scores were calculated using SuperLink v1.6 program of Easy Linkage v5.02 software. The markers that yield a LOD score value higher than 1 was used for the haplotype analysis. The limit for choosing the markers for haplotype analysis was selected as 1.0 since maximum LOD score (power of the family) was around 1.9 for the family. Result of the two point LOD score analysis for the family P444 was given in Figure 5.16.

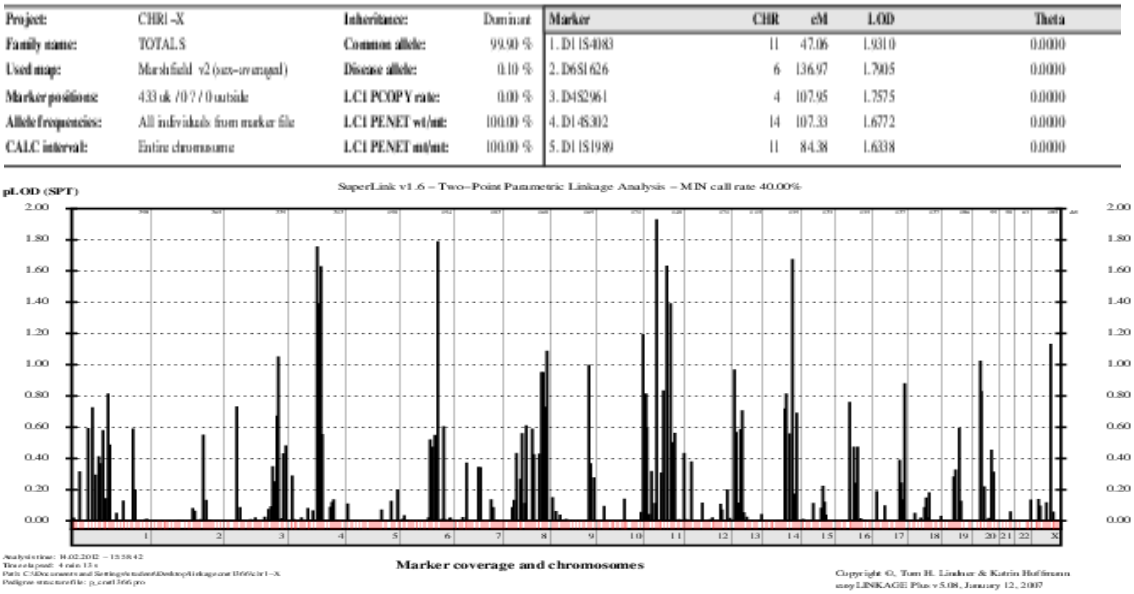

Figure 5.16. Two point LOD score results of whole genome linkage analysis for family P444.

Thirteen markers on nine chromosomes gave a LOD score higher than 1.0 (Table 5.2). The highest LOD score was 1.93 for marker D11S4083 on chromosome 11. Two further STR markers gave LOD scores around 1.6 and 1.4 on chromosome 11.

Table 5.2. STR markers that gave LOD scores higher than 1.0.

Chromosome	**Name of the STR marker**	**LOD score**
3	D3S3583	1.05
4	D4S2961	1.76
4	D4S1611	1.63
4	D4S3240	1.39
6	D6S1626	1.79
8	D8S1837	1.09
10	D10S1651	1.20
11	D11S4083	1.93
11	D11S1989	1.63
11	D11S1394	1.39
14	D14S302	1.68
20	D20S163	1.03
X	DXS1210	1.13

Three of these loci on chromosomes 3, 8 and X were excluded since they were shared by affected and unaffected members of the family (haplotypes are given on Appendix A). By the help of recombinations and considering the regions shared with affected and unaffected individuals, the regions on chromosome 4, 6, 10, 11, 14 and 20 were delineated and seven loci on these chromosomes that segregated with the disease were determined. In order to identify the candidate genes, exome sequencing data was examined for these seven loci. The data revealed nonsynonymous exonic change, splice site or 5'UTR variations for four loci, which are found on chromosomes 11, 14 and 20.

Using Matlab, a simple program (ExomeSequencer) was written in order to delineate the candidate genes from exome sequencing data of two patients and one control from the same family. The program computes a matrix from processed exome sequencing data (spreadsheets) and produces a spreadsheet file in the same format, listing common

variations among patients that are not found in the control according to the input pattern of segregation (dominant or recessive). The program also computes the size of the region shared by the two patients similar to the haplotype analysis using polymorphic markers though in a simple way. The program also marks the variation in genes that are overexpressed in nervous tissue. In order to increase the accuracy and limit the false positives, the program includes settings regarding the number of minimum reads and the ratio of alternative reads to total reads.

Exome sequencing data did not reveal any novel nonsynonymous, nonsense, frameshift insertions and deletions on exons, and variants on splice site or 5'UTR for the following loci, which are delineated after haplotype analysis:

- The locus (between the markers D4S2393 and D4S2395) on chromosome 4 was around 48Mb (Figure 5.17).

- The locus (between the markers GATA28G05 and D6S383) on chromosome 6 was around 18Mb (Figure 5.18).

- The locus (between GGAT14G01 marker and telomere) on chromosome 10 was around 5Mb (Figure 5.19).

For the Figures 5.17-5.22 and 5.28;

Squares and circles represent males and females respectively. Black filled boxes with 'A' show affected individuals. 'P' indicates the proband. Double line shows the consanguineous marriage. Different colored bars indicate different haplotypes. Numbers represent the length of the amplicons that include STRs. Yellow bars show the segregation of disease phenotype. The order of the STR markers used in haplotype analysis is given on the box. STR markers in bold had yielded the LOD scores higher than 1.0.

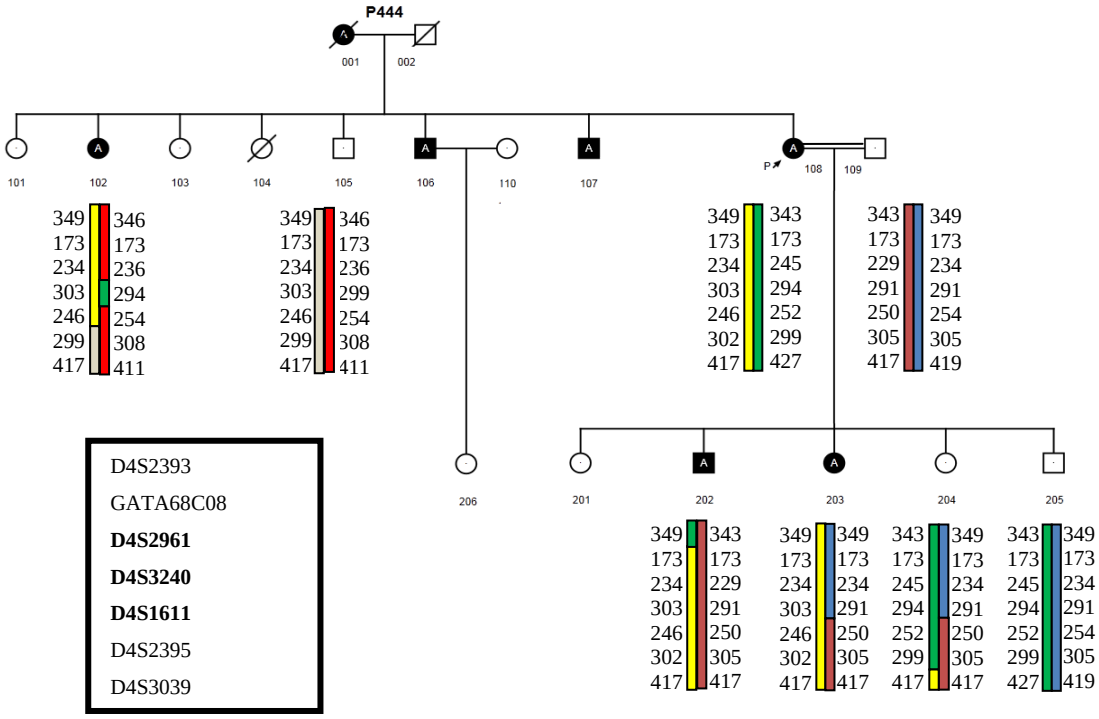

Figure 5.17. Haplotype analysis for family P444 for the locus on chromosome 4.

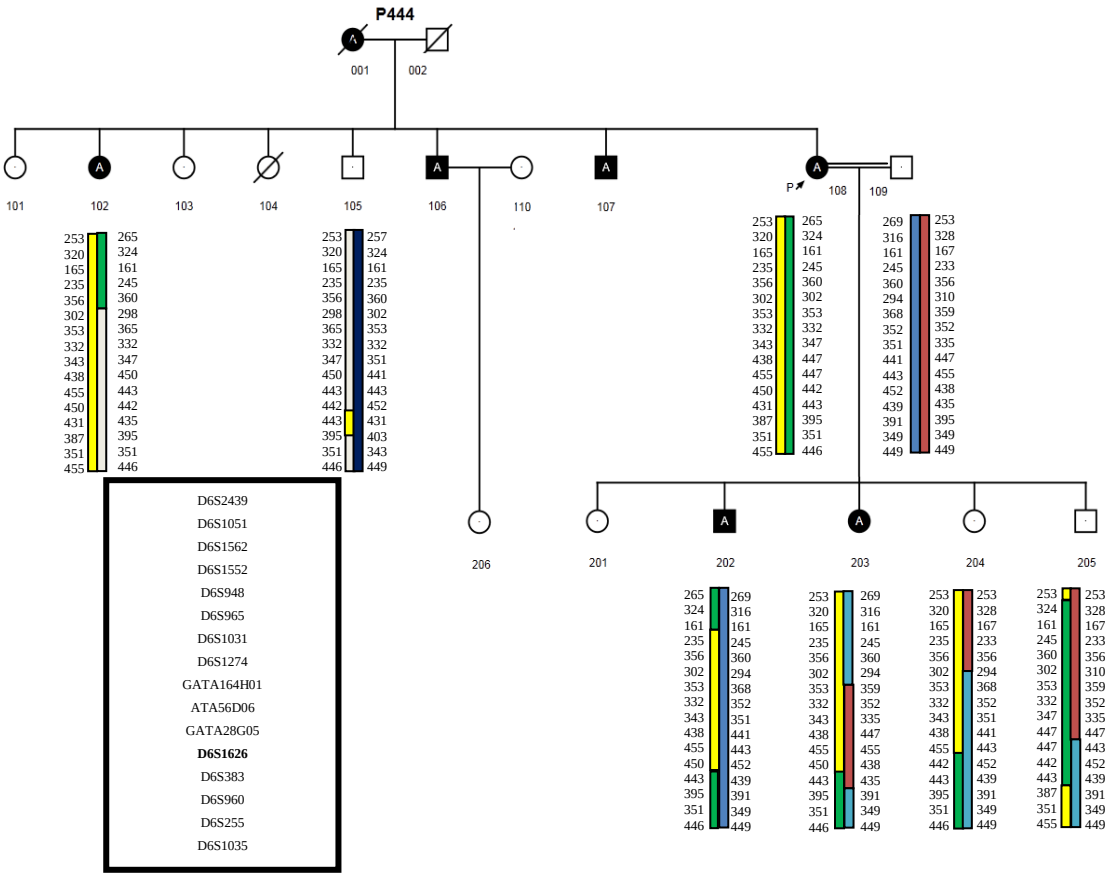

Figure 5.18. Haplotype analysis for family P444 for the locus on chromosome 6.

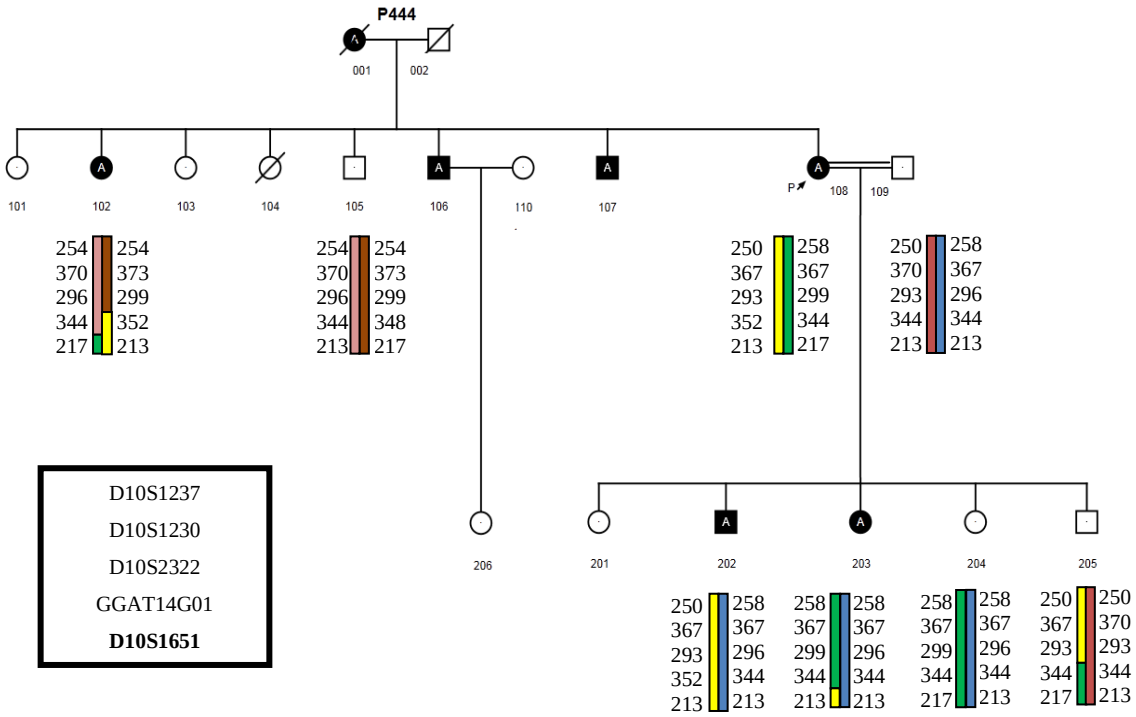

Figure 5.19. Haplotype analysis for family P444 for the locus on chromosome 10.

For the loci on chromosomes 11, 14 and 20 that were delineated, exome sequencing data yield some novel variants. The regions and variants are given below:

- Two loci identified on chromosome 11 were between the markers D11S2014-D11S2006 and D11S4139-D11S897 (Figure 5.20). The size of the regions was around 56Mb in total.

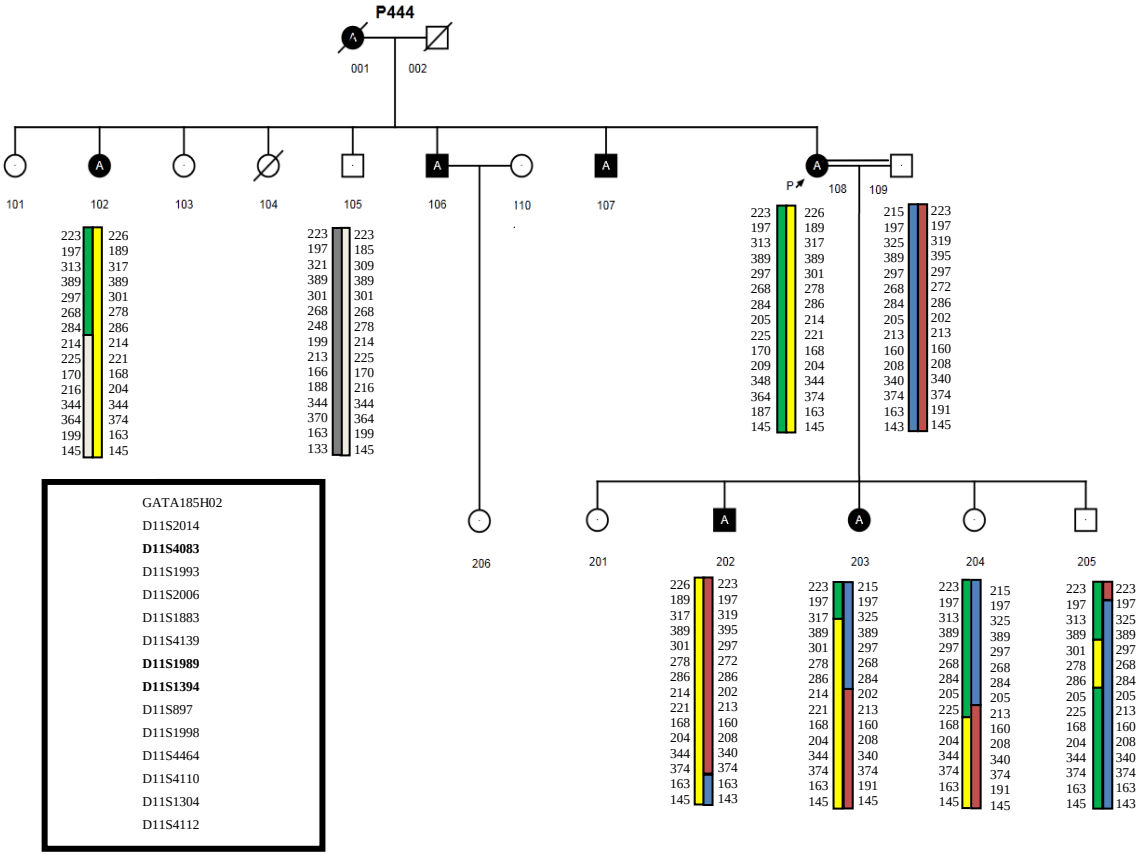

Figure 5.20. Haplotype analysis for family P444 for the locus on chromosome 11.

The 56Mb region on chromosome 11 that was delineated after haplotype analysis showed four nonsynonymous novel exonic variants in exome sequencing data that are given in Table 5.3.

Table 5.3. Variants identified by exome sequencing on chromosome 11 for two affected members of family P444.

Gene	Exon #	Nucleotide change	Amino acid change
BTBD18	Exon 3	c.827C>T	p.T276I
MYO7A	Exon 33	c.4360G>A	p.V1454I
ARAP1	Exon 11	c.1423C>G	p.H475D
SLC35F2	Exon 7	c.797T>C	p.V266A

- The region identified on chromosome 14 was around 30Mb. The delineated locus was between the markers D14S125-D14S611 (Figure 5.21).

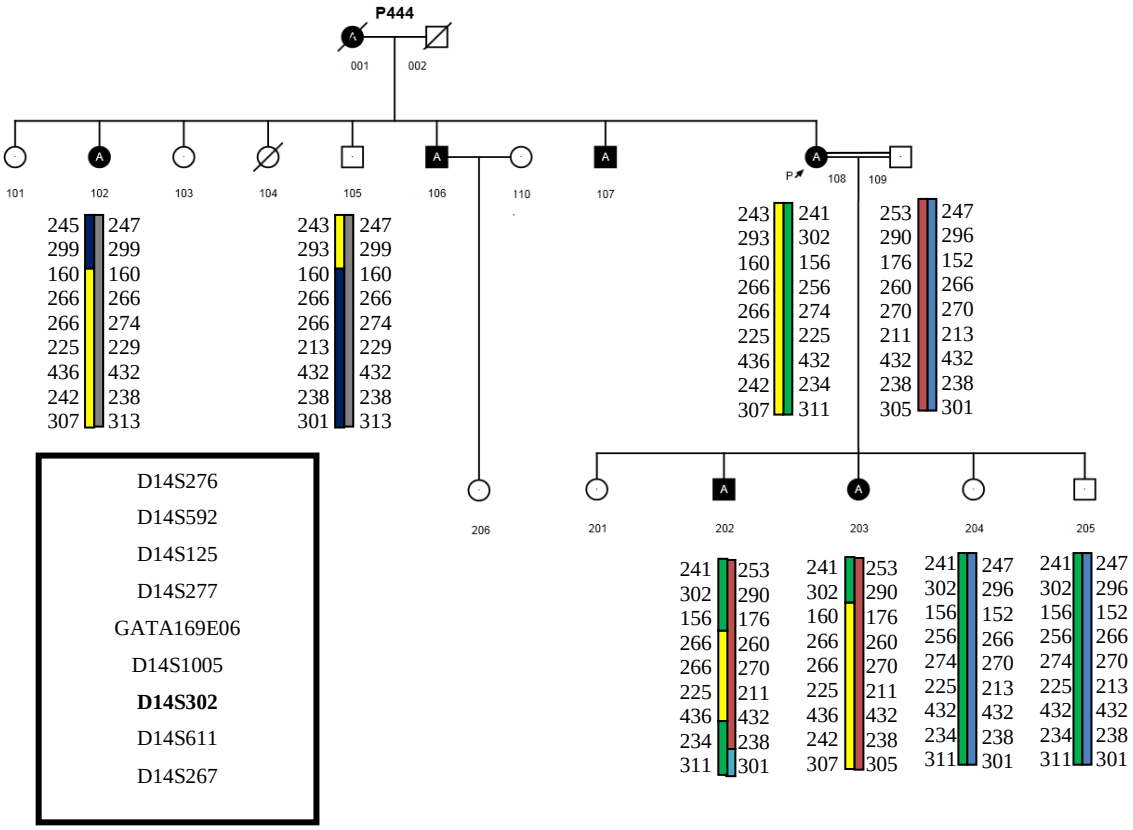

Figure 5.21. Haplotype analysis for family P444 for the locus on chromosome 14.

In exome sequencing data, a novel nonsynonymous exonic variation was identified for the 30Mb region on chromosome 14 that was delineated after haplotype analysis (Table 5.4).

Table 5.4. Variant identified after exome sequencing on chromosome 14 for two affected members of family P444.

Gene	Exon #	Nucleotide change	Amino acid change
SERPINA3	Exon 3	c.787G>T	p.V263L

- The region delineated on chromosome 20 was between the markers GATA72E1-GATA141H08 (Figure 5.22). The locus was around 30Mb.

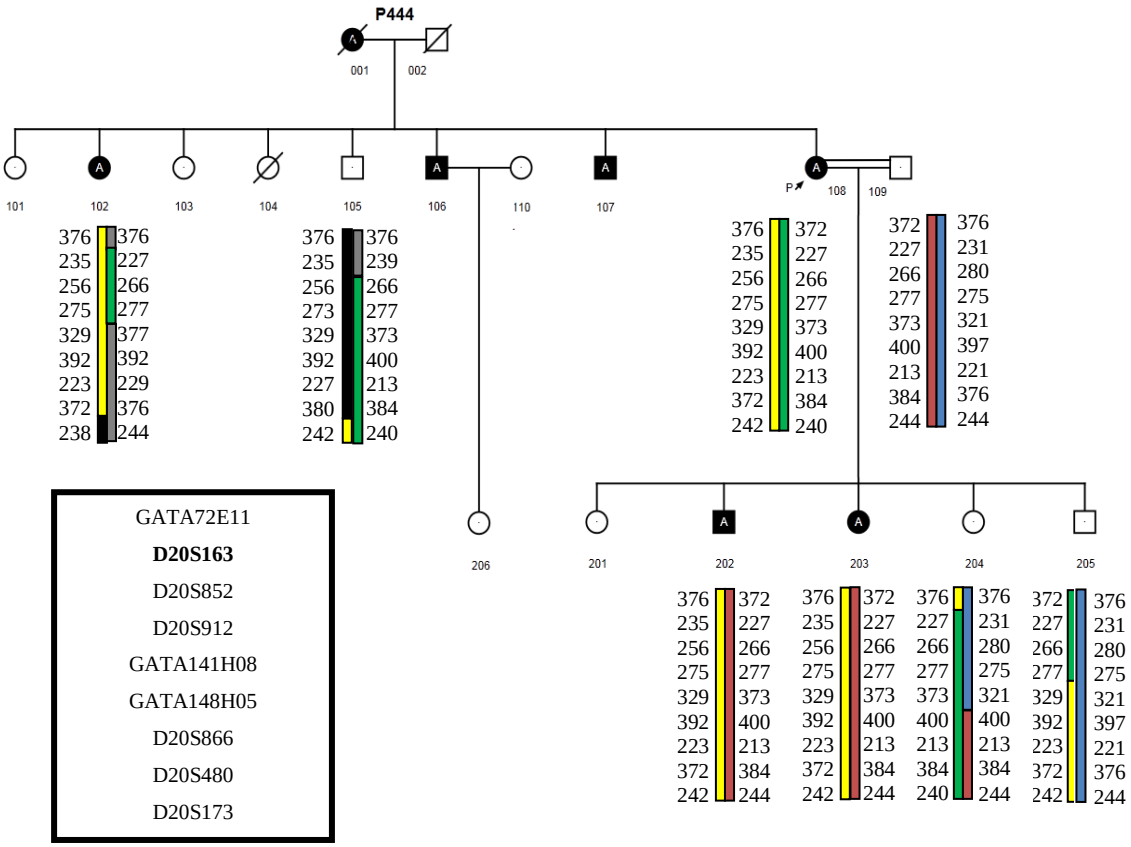

Figure 5.22. Haplotype analysis for family P444 for the locus on chromosome 20.

A novel nonsynonymous exonic variation was found in exome sequencing data for the 30Mb region on chromosome 20, which was delineated after haplotype analysis (Table 5.5).

Table 5.5. Variant identified after exome sequencing on chromosome 20 for two affected members of family P444.

Gene	Exon #	Nucleotide change	Amino acid change
ID1	Exon 1	c.442G>A	p.D148N

The segregation of these six variants in the family was analyzed to eliminate some of these candidate genes. The variant regions were amplified and sequenced using the primers listed in Table 3.9. Four affected individuals were heterozygous for the variations identified in *MYO7A, ARAP1, SLC35F2* and *SERPINA3* while four unaffected individuals were negative for the same variations (Figure 5.23-5.26). On the other hand, the

heterozygous change found on *BTBD18* and *ID1* genes were shown not to segregate with the disease phenotype since unaffected individuals were also carriers for these variants (Appendix B).

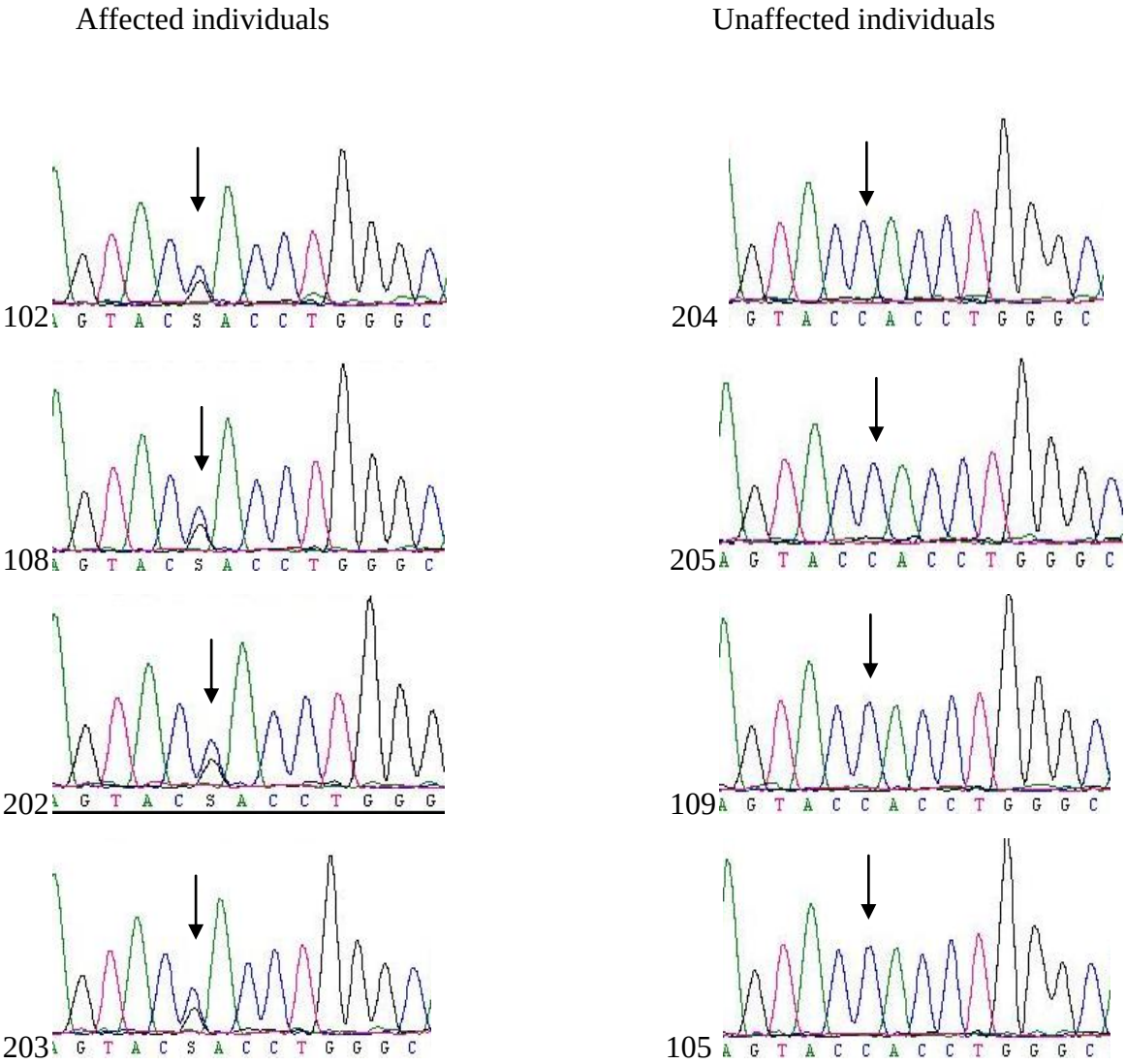

Figure 5.23. Segregation pattern for the variant c.1423C>G on *ARAP1* gene among family members of patient P444. Numbers near the chromatograms indicate the individuals' number that is given on the pedigree.

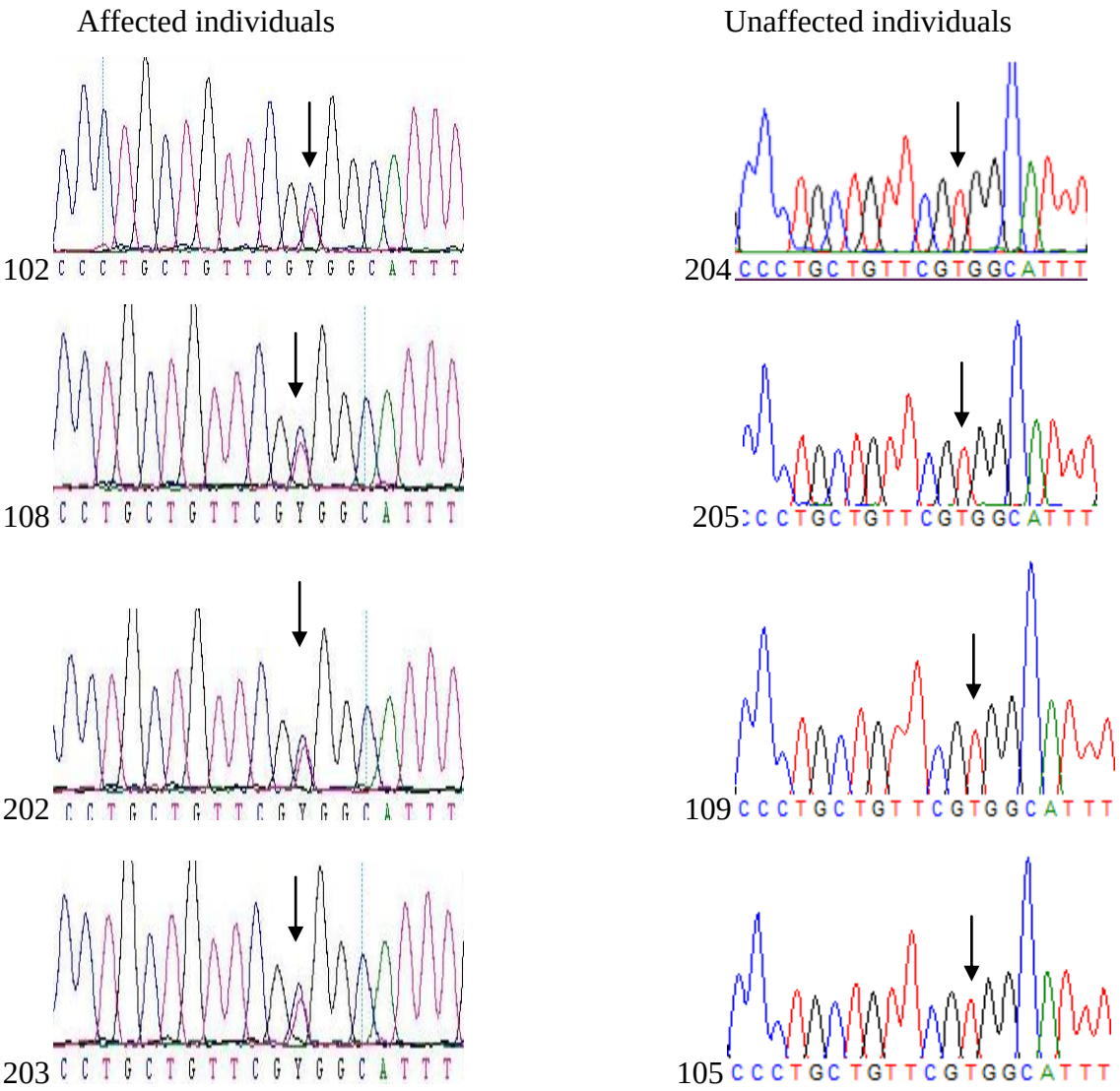

Figure 5.24. Segregation pattern for the variant c.797T>C on *SLC35F2* among family members of patient P444. Numbers near the chromatograms indicate the individuals' number that is given on pedigree.

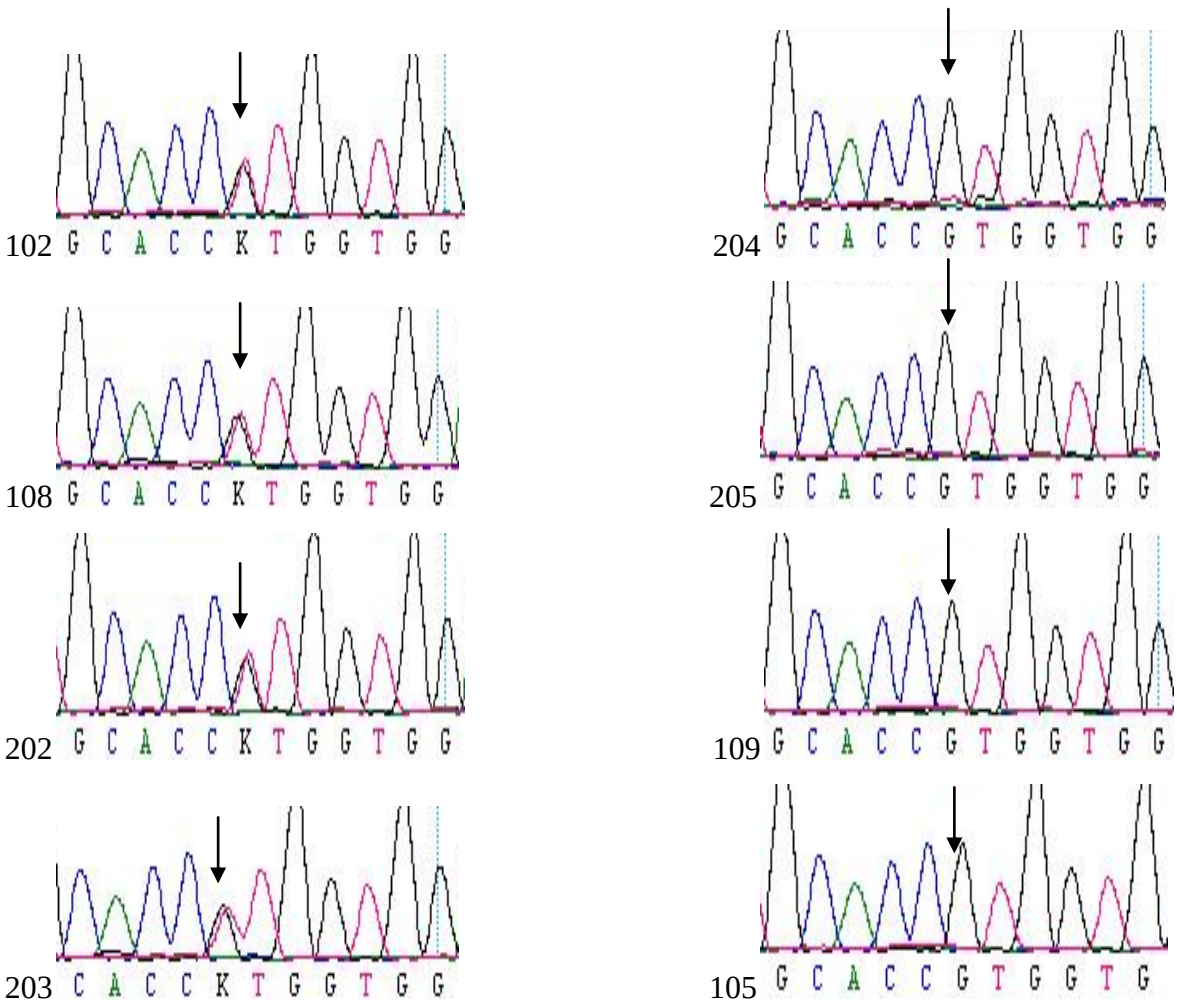

Figure 5.25. Segregation pattern for the variant c.787G>T on *SERPINA3* among family members of patient P444. Numbers near the chromatograms indicate the individuals' number that is given on pedigree.

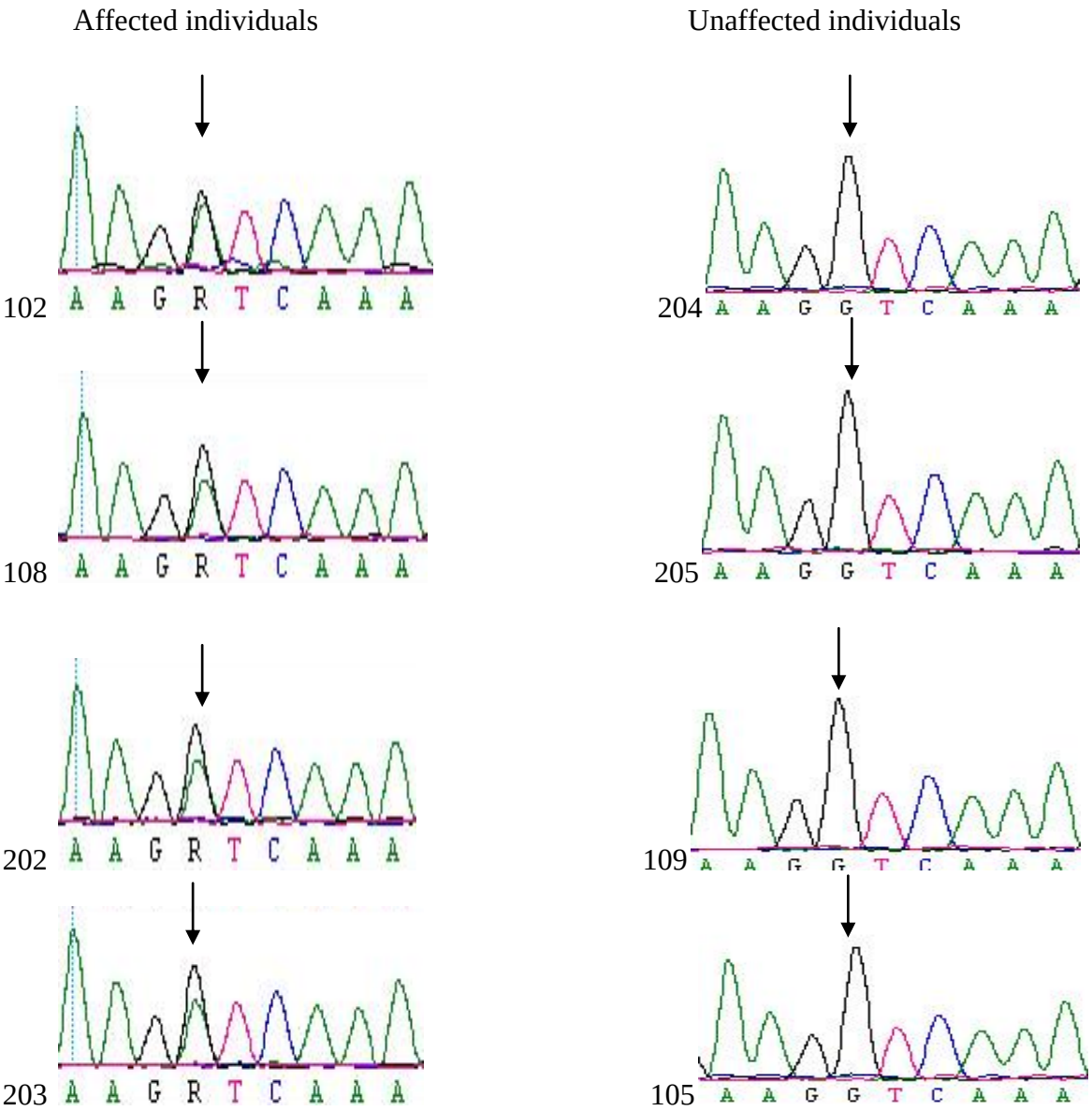

Figure 5.26. Segregation pattern for the variant c.4360G>A on *MYO7A* family members of patient P444. Numbers near the chromatograms indicate the individuals' number that is given on pedigree.

Segregation analyses excluded two of the candidate genes, *BTBD18* and *ID1* since the variants were also observed in unaffected members of the family. Thus, four genes, *ARAP1*, *MYO7A*, *SERPINA3* and *SLC35F2* remained as candidates.

Further elimination of candidate genes was achieved by screening the control individuals for the variants. None of the controls, among 91 Turkish and 231 non-Turkish

individuals, showed the variation on *ARAP1* gene. The variant on *SERPINA3* gene was also absent among 95 Turkish and 180 non-Turkish controls. For the variant on *MYO7A* gene, 88 Turkish controls were screened and none of them had the variant. Ninety five Turkish controls were screened for the variant on *SLC35F2* gene and one of them has the same heterozygous change, which was observed in the affected individuals of the P444 family. Therefore, since this variant cannot be designated as pathogenic, *SLC35F2* gene was eliminated. After all these analyses genes *ARAP1*, *MYO7A* and *SERPINA3* were left as candidate genes.

5.4. X Chromosome Linkage Analysis

X chromosome linkage analysis was performed with 30 STR markers for four families; P224, P381, P408 and P636. Two point LOD score analysis was performed by using EasyLinkage software howeverit did not reveal any linked loci for the families P224 and P381. For family P636, many markers yielded the same LOD score suggesting that no specific locus on X chromosome linked to disease; therefore, we concluded that the STR markers were uninformative for the family. For the family P408, one marker (DXS8107) yielded the highest LOD score which was 0.3010 (Figure 5.27).

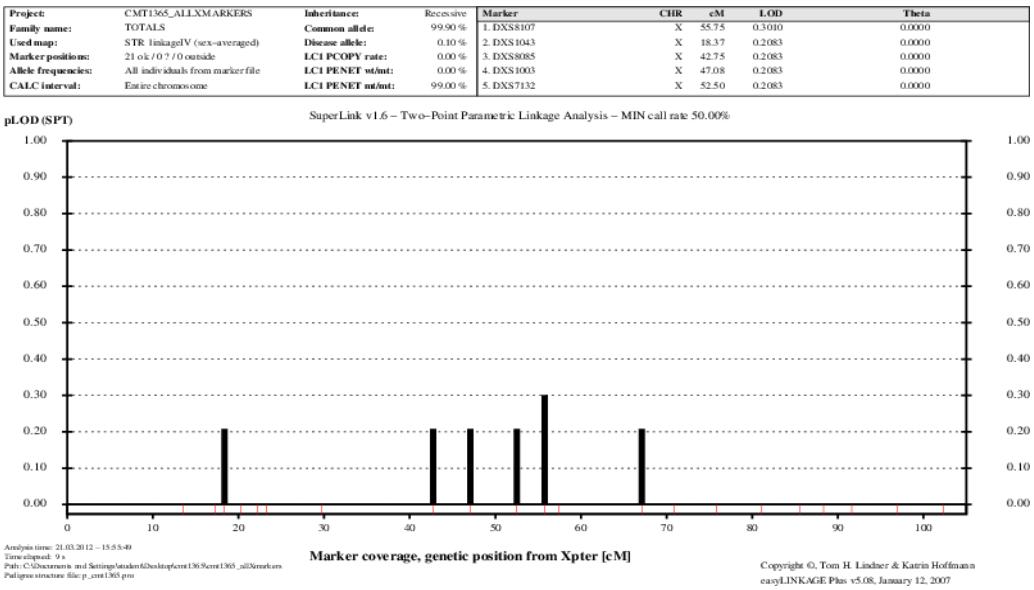

Figure 5.27. Two point LOD score results of X chromosome linkage analysis for family P408.

A haplotype was constructed using this marker with its adjacent markers, and recombinations delineated a locus between markers DXS8014-DXS1227 that was around 102Mb (Figure 5.28). This locus includes around 1100 genes, thus, the analysis was uninformative.

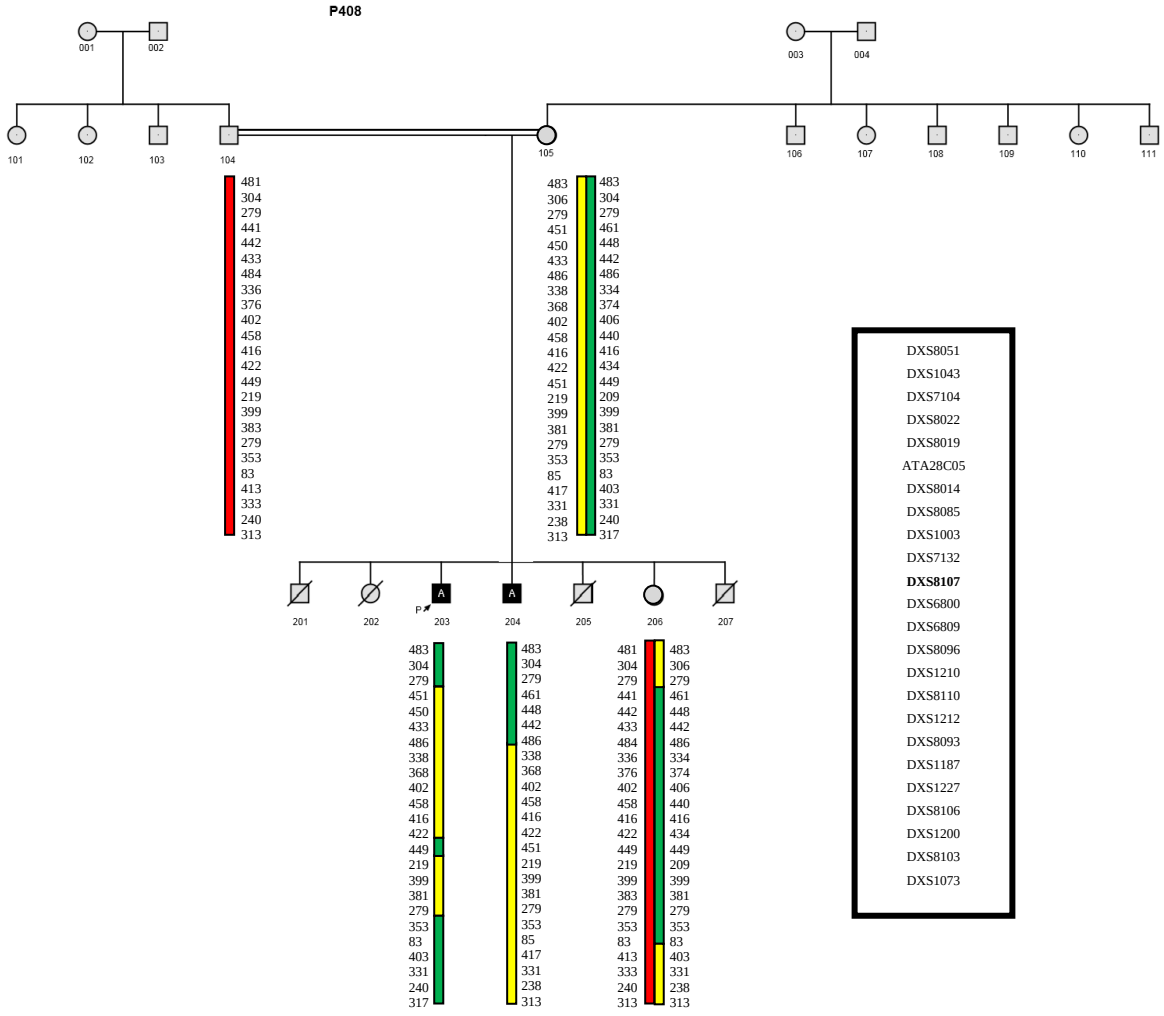

Figure 5.28. Haplotype analysis for family P408 for chromosome X.

6. DISCUSSION

During this study, 34 Turkish CMT patients were screened for mutations for one or more of the following genes depending on the segregation pattern, progression of the disease and presence of additional symptoms: *GJB1, PRPS1, GDAP1* and *SH3TC2*. Four variations were identified in *GJB1*; two of them are in 5'UTR of the gene. Two other variations were found in *GDAP1* and *SH3TC2*. Two families (P158 and P444) were exome sequenced and whole genome linkage analysis was performed for family P444. After combination of these two analyses for family P444, three candidate genes were identified. For family P158, a variation was found in 5'UTR of *GJB1*. X chromosome linkage analysis was conducted for four families and it was inconclusive for all of the families.

6.1. Mutation Analysis for CDS of *GJB1*

GJB1 (*Cx32*) is the most frequently mutated CMTX gene, responsible almost 90% of all CMTX and 10% of all CMT cases (Ressot and Bruzzone, 2000; Scherer, 1996). Mutations in *GJB1* are the second most common cause of CMT after *PMP22* duplications that results in CMT1A (Dubourg *et al.,* 2001).

In this study, two mutations were identified among 11 patients, which shows that 18% of this cohort has mutations in the CDS of *GJB1*. More than 300 mutations have been reported for the gene so far and all mutation types; missense, nonsense, frameshift deletions and insertions were observed (Figure 6.1). As shown in Figure 6.1, the protein has four transmembrane domains, two extracellular loops and three cytoplasmic domains.

Mutations in the CDS of *GJB1* mostly result in loss of function. For instance, some *in vitro* studies show that S26L alteration and deletion of amino acids between positions 111-116 result in reduction in the permeability of important molecules such as glucose, cAMP, IP_3 and Ca^{2+}. Since transfer of these important molecules is disrupted due to defect in connexin channels in Schwann cells, signals for the intracellular pathways may be altered and/or disturbed (Bicego *et al.,* 2006). Another study showed that conductance-voltage relation of hemichannels is altered when Cx32 is mutated in *Xenopus* oocytes;

therefore, the communication pathway between cells through hemichannels is affected. Average homotypic conductance is decreased significantly in R15W, H94Y and V139M mutants. The study was another evidence for the loss of function of Cx32 (Abrams *et al.*, 2001). Although most of its mutations are associated with loss of function of the Cx32, some mutations may lead to gain of function of the protein. For example, S85C and F235C mutants result in decline of ionic gradients and/or Ca^{+2} inflow due to formation of functional but mutated hemichannels, suggesting a gain of function mechanism (Abrams *et al.*, 2002; Liang *et al.*, 2005).

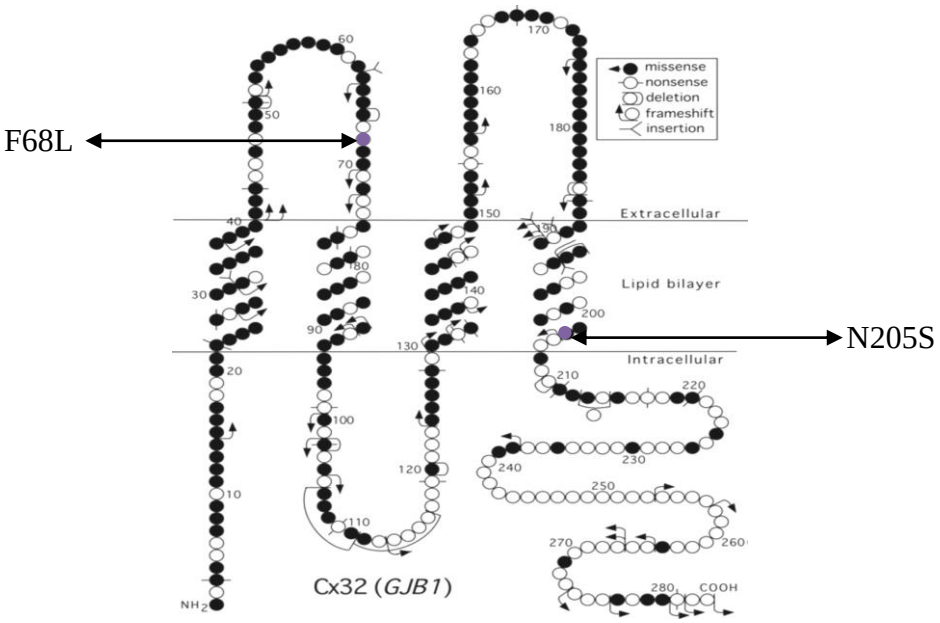

Figure 6.1. Schematic view of Cx32 mutations . Purple circles represent missense mutations identified in this study.

In this study, two mutations in the coding sequence of *GJB1* were identified in patients P824-1, P824-2 and P788. P824-1 and P824-2, who are siblings, have N205S alteration in Cx32. As expected, female sibling is less affected compared to her brother due to X inactivation. Motor nerve conduction velocity for female is around 43 m/s that was normal. She has abnormal mobility without dependency to wheelchair, distal weakness at hand wrist and *pes cavus.* This amino acid substitution is previously reported by Sorour and Upadhyaya in 1995. In another study performed by Bähr *et al.* in 1999, which investigated a family with N205S alteration, indicated that, the male patients has similar symptoms such as weakness in hands and *pes cavus*. Beside male patients, this family had

also female patients like our case. The substituted amino acid asparagine with polar uncharged side chains is found on 4th transmembrane domain of the protein. Serine is also a polar amino acid with uncharged side chains but 2nd and 4th transmembrane domains of Cx32 are important for connexon conformation and packing (Milks *et al.,* 1988). Bähr suggested that since this alteration is at 4th TMD, it may affect the channel formation (Bahr *et al.,* 1999). However, another study proved that, this alteration does not affect the formation of homotypic gap junction in N2A cells (Wang *et al.,* 2004) implicating that it affects some other pathways like myelin formation leading to demyelination. Another alteration found during this study was F68L in P788. This patient has abnormal mobility, distal weakness at hand wrist and no wheelchair use. This variation is novel, and predicted as possibly damaging in PolyPhen-2 tool (Adzhubei *et al.,* 2010). Phenyalanine at that position is highly conserved among species and the variation is not found in dbSNP, 1000genome and NHLBI Exome Sequencing Project databases. Both phenylalanine and leucine are amino acids with hydrophobic side chains but phenylalanine has an aromatic ring that might not be compensated. To understand how this mutation alters the formation of gap junctions and Cx32 itself, *in vitro* studies can be performed by using site-directed mutagenesis.

6.2. Mutation Analysis of *PRPS1*

PRPS1 is the second causative CMT gene that resides on the X chromosome. Up to date, only one family has been reported to have a mutation in this gene. In our cohort of 13 patients with a possible X-linked inheritance, none of them showed variations using PCR-SSCP technique. This result supports the rareness of *PRPS1* mutations among CMT cases.

6.3. Mutation Analysis of *GDAP1*

GDAP1 is the most frequent causative gene that results in CMT4. Mutations in *GDAP1* can be missense, nonsense and frameshift deletions and insertions. The role of GDAP1 protein is not fully understood but studies showed that it has a role in the fission of mitochondria (Niemann *et al.,* 2005). Even if CMT4 is classified as a subtype for recessive form of demyelinating CMT, some recessive mutations of this same gene may lead to

axonal degeneration (Claramunt *et al.,* 2005). This supports the controversies in classification of CMT.

In this study, 17 patients were screened for GDAP1 mutations and a novel nonsense mutation was found in one family. Two sisters from the family P950 have a homozygous change c.112C>T that leads to Q38X change at amino acid level. The mutation hypothetically results in truncated protein translation. Up to date, homozygous nonsense mutations in *GDAP1* were reported as leading to severe phenotype with a very early onset. Homozygous nonsense mutations may lead axonal degeneration, demyelination or both (Cassereau *et al.,* 2011). The proband, in our study, has axonal features and also a severe phenotype with wheelchair use and distal weakness at hand wrist. Age of onset for the patient is at birth. Niemann and his colleagues indicated that, the effect of homozygous nonsense mutation is the complete loss of function of the protein. Their study showed that, mitochondria targeting for some truncated GDAP1 proteins (T288fs290X, S194X) were significantly reduced. Q163X GDAP1 protein cannot be detected in the mitochondria indicating that stability of truncated GDAP1 protein is abolished (Niemann *et al.,* 2005). The variation found in this study is absent in dbSNP, 1000genome database and NHLBI Exome Sequencing Project database. In the light of these findings, the variation c.112C>T is a novel pathogenic mutation and the truncated protein possibly cannot reach to the mitochondria, leading to a severe phenotype with very early onset.

6.4. Mutation Analysis of *SH3TC2*

SH3TC2 (CMT4C) is one of the most frequently mutated causative genes that lead to recessive demyelinating CMT (CMT4). So far, 21 different mutations were reported in *SH3TC2* but the most frequent mutation is c.2860C>T that result in R954X and leads to truncated protein translation. It is a founder mutation in exon 11 that represents a hot spot, (Inherited peripheral neuropathies mutation database, 2007; Gosselin *et al.,* 2008). The patients with CMT4C have demyelination and more specifically scoliosis with an early onset (Senderek *et al.,* 2003). In this study, 12 patients were screened for *SH3TC2* mutations and one family, P909, had the founder mutation. Both affected sisters have abnormal mobility but no requirement for wheelchair, *pes cavus,* and distal weakness at hand wrist. Additionally, the affected sisters have scoliosis that is a characteristic feature

associated with SH3TC2 mutations. Motor NCVs for affected sisters are around 22 m/s and 29 m/s that delineate demyelination.

Although the role of SH3TC2 protein is uncertain, it is known that it is found in both early and late endosomes and therefore may have a role in endocytic pathway. *In vitro* studies showed that truncated SH3TC2 protein (R954X) localized normally when compared to wild type protein suggesting the localization of protein seems irrelevant for the pathogenesis of mutated SH3TC2 and due to co-localization of this protein with the components of the endocytic pathway, the study indicates that this protein has a function in endocytic pathway and defects in this protein result in demyelination (Lupo *et al.,* 2009).

6.5. Exome Sequencing for Family P158

Family P158 was found to be negative for point mutations in the coding region of *GJB1, PMP22* and *MPZ. PMP22* duplication was not also found in the proband of family P158. Since, almost 85% of functional variations were found in exome and it is more cost effective than the whole genome sequencing (Botstein and Risch, 2003; Lupski *et al.,* 2010), we decided to perform exome sequencing for this family.

Two affected and one unaffected individual from the family were exome sequenced. After a detailed analysis of the spreadsheet file (analysis criteria was given in Results 5.2), c.-18A>G variation was identified in two affected individuals and absent in unaffected member of the family P158. Position -18 is important since it is the acceptor site for splicing found between exon 1 and exon 2 of *GJB1* for nerve specific transcript. So far, only one splice site mutation, c.-373G>A, was published for *GJB1* in two families (Murphy *et al.,* 2011). The variation was located at the last base of exon 1, which is the untranslated exon of *GJB1*. This variation is not reported in dbSNP and absent in controls and segregating with the disease phenotype in the families. The nucleotide (-373) is highly conserved among mammalian species. Since the last base of the exons is one of the most conserved ones at exon-intron boundaries, mutations at this base affect the splicing in many genes (Ladopulou *et al.,* 2002). In our case, the variation, c.-18A>G, segregates with the CMT phenotype. Hemizygous variation was also observed in other affected male members of the family. Mildly affected females were heterozygous for the variation and

unaffected individuals had wild type allele. The variation was absent in 95 Turkish and 92 non-Turkish controls and also not observed in dbSNP, 1000genome database and NHLBI Exome Sequencing Project database. Moreover, online program (Desmet *et al.,* 2009) that predicts the splice sites suggests that if this nucleotide is mutated splicing will be affected. The same program also predicts that binding of SRp40 protein, which activates exonic splicing enhancer (ESE) necessary for efficient 3' splicing, to acceptor site is completely abolished. In the light of these data, this variation can be described as a pathogenic novel mutation resulting in CMT.

Since this mutation is found at 5'UTR of *GJB1,* we decided to screen 5'UTR of *GJB1* for mutations in CMT patients, who were found to be negative for mutations in CDS of *GJB1*.

6.6. Mutation Analysis for 5'UTR of *GJB1*

Mutations in 5'UTR of *GJB1* is very rare and only few cases have been reported related with CMT phenotype (Inherited peripheral neuropathies mutation database, 2007). Up to now, some mutations were reported in the promoter region, internal ribosome entry site or splice sites of nerve specific transcript of *GJB1*, which is initiated from promoter P2 (Ionasescu *et al.,* 1996; Murphy *et al.,* 2011).

In this study, another group of patients, who were found to be negative for mutations in the coding sequence of *GJB1*, were screened for mutations for the 5'UTR of *GJB1*. Two patients had novel mutations out of 15 (14%). The first variation in patient P232 (c.-541 A>G) was in the promoter P2. This region is known to be important for activity of SOX10 transcription factor. SOX10 has two binding sites, S1 and S2, and this variation is found on the S1 binding site, which is important for dimeric binding of SOX10. Mutations on this site were shown to decrease the dimeric binding of SOX10 dramatically and affect the SOX10 activity (Bondurand *et al.,* 2001). Moreover, the variation was not reported in dbSNP, 1000genome database and NHLBI Exome Sequencing Project database. Ninety-five Turkish and 92 non-Turkish individuals were sequenced but this variation was absent in any of the controls. This is the first pathogenic mutation found in S1 binding site of SOX10. Second variation identified in this study was c.528T>C found in patient P727.

This variation is segregating with the disease, found also in other affected individuals and was not observed in non-affected family members. It is also located on promoter 2 but in S2 binding site of SOX10 (Bondurand *et al.*, 2001). So far, three other mutations have been identified at this site, c.-527G>C and c.-529T>G, c.-529T>C, that result in CMT phenotype (Inherited peripheral neuropathies mutation database, 2007). Binding of SOX10 to promoter 2 is completely destroyed when S2 binding site is mutated (Bondurand *et al.*, 2001), suggesting that mutations in binding site, S2, of SOX10 affect the transcription efficiency and lead to CMT phenotype. Beside these information, since this variation was absent in 95 Turkish and 92 non-Turkish controls and in dbSNP, 1000genome and NHLBI Exome Sequencing Project databases, the variation can be defined as a pathogenic mutation.

Since three different mutations in three families have been identified at 5'UTR of *GJB1* among 16 patients (including exome sequenced family P158), we suggest 5'UTR of the gene should also be screened with its coding sequences in order not to miss the pathogenic mutations of *GJB1*.

In the case of both 5'UTR and CDS of *GJB1*, the mutation frequency was 19%; five families among 27 had mutations in *GJB1*. In this study, since we have studied with X-linked families for screening *GJB1*, it was expected to have mutation frequency higher than 10%, which is the frequency of *GJB1* mutations among all CMT cases.

6.7. Exome Sequencing and Whole Genome Linkage Analysis for Family P444

Family P444 has been previously found to be negative for two most frequent genetic causes of CMT; *PMP22* duplication and point mutations in *GJB1*. Then, exome sequencing was performed for three individuals from this family, two of them are affected and one of them is unaffected.

Since exome sequencing did not reveal any mutations in the known causative CMT genes, whole genome linkage analysis was also performed with highly polymorphic STR markers were used during this analysis in order to have different alleles for individuals. In this way haplotype construction was easier and more informative. Comparison of

haplotype analysis and exome sequencing data allowed us to find out three candidate genes (*ARAP1*, *MYO7A* and *SERPINA3*) that may lead to CMT.

We are currently screening other dominant CMT families to find a variation in one of these genes' exonic or splice site regions. Functional analysis can then be performed in order to understand how the mutated protein leads to CMT phenotype.

6.7.1. ARAP1

After whole genome linkage analysis two loci were identified on chromosome 11, which are between markers D11S2014-D11S2006 and D11S4139-D11S897. When exome sequencing data was analyzed for these loci, the variation c.1423C>G was identified in *ARAP1* located between the markers D11S4139-D11S897. It was observed in all affected individuals of the family P444 and not present in unaffected individuals. This alteration leads to p.H475D and is predicted as benign in PolyPhen-2 tool (Adzhubei *et al.,* 2010). But, some variations that are published as a pathogenic mutation may be a benign variation in this tool.

ARAP1 is a 162 kDa protein contains Sam, Arf-GAP, Rho-GAP, ankyrin repeat, Ras-associating, and PH domains. It regulates Arf and Rho proteins. Rho GAPs are involved in cytoskeleton dynamics through Rho GTPases, having a key role in remodeling of actin microfilaments (Etienne-Manneville and Hall 2002). ARAP1 regulates endocytic trafficking of the epidermal growth factor receptor (EGFR). Two PH domains specifically bind phosphatidylinositol (3,4,5)-triphosphate (PIP_3), which recruits ARAP1 to the PM or endosome (Yoon *et al.,* 2008). ARAP1 knock down (KD) alters the organization of the endosomal compartment (Daniele *et al.,* 2008). Since some CMT proteins (such as SH3TC2) are involved in endocytic pathway, mutated ARAP1 may also result in CMT phenotype. Moreover like ARAP1, some CMT proteins (such as GDAP1 and MTMR2) are also involved in PIP_3 pathway. This makes the ARAP1 the strongest candidate for CMT among the three candidates.

6.7.2. MYO7A

MYO7A is located on chromosome 11 between markers D11S4139-D11S897. The family showed linkage to that locus and when we referred to exome sequencing data, *MYO7A* c.4360G>A alteration was identified in all affected individuals. Unaffected individuals of family P444 did not have this variation. It leads to V1454I change at amino acid level. To predict the pathogenicity of this variation, PolyPhen-2 tool was used (Adzhubei *et al.*, 2010) and this variation was predicted as benign.

MYO7A protein is a member of myosin family and has a molecular mass of 254 kDa. The protein has four domains, which are a motor domain, an actin binding domain, a neck domain providing the interaction of MYO7A with other proteins, and a tail domain, acting as an anchor. MYO7A is expressed mainly in cochlea and retina. In human, this gene has already been associated with disease, Usher syndrome 1B characterized by deafness, vestibular dysfunction and blindness (Weil *et al.*, 1995).

6.7.3. SERPINA3

SERPINA3 is located on chromosome 14 and the family showed linkage to the locus, which is found between the markers D14S125-D14S611. Exome sequencing data revealed nonsynonymous c.787G>T variation for this locus in all affected members of the family P444. This variation leads to p.V263L alteration. No variation was observed in unaffected individual members of the family P444. This alteration was predicted as possibly damaging by using PolyPhen-2 tool (Adzhubei *et al.*, 2010).

SERPINA3 is a member of the serine protease inhibitor family. It is highly expressed in liver and pancreas. Although its biological role has not been understood yet, it inhibits the cathepsin G and chymotypsin-like enzymes (Travis and Salyesen, 1983). The protein inhibits the proteases by making covalent linkage after serpin site cleavage by proteases. The complex of serpin-protease is highly stable and inactive (Baumann *et al.*, 1991). Polymorphisms in *SERPINA3* are tissue specific and affect the protease targeting. Variations in this gene are also associated with various diseases. For instance, polymorphism in the promoter region of *SERPINA3* has been implicated in Alzheimer’s

disease and increases the SERPINA3 concentration in the senile plaques (Abraham *et al.*, 1988).

6.8. X Chromosome Linkage Analysis

In this study, X chromosome linkage analysis was performed for four X-linked CMT families. Two point LOD score values calculated by EasyLinkage software did not revealed linkage to any loci for the families P224 and P381. For the family P636, many markers gave the same LOD score suggesting that this analysis is uninformative for the family. Linkage analysis is generally an efficient method for large families. For small families, it may be less informative and even some loci, which may contain the causative gene, can be excluded due to misleading LOD scores (Krueger *et al.*, 2009). Family P636 was also a small family with four members among which two was affected. The other important point for linkage analysis is the selection of the markers. As mentioned earlier the selected markers were polymorphic and spread roughly equal intervals in order to make the analysis informative. If the parents have different alleles, it is easy to understand the origin of alleles for the children (in X chromosome case, females have two alleles). Even if the chosen markers seem highly polymorphic according to the NCBI database, some of the markers may not be polymorphic enough in our population. For the family P408, linkage to a locus was identified between markers DXS8014-DXS1227, which is around 102Mb. Since this locus is too large and contains almost 1100 gene, additional procedures should be performed. One of them may be use some additional polymorphic markers to delineate the locus. The more efficient way may be to perform another genetic analysis such as exome sequencing. Combination of both analyses can be more efficient way to obtain informative results.

7. CONCLUSION

In this study, we identified some novel and previously reported mutations in causative CMT genes (*GJB1, GDAP1* and *SH3TC2*). Especially, three novel mutations that were identified in 5'UTR of *GJB1* have critical importance since few mutations were reported in this region up to date. We have also successfully determined three candidate genes (*ARAP1, MYO7A* and *SERPINA3*) for the family P444 that were previously excluded for mutations in the known CMT genes. To identify the exact causative gene, these genes should be screened in other dominant CMT cases. Further functional studies can also be performed to understand how this novel gene leads to pathogenicity. We hope this study can contribute to illumination of genetics of CMT and help development of therapies for patients.

APPENDIX A : EXCLUDED LOCI FOR FAMILY P444

Haplotypes of the family P444 that excluded the regions on chromosomes 3, 8 and X are given in Figures A.1-Figure A.3. In all figures, squares and circles represent males and females, respectively. Black filled boxes with 'A' show affected individuals. 'P' indicates the proband. Double line shows the consanguineous marriage. Different colored bars indicate different haplotypes. Numbers represent the length of the amplicons that include STRs. The order of the STR markers used in haplotype analyses are given on the boxes in each figure. STR markers in bold had yielded the LOD scores higher than 1.0.

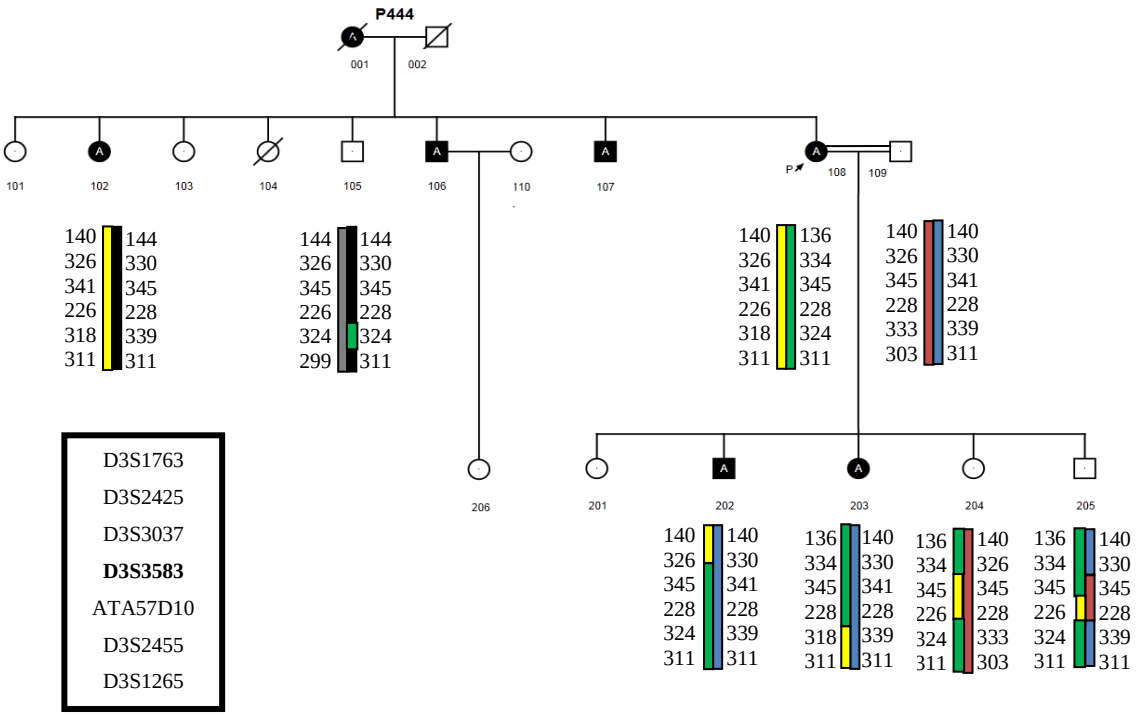

Figure A.1. Haplotype analysis for family P444 for the locus on chromosome 3.

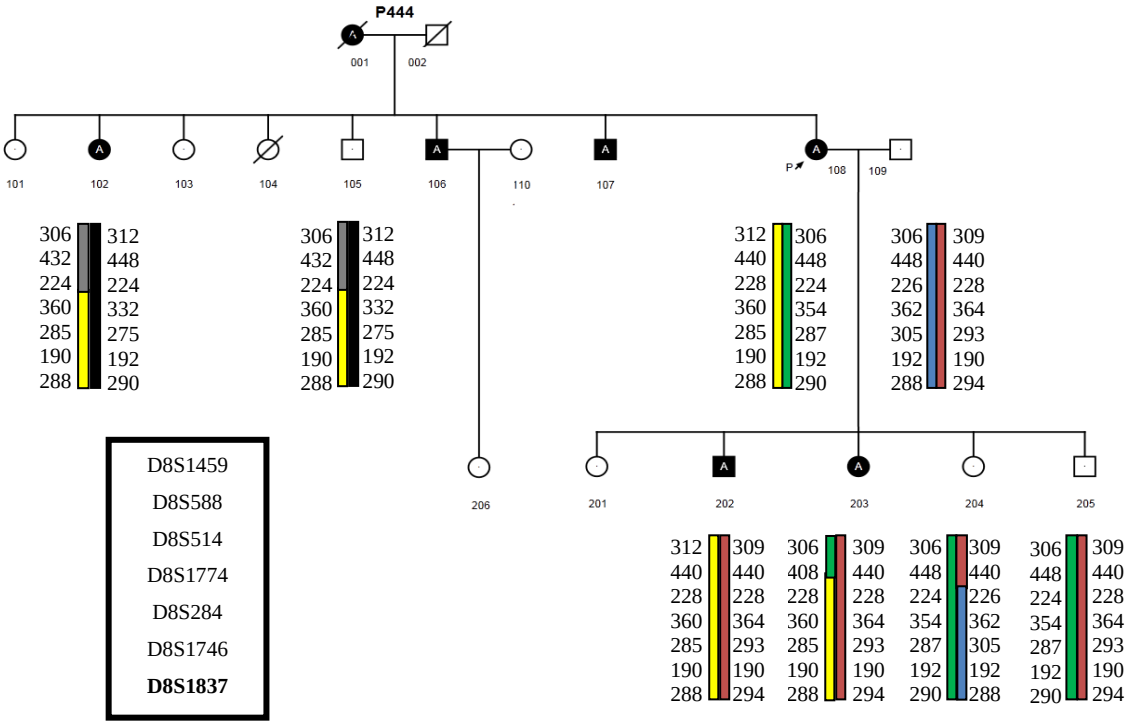

Figure A.2. Haplotype analysis for family P444 for the locus on chromosome 8.

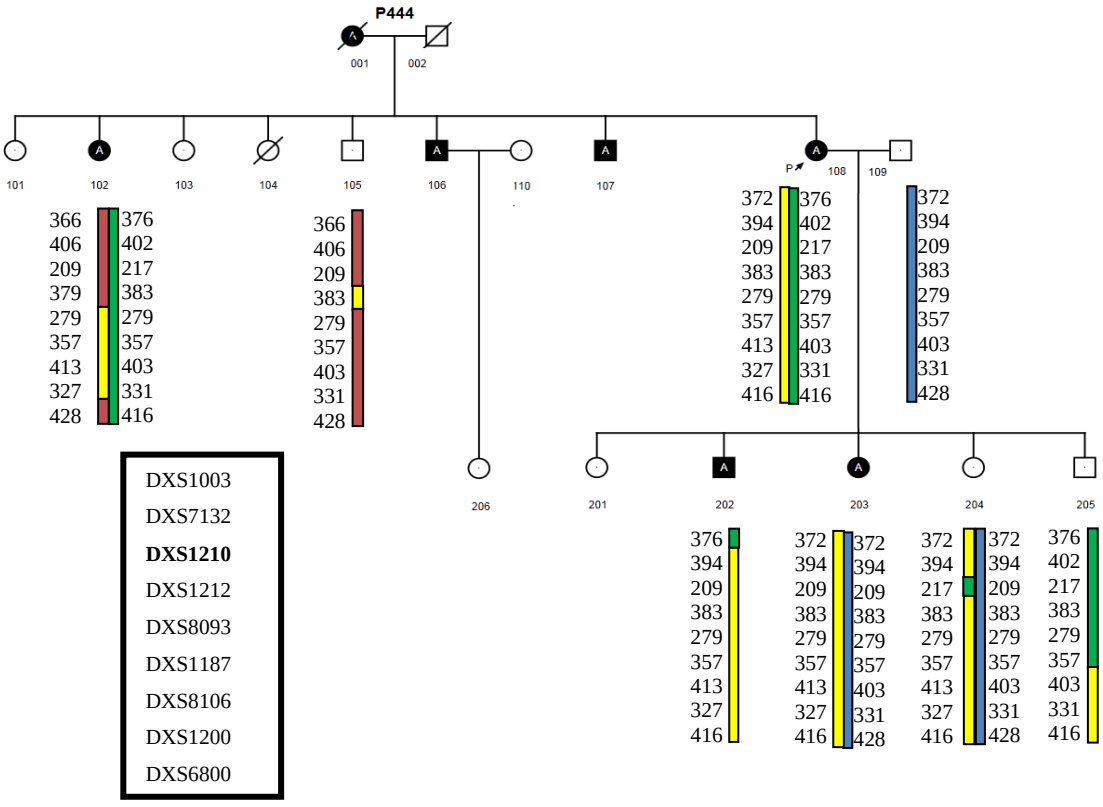

Figure A.3. Haplotype analysis for family P444 for the locus on chromosome X.

APPENDIX B : EXCLUSION OF *BTBD18* and *ID1* GENES FOR FAMILY P444

Variants on *BTBD18* and *ID1* genes were also observed in unaffected individuals. The sequencing results for one affected and one unaffected individual carrying the variation was given in Figure B.1 and Figure B.2. Numbers to the left of the chromatograms indicate the individuals' number that is given on pedigree.

Affected individual

Unaffected individual

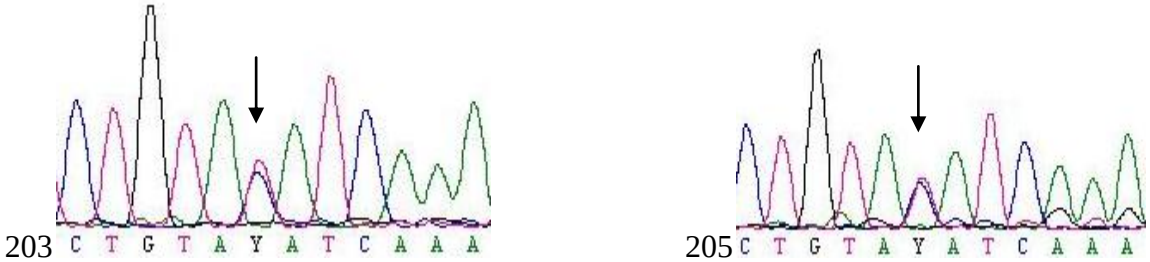

Figure B.1. The variant c.827C>T on *BTBD18* was observed in both affected (203) and unaffected (205) individuals of family P444.

Affected individual

Unaffected individual

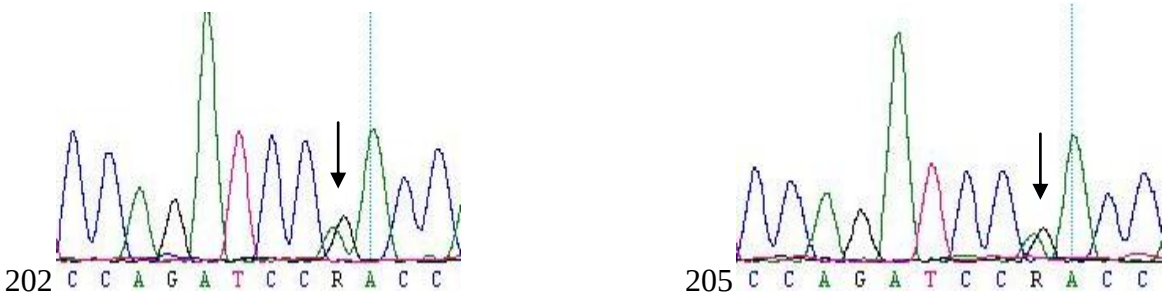

Figure B.2. The variant c.442G>A on *ID1* was observed in both affected (202) and unaffected (205) individuals in family P444.

APPENDIX C : X CHROMOSOME LINKAGE ANALYSIS FOR FAMILY P636

Among 30 STR markers used for the analysis and 12 of them yielded the same LOD score for family P636 (Figure C.1). The analysis was inconclusive on the assumption that the markers gave uninformative results.

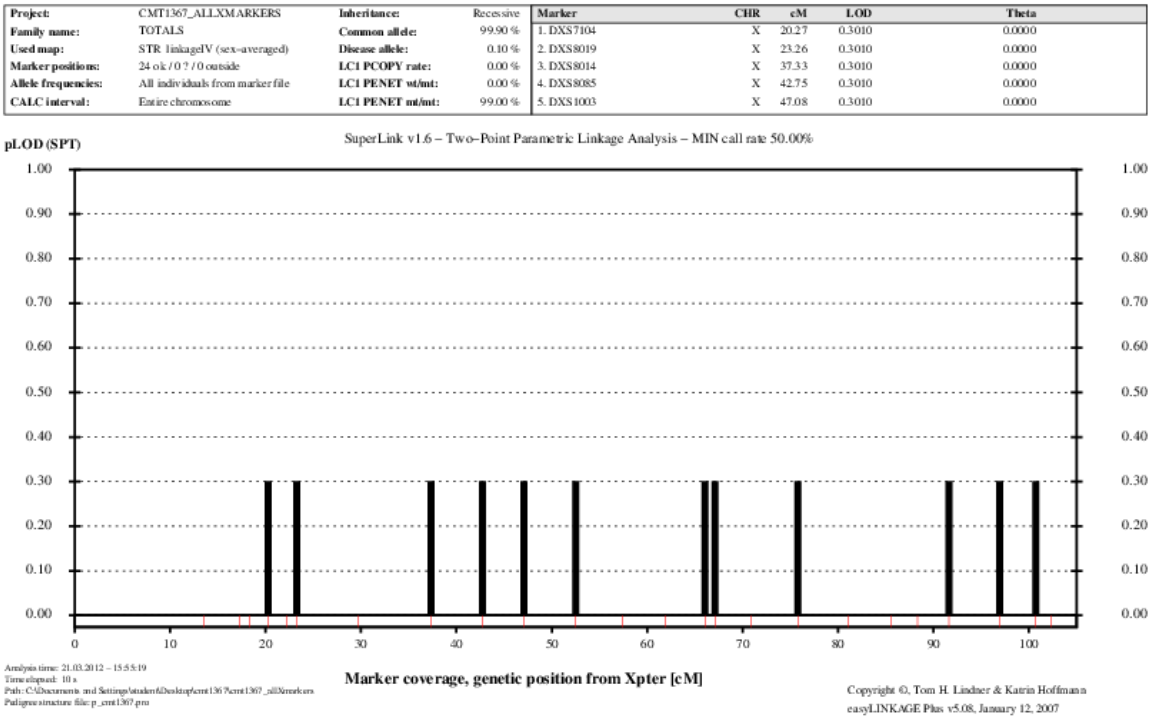

Project:	CMT1367_ALLXMARKERS	Inheritance:	Recessive
Family name:	TOTALS	Common allele:	99.90 %
Used map:	STR linkageIV (sex-averaged)	Disease allele:	0.10 %
Marker positions:	24 ok / 0 ? / 0 outside	LC1 PCOPY rate:	0.00 %
Allele frequencies:	All individuals from marker file	LC1 PENET wt/mt:	0.00 %
CALC interval:	Entire chromosome	LC1 PENET mt/mt:	99.00 %

Marker	CHR	cM	LOD	Theta
1. DXS7104	X	20.27	0.3010	0.0000
2. DXS8019	X	23.26	0.3010	0.0000
3. DXS8014	X	37.33	0.3010	0.0000
4. DXS8085	X	42.75	0.3010	0.0000
5. DXS1003	X	47.08	0.3010	0.0000

Figure C.1. X chromosome linkage analysis for family P636.

APPENDIX D : STR MARKERS USED FOR WHOLE GENOME LINKAGE ANALYSIS FOR FAMILY P444

In this section, all markers used during whole genome linkage analysis for each chromosome are given in Table D.1-D.23.

Table D.1. Name of the STR markers and their position for chromosome 1.

Name of the STR marker	**Position (cM)**
D1S2845	8.85
D1S1646	14.594
D1S244	20.613
D1S434	29.932
D1S1592	38.51
D1S552	45.332
D1S513	57.28
D1S1616	75.671
D1S405	86.772
ATA52G05	98.214
GATA193D02	104.794
D1S551	113.694
D1S2865	120.28
D1S1588	125.511
D1S2767	132.47
ATA42G12	139.023
D1S187	146.531
D1S442	154.74
D1S1653	164.091
ATA38A05	178.42
D1S1619	188.853
D1S2786	192.061
D1S1642	201.583
D1S1647	216.821

Table D.1. Name of the STR markers and their position for chromosome 1 (cont.).

D1S2636	222.84
D1S1667	231.671
D1S395	239.66
D1S459	247.233
D1S2850	256.261
D1S180	267.511
D1S1609	274.534
D1S2682	288.29

Table D.2. Name of the STR markers and their position for chromosome 2.

Name of the STR marker	**Position (cM)**
D2S2166	10.86
D2S1275	22.101
D2S1400	27.6
D2S1360	38.331
D2S144	45.837
D2S352	50.652
D2S2230	56.15
D2S2306	63.41
D2S2739	73.61
D2S1772	85.482
D2S1394	90.822
D2S1777	99.411
D2S2161	103.172
D2S1343	115.27
D2S1265	124.032
D2S2215	134.45
D2S2256	141.622
D2S1326	149.891
D2S2241	157.551
D2S1353	164.51

Table D.2. Name of the STR markers and their position for chromosome 2 (cont.).

D2S2345	171.04
D2S1267	177.531
D2S1391	188.114
D2S273	193.262
GATA161E02	199.185
D2S1369	206.741
D2S2382	213.49
D2S126	221.13
D2S1363	227.002
D2S427	236.7
D2S2968	251.94
D2S140	263.56

Table D.3. Name of the STR markers and their position for chromosome 3.

Name of the STR marker	**Position (cM)**
D3S1297	8.31
D3S1560	18.97
D3S3589	32.362
D3S2385	38.54
D3S3038	44.811
D3S2432	57.921
D3S2304	67.947
D3S2408	74.351
D3S1312	82.242
D3S1287	88.6
D3S3544	96.66
D3S2323	109.228
D3S2318	112.961
D3S3045	124.165
D3S3526	129.732
D3S2460	134.64

Table D.3. Name of the STR markers and their position for chromosome 3 (cont.).

D3S1541	146.604
D3S1764	153.185
D3S1744	161.046
D3S1746	170.141
D3S1763	176.545
D3S2425	185.402
D3S3037	191.043
D3S3583	195.602
ATA57D10	206.432
D3S2455	214.452
D3S1265	222.83

Table D.4. Name of the STR markers and their position for chromosome 4.

Name of the STR marker	**Position (cM)**
D4S2366	12.93
D4S2983	17.49
D4S2315	25.361
GGAT18G02	29.685
D4S1533	36.091
D4S2408	45.971
D4S1581	51.603
D4S2382	56.95
GATA61B02	64.243
D4S2308	75.202
D4S1543	78.972
D4S2393	85.18
GATA68C08	93.48
D4S2961	107.95
D4S3240	114.04
D4S1611	121.61
D4S2395	126.71

Table D.4. Name of the STR markers and their position for chromosome 4 (cont.).

D4S3039	132.72
D4S1644	143.312
GATA72A08	155.75
D4S1626	161.912
D4S2368	167.56
D4S2637	176.194
D4S2417	181.93
D4S2920	190.021
D4S408	195.06
D4S1652	208.073

Table D.5. Name of the STR markers and their position for chromosome 5.

Name of the STR marker	**Position (cM)**
D5S2849	7.771
D5S807	19.022
D5S1991	26.73
D5S2845	36.254
GATA63C02	49.54
D5S1457	59.856
GGAT1D10	66.812
D5S647	74.07
D5S1501	85.25
GATA142H05	92.387
D5S1463	99.423
D5S1462	105.29
D5S1346	113.081
D5S2501	117.511
D5S1484	123.451
D5S1505	129.833
D5S816	140.726
ATA26G09	147.498

Table D.5. Name of the STR markers and their position for chromosome 5 (cont.).

D5S1499	160.874
D5S2066	165.13
D5S1471	172.13
D5S394	179.76
D5S2111	187.811
D5S2073	194.88

Table D.6. Name of the STR markers and their position for chromosome 6.

Name of the STR marker	**Position (cM)**
D6S477	9.183
D6S296	14.612
D6S429	26.716
D6S285	34.232
D6S2439	42.273
D6S1051	50.751
D6S1562	57.96
D6S1552	63.281
D6S948	73.143
D6S965	82.595
D6S1031	88.634
D6S1274	102.812
GATA164H01	109.194
ATA56D06	118.08
GATA28G05	125.714
D6S1626	136.97
D6S383	144.465
D6S960	151.42
D6S255	157.841
D6S1035	164.78
D6S1277	173.31
D6S264	179.07

Table D.6. Name of the STR markers and their position for chromosome 6 (cont.).

D6S503	182.113
D6S281	190.14

Table D.7. Name of the STR markers and their position for chromosome 7.

Name of the STR marker	**Position (cM)**
D7S531	5.282
D7S2201	10.681
D7S2464	17.74
D7S2508	27.66
D7S2210	33.09
D7S617	43.843
D7S1869	47.082
D7S656	52.701
D7S2209	57.791
D7S691	63.67
D7S1793	69.56
D7S672	84.521
D7S2204	90.95
GATA73F12	98.441
D7S1820	105.92
D7S796	113.391
GATA141H10	121.416
D7S650	126.75
D7S1804	136.95
D7S509	143.33
GATA63F08	149.9
GATA150C06	155.103
D7S2426	160.09
D7S483	165.182
D7S637	173.031
D7S2423	181.971

Table D.8. Name of the STR markers and their position for chromosome 8.

Name of the STR marker	**Position (cM)**
D8S518	5.63
D8S1469	16.19
D8S1759	22.173
D8S1827	30.491
D8S261	37.04
D8S560	43.41
GATA31A06	46.262
D8S1125	60.879
GATA116E08	61.406
D8S1110	67.279
D8S507	75.39
D8S1136	82.261
D8S570	90.332
D8S1126	96.211
GATA8B01	103.694
D8S506	110.203
D8S1459	117.631
D8S588	124.41
D8S514	130.002
D8S1774	137.923
D8S284	143.82
D8S1746	149.46
D8S1837	156.59

Table D.9. Name of the STR markers and their position for chromosome 9.

Name of the STR marker	**Position (cM)**
D9S1871	9.832
D9S2169	14.782
D9S775	21.88
D9S274	28.42

Table D.9. Name of the STR markers and their position for chromosome 9 (cont.).

D9S1870	37.582
D9S1121	44.28
D9S270	51.813
D9S1118	58.26
GATA124G05	63.65
D9S284	70.331
GATA152H04	84.901
D9S253	94.851
D9S1786	104.48
D9S2026	117.374
D9S934	127.981
D9S1798	136.475
D9S752	141.69
D9S164	147.91
D9S1826	159.61

Table D.10. Name of the STR markers and their position for chromosome 10.

Name of the STR marker	**Position (cM)**
D10S1706	5.221
D10S1729	14.331
D10S1172	22.28
D10S1412	28.315
D10S527	33.482
D10S674	41.79
GATA179E06	52.102
D10S1228	57.961
D10S1208	63.301
D10S1220	70.235
D10S609	80.771
D10S676	91.132

Table D.10. Name of the STR markers and their position for chromosome 10 (cont.).

D10S556	95.04
D10S2327	100.92
D10S1774	106.652
D10S564	112.582
GATA114H09	127.112
D10S1237	134.7
D10S1230	142.781
D10S2322	149.254
GGAT14G01	162.38
D10S1651	168.771

Table D.11. Name of the STR markers and their position for chromosome 11.

Name of the STR marker	**Position (cM)**
D11S1758	8.644
GATA13F08	12.922
D11S1981	21.477
GATA185H02	29.183
D11S2014	40.902
D11S4083	47.06
D11S1993	54.091
D11S2006	59.777
D11S1883	65.05
D11S4139	72.82
D11S1989	84.383
D11S1394	98.99
D11S897	105.747
D11S1998	113.403
D11S4464	123.002
D11S4110	129.02
D11S1304	141.915
D11S4112	147.771

Table D.12. Name of the STR markers and their position for chromosome 12.

D12S372	7.122
D12S1673	12.606
GATA167A06	20.271
D12S358	26.231
D12S373	36.061
GATA91H01	42.1
D12S1042	48.701
GATA123B12	55.992
D12S297	66.031
D12S1056	75.761
D12S375	80.52
D12S326	86.406
D12S379	93.69
GATA7A02	101.985
D12S1727	107.19
D12S815	113.91
D12S1645	119.551
D12S1023	125.31
D12S2082	130.94
D12S395	136.822
GATA21B11	149.601
D12S1659	155.941
D12S392	165.69
D12S372	7.122

Table D.13. Name of the STR markers and their position for chromosome 13.

Name of the STR marker	**Position (cM)**
D13S742	10.71
D13S1242	17.211
D13S260	23.651
GATA125C04	32.9

Table D.13. Name of the STR markers and their position for chromosome 13 (cont.).

D13S1247	38.96
D13S788	45.563
D13S258	55.31
D13S317	64.972
D13S886	70.13
D13S779	82.93
D13S1311	90.275
D13S778	96.7
D13S1295	110.552

Table D.14. Name of the STR markers and their position for chromosome 14.

Name of the STR marker	**Position (cM)**
D14S261	6.46
D14S283	13.89
D14S1280	25.87
D14S297	31.755
D14S741	36.76
D14S306	44.061
D14S748	51.091
D14S276	56.36
D14S592	66.813
D14S125	69.823
D14S277	79.07
GATA169E06	84.692
D14S1005	96.421
D14S302	107.33
D14S611	115.911
D14S267	121.95
D14S985	126.611
D14S260	134.301

Table D.15. Name of the STR markers and their position for chromosome 15.

Name of the STR marker	**Position (cM)**
D15S128	6.113
GATA143C02	6.921
D15S165	20.241
D15S995	25.86
D15S118	32.58
D15S659	43.47
GATA153F11	48.98
D15S1036	57.371
D15S125	64.2
D15S818	72.373
D15S653	78.926
D15S116	85.642
D15S652	90.02
D15S649	98.44
D15S657	104.86
D15S966	112.58

Table D.16. Name of the STR markers and their position for chromosome 16.

Name of the STR marker	**Position (cM)**
ATA67B07	7.051
D16S3128	13.672
D16S519	20.773
D16S2619	28.301
D16S3036	39.041
D16S3145	52.262
D16S685	57.794
D16S3396	63.78
D16S3034	67.401
D16S489	73.201
GATA67G11	81.153

Table D.16. Name of the STR markers and their position for chromosome 16 (cont.).

D16S752	88.185
D16S3118	92.103
D16S516	100.39
D16S3098	108.32
GATA86C08	120.59
D16S476	128.53

Table D.17. Name of the STR markers and their position for chromosome 17.

Name of the STR marker	**Position (cM)**
D17S1298	10.72
D17S960	15.782
GATA134G03	22.245
D17S922	35.551
D17S2196	44.622
D17S1824	50.742
D17S907	57.715
D17S2180	66.859
D17S809	74.454
D17S1154	83.402
D17S2193	89.32
GATA65G11	99.215
D17S939	105.685
D17S1847	111.22
D17S1822	116.86

Table D.18. Name of the STR markers and their position for chromosome 18.

Name of the STR marker	**Position (cM)**
D18S63	8.3
D18S62	18.702
D18S843	28.1
D18S1158	38.92

Table D.18. Name of the STR markers and their position for chromosome 18 (cont.).

GATA41G05	49.552
GATA173A03	62.841
D18S450	68.914
D18S539	74.93
D18S1152	80.41
D18S1357	88.622
D18S857	99.313
GATA7G11	104.17
D18S1009	116.441
D18S1122	122.61

Table D.19. Name of the STR markers and their position for chromosome 19.

Name of the STR marker	**Position (cM)**
D19S591	9.84
D19S427	20.752
D19S922	26.371
D19S586	32.941
ATA37G08	42.293
D19S1037	47.67
D19S414	54.682
D19S220	62.036
D19S217	68.08
D19S867	77.54
D19S926	94.56
D19S404	100.382

Table D.20. Name of the STR markers and their position for chromosome 20.

Name of the STR marker	**Position (cM)**
D20S199	6.25
GATA72E11	21.15
D20S163	32.941

Table D.20. Name of the STR markers and their position for chromosome 20 (cont.).

D20S852	36.58
D20S912	46.71
GATA141H08	55.742
GATA148H05	62.321
D20S866	72.271
D20S480	79.91
D20S173	98.093

Table D.21. Name of the STR markers and their position for chromosome 21.

Name of the STR marker	**Position (cM)**
D21S1441	14.205
D21S1280	28.485
D21S1440	38.654
D21S1893	43.67

Table D.22. Name of the STR markers and their position for chromosome 22.

Name of the STR marker	**Position (cM)**
D22S420	4.06
D22S1174	19.32
D22S1045	42.811
D22S534	46.425
D22S927	48.202
D22S1161	59.5

Table D.23. Name of the STR markers and their position for chromosome X.

Name of the STR marker	**Position (cM)**
DXS9900	4.03
DXS6807	13.505
DXS1043	18.372
DXS8019	23.26
ATA28C05	29.761

Table D.23. Name of the STR markers and their position for chromosome X (cont.).

DXS8085	42.752
DXS1003	47.081
DXS7132	52.511
DXS1210	68.753
DXS1212	77.152
DXS8093	81.02
DXS1187	85.34
DXS8106	91.64
DXS1200	96.941

APPENDIX E : STR MARKERS USED FOR X CHROMOSOME LINKAGE ANALYSIS

STR markers used for X chromosome linkage analysis for families P224. P381. P408 and P636 are listed in Table E.1.

Table E.1. Name of the STR markers and their position for X chromosome linkage analysis.

Name of the STR marker	**Position (cM)**
DXS9900	4.03
DXS6807	13.505
DXS8051	17.29
DXS1043	18.372
DXS7104	20.27
DXS8022	22.18
DXS8019	23.26
ATA28C05	29.761
DXS1036	33.54
DXS1068	37.33
DXS8014	37.33
DXS8085	42.752
DXS1003	47.081
DXS7132	52.511
DXS8107	55.75
DXS6800	57.37
DXS6809	61.88
DXS8096	66.04
DXS1210	68.753
DXS8110	70.91
DXS1212	77.152
DXS8093	81.02
DXS8009	82.07

Table E.1. Name of the STR markers and their position for X chromosome linkage analysis (cont.).

DXS1211	83.92
DXS1187	85.34
DXS1227	88.33
DXS8106	91.64
DXS1200	96.941
DXS8103	100.73
DXS1073	102.35

REFERENCES

Abraham, C.R., D.J. Selkoe, and H. Potter, 1988, "Immunochemical Identification of the Serine Protease Inhibitor Alpha 1-antichymotrypsin in the Brain Amyloid Deposits of Alzheimer's Disease", *Cell*, Vol. 52, No. 4, pp. 487-501.

Abrams, C.K., M.M. Freidin, V.K. Verselis, M.V. Bennett, and T.A. Bargiello, 2001, "Functional Alterations in Gap Junction Channels Formed by Mutant Forms of Connexin 32: Evidence for Loss of Function as a Pathogenic Mechanism in the X-linked Form of Charcot-Marie-Tooth Disease", *Brain Research*, Vol. 900, No. 6, pp. 9-25.

Abrams, C.K., M.V. Bennett, V.K. Verselis, and T.A. Bargiello, 2002, "Voltage Opens Unopposed Gap Junction Hemichannels Formed by a Connexin 32 Mutant Associated with X-linked Charcot-Marie-Tooth Disease", *Proceedings of the National Academy of Sciences of the United States of America*, Vol. 99, No. 1, pp. 3980-3984.

Adzhubei, I.A., S. Schmidt, L. Peshkin, V.E. Ramensky, A. Gerasimova, P. Bork, A.S. Kondrashov, and S.R. Sunyaev, 2010, "A Method and Server for Predicting Damaging Missense Mutations", *Nature Methods*, Vol. 7, No. 4, pp. 248-249.

Azzedine, H., N. Ravise, C. Verny, A. Gabreels-Festen, M. Lammens, D. Grid, J.M. Vallat, G. Durosier, J. Senderek, S. Nouioua, T. Hamadouche, A. Bouhouche, A. Guilbot, C. Stendel, M. Ruberg, A. Brice, N. Birouk, O. Dubourg, M. Tazir, and E. Leguern, 2006, "Spine Deformities in Charcot-Marie-Tooth 4c Caused by Sh3tc2 Gene Mutations", *Neurology*, Vol. 67, No. 4, pp. 602-606.

Bahr, M., F. andres, V. Timmerman, M.E. Nelis, C. Van Broeckhoven, and J. Dichgans, 1999, "Central Visual, Acoustic, and Motor Pathway Involvement in a Charcot-Marie-Tooth Family with an Asn205Ser Mutation in the Connexin 32 Gene", *Journal of Neurology, Neurosurgery and Psychiatry*, Vol. 66, No. 2, pp. 202-206.

Bailey-Wilson, J.E., and A.F. Wilson, 2011, "Linkage Analysis in the Next-generation Sequencing Era", *Human Heredity*, Vol. 72, No. 4, pp. 228-236.

Baumann, U., R. Huber, W. Bode, D. Grosse, M. Lesjak, and C.B. Laurell, 1991, "Crystal Structure of Cleaved Human Alpha 1-antichymotrypsin at 2.7 a Resolution and Its Comparison with Other Serpins", *Journal of Molecular Biology*, Vol. 218, No. 3, pp. 595-606.

Baxter, R.V., K. Ben Othmane, J.M. Rochelle, J.E. Stajich, C. Hulette, S. Dew-Knight, F. Hentati, M. Ben Hamida, S. Bel, J.E. Stenger, J.R. Gilbert, M.A. Pericak-Vance, and J.M. Vance, 2002, "Ganglioside-induced Differentiation-associated Protein-1 Is Mutant in Charcot-Marie-Tooth Disease Type 4a/8q21", *Nature Genetics*, Vol. 30, No. 1, pp. 21-22.

Berciano, J., E. Gallardo, A. Garcia, A.L. Pelayo-Negro, J. Infante, and O. Combarros, 2011, "New Insights into the Pathophysiology of Pes Cavus in Charcot-Marie-Tooth Disease Type 1a Duplication", *Journal of Neurology*, Vol. 258, No. 9, pp. 1594-1602.

Bergoffen, J., S.S. Scherer, S. Wang, M.O. Scott, L.J. Bone, D.L. Paul, K. Chen, M.W. Lensch, P.F. Chance, and K.H. Fischbeck, 1993, "Connexin Mutations in X-linked Charcot-Marie-Tooth Disease", *Science*, Vol. 262, No. 5142, pp. 2039-2042.

Bevans, C.G., M. Kordel, S.K. Rhee, and A.L. Harris, 1998, "Isoform Composition of Connexin Channels Determines Selectivity among Second Messengers and Uncharged Molecules", *the Journal of Biological Chemistry*, Vol. 273, No. 5, pp. 2808-2816.

Bicego, M., S. Morassutto, V.H. Hernandez, M. Morgutti, F. Mammano, P. D'andrea, and R. Bruzzone, 2006, "Selective Defects in Channel Permeability Associated with Cx32 Mutations Causing X-linked Charcot-Marie-Tooth Disease", *Neurobiology of Disease*, Vol. 21, No. 3, pp. 607-617.

Boerkoel, C.F., H. Takashima, C.A. Garcia, R.K. Olney, J. Johnson, K. Berry, P. Russo, S. Kennedy, A.S. Teebi, M. Scavina, L.L. Williams, P. Mancias, I.J. Butler, K. Krajewski, M. Shy, and J.R. Lupski, 2002, "Charcot-Marie-Tooth Disease and Related Neuropathies: Mutation Distribution and Genotype-phenotype Correlation", *Annals of Neurology*, Vol. 51, No. 2, pp. 190-201.

Bondurand, N., M. Girard, V. Pingault, N. Lemort, O. Dubourg, and M. Goossens, 2001, "Human Connexin 32, a Gap Junction Protein Altered in the X-linked Form of Charcot-Marie-Tooth Disease, Is Directly Regulated by the Transcription Factor Sox10", *Human Molecular Genetics*, Vol. 10, No. 24, pp. 2783-2795.

Botstein, D., and N. Risch, 2003, "Discovering Genotypes Underlying Human Phenotypes: Past Successes for Mendelian Disease, Future Approaches for Complex Disease", *Nature Genetics*, Vol. 33, No. 3s, pp. 228-237.

Bray, G.M., and A.J. Aguayo, 1974, "Regeneration of Peripheral Unmyelinated Nerves. Fate of the Axonal Sprouts Which Develop After Injury", *Journal of Anatomy*, Vol. 117, No. 3, pp. 517-529.

Bronstein, J.M., 2000, "Function of Tetraspan Proteins in the Myelin Sheath", *Current Opinion in Neurobiology*, Vol. 10, No. 5, pp. 552-557.

Campagnoni, A.T., 1988, "Molecular Biology of Myelin Proteins from the Central Nervous System", *Journal of Neurochemistry*, Vol. 51, No. 1, pp. 1-14.

Cassereau, J., A. Chevrollier, N. Gueguen, V. Desquiret, C. Verny, G. Nicolas, F. Dubas, P. Amati-Bonneau, P. Reynier, D. Bonneau, and V. Procaccio, 2011, "Mitochondrial Dysfunction and Pathophysiology of Charcot-Marie-Tooth Disease Involving Gdap1 Mutations", *Experimental Neurology*, Vol. 227, No. 1, pp. 31-41.

Charcot, J.M. and P. Marie, 1886, "Sur Une forme Particuliére D`atrophie Musculaire Progressive, Souvent Familiale, Debutant Par Les Pieds Et Les Jambes Et atteignant Plus Tard Les Mains", *Revue Médicale*, Vol. 6, pp. 97-138.

Choi, M., U.I. Scholl, W. Ji, T. Liu, I.R. Tikhonova, P. Zumbo, A. Nayir, A. Bakkaloglu, S. Ozen, S. Sanjad, C. Nelson-Williams, A. Farhi, S. Mane, and R.P. Lifton, 2009, "Genetic Diagnosis by Whole Exome Capture and Massively Parallel DNA Sequencing", *Proceedings of the National Academy of Sciences of the United States of America*, Vol. 106, No. 45, pp. 19096-19101.

Choi, B.O., S.K. Koo, M.H. Park, H. Rhee, S.J. Yang, K.G. Choi, S.C. Jung, H.S. Kim, Y.S. Hyun, K. Nakhro, H.J. Lee, H.M. Woo, and K.W. Chung, 2012, "Exome Sequencing Is an Efficient Tool for Genetic Screening of Charcot-Marie-Tooth Disease", *Human Mutation*.

Claramunt, R., L. Pedrola, T. Sevilla, A. Lopez De Munain, J. Berciano, A. Cuesta, B. Sanchez-Navarro, J.M. Millan, G.M. Saifi, J.R. Lupski, J.J. Vilchez, C. Espinos, and F. Palau, 2005, "Genetics of Charcot-Marie-Tooth Disease Type 4a: Mutations, Inheritance, Phenotypic Variability, and Founder Effect", *Journal of Medical Genetics*, Vol. 42, No. 4, pp. 358-365.

Cuesta, A., L. Pedrola, T. Sevilla, J. Garcia-Planells, M.J. Chumillas, F. Mayordomo, E. Leguern, I. Marin, J.J. Vilchez, and F. Palau, 2002, "The Gene Encoding Ganglioside-induced Differentiation-associated Protein 1 Is Mutated in Axonal Charcot-Marie-Tooth Type 4a Disease", *Nature Genetics*, Vol. 30, No. 1, pp. 22-25.

Daniele, T., G. Di Tullio, M. Santoro, G. Turacchio, and M.A. De Matteis, 2008, "Arap1 Regulates Egf Receptor Trafficking and Signalling", *Traffic*, Vol. 9, No. 12, pp. 2221-2235.

De Sandre-Giovannoli, A., M. Chaouch, S. Kozlov, J.M. Vallat, M. Tazir, N. Kassouri, P. Szepetowski, T. Hammadouche, A. Vandenberghe, C.L. Stewart, D. Grid, and N. Levy, 2002, "Homozygous Defects in Lmna, Encoding Lamin A/C Nuclear-Envelope Proteins, Cause Autosomal Recessive Axonal Neuropathy in Human (Charcot-Marie-Tooth Disorder Type 2) and Mouse", *The American Journal of Human Genetics*, Vol. 70, No. 3, pp. 726-736.

den Dunnen, J.T., and S.E. Antonarakis, 2000, "Mutation Nomenclature Extensions and Suggestions to Describe Complex Mutations: A Discussion", *Human Mutation*, Vol. 15, No. 1, pp. 7-12.

Desmet, F.O., D. Hamroun, M. Lalande, G. Collod-Beroud, M. Claustres, and C. Beroud, 2009, "Human Splicing Finder: An Online Bioinformatics Tool to Predict Splicing Signals", *Nucleic Acids Research*, Vol. 37, No. 9, pp. e67.

Dubourg, O., H. Azzedine, C. Verny, G. Durosier, N. Birouk, R. Gouider, M. Salih, A. Bouhouche, A. Thiam, D. Grid, M. Mayer, M. Ruberg, M. Tazir, A. Brice, and E. Leguern, 2006, "Autosomal-Recessive Forms of Demyelinating Charcot-Marie-Tooth Disease", *Neuromolecular Medicine*, Vol. 8, No. 1-2, pp. 75-86.

Dyck, P. J., P. Chance, R. Lebo, J. A. Carney and P.K. Thomas, 1993, "Hereditary Motor and Sensory Neuropathy", *Peripheral Neuropathy*, W. B. Saunders, Philadelphia, 3rd edition.

Dyck, P.J., W.J. Litchy, S. Minnerath, T.D. Bird, P.F. Chance, D.J. Schaid, and A.E. Aronson, 1994, "Hereditary Motor and Sensory Neuropathy with Diaphragm and Vocal Cord Paresis", *Annals of Neurology*, Vol. 35, No. 5, pp. 608-615.

Edgar, J.M., and J. Garbern, 2004, "The Myelinated Axon Is Dependent on the Myelinating Cell for Support and Maintenance: Molecules Involved", *Journal of Neuroscience Research*, Vol. 76, No. 5, pp. 593-598.

England, J.D., and C.A. Garcia, 1996, "Electrophysiological Studies in the Different Genotypes of Charcot-Marie-Tooth Disease", *Current Opinion in Neurology*, Vol. 9, No. 5, pp. 338-342.

Fischbeck, K.H., N. Ar-Rushdi, M. Pericak-Vance, M. Rozear, A.D. Roses, and J.P. Fryns, 1986, "X-linked Neuropathy: Gene Localization with DNA Probes", *Annals of Neurology*, Vol. 20, No. 4, pp. 527-532.

Gosselin, I., I. Thiffault, M. Tetreault, V. Chau, M.J. Dicaire, L. Loisel, M. Emond, J. Senderek, J. Mathieu, N. Dupre, M. Vanasse, J. Puymirat, and B. Brais, 2008, "Founder Sh3tc2 Mutations Are Responsible for a Cmt4c French-Canadians Cluster", *Neuromuscular Disorders*, Vol. 18, No. 6, pp. 483-492.

Hoffman, J. 1889, ''Ueber Progressive Neurotische Muskelatrophie.'' *Psychiat Nervenkr*, Vol. 20, pp. 660-70.

Houlden, H., M. Girard, C. Cockerell, D. Ingram, N.W. Wood, M. Goossens, R.W. Walker, and M.M. Reilly, 2004, "Connexin 32 Promoter P2 Mutations: A Mechanism of Peripheral Nerve Dysfunction", *Annals of Neurology*, Vol. 56, No. 5, pp. 730-734.

Ionasescu, V.V., C. Searby, R. Ionasescu, I.M. Neuhaus, and R. Werner, 1996, "Mutations of the Noncoding Region of the Connexin32 Gene in X-Linked Dominant Charcot-Marie-Tooth Neuropathy", *Neurology*, Vol. 47, No. 2, pp. 541-544.

Jessen, K.R., and R. Mirsky, 2005, "The Origin and Development of Glial Cells in Peripheral Nerves", *Nature Reviews Neuroscience*, Vol. 6, No. 9, pp. 671-682.

Jordanova, A., J. Irobi, F.P. Thomas, P. Van Dijck, K. Meerschaert, M. Dewil, I. Dierick, A. Jacobs, E. De Vriendt, V. Guergueltcheva, C.V. Rao, I. Tournev, F.A. Gondim, M. D'Hooghe, V. Van Gerwen, P. Callaerts, L. Van Den Bosch, J.P. Timmermans, W. Robberecht, J. Gettemans, J.M. Thevelein, P. De Jonghe, I. Kremensky, and V. Timmerman, 2006, "Disrupted Function and Axonal Distribution of Mutant Tyrosyl-Trna Synthetase in Dominant Intermediate Charcot-Marie-Tooth Neuropathy", *Nature Genetics*, Vol. 38, No. 2, pp. 197-202.

Juarez, P., and F. Palau, 2012, "Neural and Molecular Features On Charcot-Marie-Tooth Disease Plasticity and Therapy", *Neural Plasticity*.

Kim, H.J., S.H. Hong, C.S. Ki, B.J. Kim, J.S. Shim, S.H. Cho, J.H. Park, and J.W. Kim, 2005, "A Novel Locus for X-linked Recessive Cmt with Deafness and Optic Neuropathy Maps To Xq21.32-Q24", *Neurology*, Vol. 64, No. 11, pp. 1964-1967.

Kim, H.J., K.M. Sohn, M.E. Shy, K.M. Krajewski, M. Hwang, J.H. Park, S.Y. Jang, H.H. Won, B.O. Choi, S.H. Hong, B.J. Kim, Y.L. Suh, C.S. Ki, S.Y. Lee, S.H. Kim, and J.W. Kim, 2007, "Mutations in Prps1, Which Encodes the Phosphoribosyl Pyrophosphate Synthetase Enzyme Critical for Nucleotide Biosynthesis, Cause Hereditary Peripheral Neuropathy with Hearing Loss and Optic Neuropathy (Cmtx5)", T*he American Journal of Human Genetics*, Vol. 81, No. 3, pp. 552-558.

Kleopa, K.A., and S.S. Scherer, 2002, "Inherited Neuropathies", *Neurologic Clinics*, Vol. 20, No. 3, pp. 679-709.

Kleopa, K.A., and S.S. Scherer, 2006, "Molecular Genetics of X-linked Charcot-Marie-Tooth Disease", *Neuromolecular Medicine*, Vol. 8, No. 1-2, pp. 107-122.

Koval, M., 2006, "Pathways and Control of Connexin Oligomerization", *Trends in Cell Biology*, Vol. 16, No. 3, pp. 159-166.

Krajewski, K.M., R.A. Lewis, D.R. Fuerst, C. Turansky, S.R. Hinderer, J. Garbern, J. Kamholz, and M.E. Shy, 2000, "Neurological Dysfunction and Axonal Degeneration in Charcot-Marie-Tooth Disease Type 1a", *Brain*, Vol. 123, No. 7, pp. 1516-1527.

Krueger, K.A., S. Tsuji, Y. Fukuda, Y. Takahashi, J. Goto, J. Mitsui, H. Ishiura, J.C. Dalton, M.B. Miller, J.W. Day, and L.P. Ranum, 2009, "Snp Haplotype Mapping in a Small Als Family", *Plos One*, Vol. 4, No. 5, pp. e5687.

Kuhlenbaumer, G., P. Young, G. Hunermund, B. Ringelstein, and F. Stogbauer, 2002, "Clinical Features and Molecular Genetics of Hereditary Peripheral Neuropathies", *Journal of Neurology*, Vol. 249, No. 12, pp. 1629-1650.

Ladopoulou, A., I. Konstantopoulou, S. Armaou, E. Efstathiou, M. Mihalatos, G. Nasioulas, G. Bardi, N. Pandis, D. Yannoukakos, and athens, 2002, "A Change in the Last Base of Brca1 Exon 23, 5586G>A, Results in Abnormal Rna Splicing", *Cancer Genetics and Cytogenetics*, Vol. 134, No. 2, pp. 175-177.

Leguern, E., A. Guilbot, M. Kessali, N. Ravise, J. Tassin, T. Maisonobe, D. Grid, and A. Brice, 1996, "Homozygosity Mapping of an Autosomal Recessive form of Demyelinating Charcot-Marie-Tooth Disease to Chromosome 5q23-q33", *Human Molecular Genetics*, Vol. 5, No. 10, pp. 1685-1688.

Lemke, G., 1988, "Unwrapping the Genes of Myelin", *Neuron*, Vol. 1, No. 7, pp. 535-543.

Liang, G.S., M. De Miguel, J.M. Gomez-Hernandez, J.D. Glass, S.S. Scherer, M. Mintz, L.C. Barrio, and K.H. Fischbeck, 2005, "Severe Neuropathy with Leaky Connexin32 Hemichannels", *Annals of Neurology*, Vol. 57, No. 5, pp. 749-754.

Louis-Dit-Picard, H., J. Barc, D. Trujillano, S. Miserey-Lenkei, N. Bouatia-Naji, O. Pylypenko, G. Beaurain, A. Bonnefond, O. Sand, C. Simian, E. Vidal-Petiot, C. Soukaseum, C. Mandet, F. Broux, O. Chabre, M. Delahousse, V. Esnault, B. Fiquet, P. Houillier, C.I. Bagnis, J. Koenig, M. Konrad, P. Landais, C. Mourani, P. Niaudet, V. Probst, C. Thauvin, R.J. Unwin, S.D. Soroka, G. Ehret, S. Ossowski, M. Caulfield, P. Bruneval, X. Estivill, P. Froguel, J. Hadchouel, J.J. Schott, and X. Jeunemaitre, 2012, "Klhl3 Mutations Cause Familial Hyperkalemic Hypertension by Impairing Ion Transport in the Distal Nephron", *Nature Genetics*, Vol. 44, No. 4, pp. 456-460.

Lupo, V., M.I. Galindo, D. Martinez-Rubio, T. Sevilla, J.J. Vilchez, F. Palau, and C. Espinos, 2009, "Missense Mutations in the Sh3tc2 Protein Causing Charcot-Marie-Tooth Disease Type 4c Affect Its Localization in the Plasma Membrane and Endocytic Pathway", *Human Molecular Genetics*, Vol. 18, No. 23, pp. 4603-4614.

Lupski, J.R., R.M. De Oca-Luna, S. Slaugenhaupt, L. Pentao, V. Guzzetta, B.J. Trask, O. Saucedo-Cardenas, D.F. Barker, J.M. Killian, C.A. Garcia, A. Chakravarti, and P.I. Patel, 1991, "DNA Duplication Associated with Charcot-Marie-Tooth Disease Type 1a", *Cell*, Vol. 66, No. 2, pp. 219-232.

Magyar, J.P., R. Martini, T. Ruelicke, A. Aguzzi, K. Adlkofer, Z. Dembic, J. Zielasek, K.V. Toyka, and U. Suter, 1996, "Impaired Differentiation of Schwann Cells in Transgenic Mice with Increased Pmp22 Gene Dosage", *Journal of Neuroscience*, Vol. 16, No. 17, pp. 5351-5360.

Marco, A., A. Cuesta, L. Pedrola, F. Palau, and I. Marin, 2004, "Evolutionary and Structural Analyses of Gdap1, Involved in Charcot-Marie-Tooth Disease, Characterize a Novel Class of Glutathione Transferase-Related Genes", *Molecular Biology and Evolution*, Vol. 21, No. 1, pp. 176-187.

Matsunami, N., B. Smith, L. Ballard, M.W. Lensch, M. Robertson, H. Albertsen, C.O. Hanemann, H.W. Muller, T.D. Bird, R. White, and P.F. Chance, 1992, "Peripheral Myelin Protein-22 Gene Maps in the Duplication in Chromosome 17p11.2 Associated with Charcot-Marie-Tooth 1a", *Nature Genetics*, Vol. 1, No. 3, pp. 176-179.

Milks, L.C., N.M. Kumar, R. Houghten, N. Unwin, and N.B. Gilula, 1988, "Topology of the 32-kD Liver Gap Junction Protein Determined by Site-directed Antibody Localizations", *the EMBO Journal*, Vol. 7, No. 10, pp. 2967-2975.

Mirsky, R., and K.R. Jessen, 1999, "The Neurobiology of Schwann Cells", Brain Pathology, Vol. 9, No. 2, pp. 293-311.

Montenegro, G., E. Powell, J. Huang, F. Speziani, Y.J. Edwards, G. Beecham, W. Hulme, C. Siskind, J. Vance, M. Shy, and S. Zuchner, 2011, "Exome Sequencing Allows for

Rapid Gene Identification in a Charcot-Marie-Tooth Family", *Annals of Neurology*, Vol. 69, No. 3, pp. 464-470.

Murphy, S.M., M. Laura, K. Fawcett, A. Pandraud, Y.T. Liu, G.L. Davidson, A.M. Rossor, J.M. Polke, V. Castleman, H. Manji, M.P. Lunn, K. Bull, G. Ramdharry, M. Davis, J.C. Blake, H. Houlden, and M.M. Reilly, 2012, "Charcot-Marie-Tooth Disease: Frequency of Genetic Subtypes and Guidelines for Genetic Testing", *Journal of Neurology, Neurosurgery and Psychiatry*, Vol. 83, No. 7, pp. 706-710.

Murphy, S.M., J. Polke, H. Manji, J. Blake, L. Reiniger, M. Sweeney, H. Houlden, S. Brandner, and M.M. Reilly, 2011, "A Novel Mutation in the Nerve-specific 5'UTR of the Gjb1 Gene Causes X-linked Charcot-Marie-Tooth Disease", *Journal of the Peripheral Nervous System*, Vol. 16, No. 1, pp. 65-70.

Nelis, E., C. Van Broeckhoven, P. De Jonghe, A. Lofgren, A. Vandenberghe, P. Latour, E. Le Guern, A. Brice, M.L. Mostacciuolo, F. Schiavon, F. Palau, S. Bort, M. Upadhyaya, M. Rocchi, N. Archidiacono, P. Mandich, E. Bellone, K. Silander, M.L. Savontaus, R. Navon, H. Goldberg-Stern, X. Estivill, V. Volpini, W. Friedl, U. Orth A. Gal, X. Estivill, V. Volpini, C. Wolf and E. Kunert, 1996, "Estimation of the Mutation Frequencies in Charcot-Marie-Tooth Disease Type 1 and Hereditary Neuropathy with Liability to Pressure Palsies: A European Collaborative Study", *European Journal of Human Genetics*, Vol. 4, No. 1, pp. 25-33.

Ng, S.B., E.H. Turner, P.D. Robertson, S.D. Flygare, A.W. Bigham, C. Lee, T. Shaffer, M. Wong, A. Bhattacharjee, E.E. Eichler, M. Bamshad, D.A. Nickerson, and J. Shendure, 2009, "Targeted Capture and Massively Parallel Sequencing of 12 Human Exomes", *Nature*, Vol. 461, No. 7261, pp. 272-276.

Nicholson, G., and A. Corbett, 1996, "Slowing of Central Conduction in X-linked Charcot-Marie-Tooth Neuropathy Shown by Brain Stem Auditory Evoked Responses", *Journal of Neurology, Neurosurgery and Psychiatry*, Vol. 61, No. 1, pp. 43-46.

Niemann, A., M. Ruegg, V. La Padula, A. Schenone, and U. Suter, 2005, "Ganglioside-induced Differentiation associated Protein 1 Is a Regulator of the Mitochondrial Network: New Implications for Charcot-Marie-Tooth Disease", *the Journal of Cell Biology*, Vol. 170, No. 7, pp. 1067-1078.

Niemann, A., P. Berger, and U. Suter, 2006, "Pathomechanisms of Mutant Proteins in Charcot-Marie-Tooth Disease", *Neuromolecular Medicine*, Vol. 8, No. 1-2, pp. 217-242.

Patel, P.I., B.B. Roa, A.A. Welcher, R. Schoener-Scott, B.J. Trask, L. Pentao, G.J. Snipes, C.A. Garcia, U. Francke, E.M. Shooter, J.R. Lupski, and U. Suter, 1992, "The Gene for the Peripheral Myelin Protein Pmp-22 Is a Candidate for Charcot-Marie-Tooth Disease Type 1a", *Nature Genetics*, Vol. 1, No. 3, pp. 159-165.

Parman, Y., F. Ciftci, M. Poyraz, A.M. Halefoglu, A.E. Oge, M. Eraksoy, G. Saruhan-Direskeneli, F. Deymeer, and E. Battaloglu, 2007, "X-Linked Charcot-Marie-Tooth Disease and Multiple Sclerosis", *Journal of Neurology*, Vol. 254, No. 7, pp. 953-955.

Poliak, S., and E. Peles, 2003, "The Local Differentiation of Myelinated Axons at Nodes of Ranvier", *Nature Reviews Neuroscience*, Vol. 4, No. 12, pp. 968-980.

Raeymaekers, P., V. Timmerman, E. Nelis, P. De Jonghe, J.E. Hoogendijk, F. Baas, D.F. Barker, J.J. Martin, M. De Visser, P.A. Bolhuis, and C. Van Broeckhoven, 1991, "Duplication in Chromosome 17p11.2 in Charcot-Marie-Tooth Neuropathy Type 1a (Cmt 1a). The Hmsn Collaborative Research Group", *Neuromuscular Disorders*, Vol. 1, No. 2, pp. 93-97.

Reilly, M.M., S.M. Murphy, and M. Laura, 2011, "Charcot-Marie-Tooth Disease", *Journal of the Peripheral Nervous System*, Vol. 16, No. 1, pp. 1-14.

Ressot, C., and R. Bruzzone, 2000, "Connexin Channels in Schwann Cells and the Development of the X-Linked form of Charcot-Marie-Tooth Disease", *Brain Research Reviews*, Vol. 32, No. 1, pp. 192-202.

Ri, Y., J.A. Ballesteros, C.K. Abrams, S. Oh, V.K. Verselis, H. Weinstein, and T.A. Bargiello, 1999, "The Role of a Conserved Proline Residue in Mediating Conformational Changes Associated with Voltage Gating of Cx32 Gap Junctions", *Biophysical Journal*, Vol. 76, No. 6, pp. 2887-2898.

Roa, B.B., P.J. Dyck, H.G. Marks, P.F. Chance, and J.R. Lupski, 1993, "Dejerine-Sottas Syndrome Associated with Point Mutation in the Peripheral Myelin Protein 22 (Pmp22) Gene", *Nature Genetics*, Vol. 5, No. 3, pp. 269-273.

Roberts, R.C., A.A. Peden, F. Buss, N.A. Bright, M. Latouche, M.M. Reilly, J. Kendrick-Jones, and J.P. Luzio, 2010, "Mistargeting of Sh3tc2 Away from the Recycling Endosome Causes Charcot-Marie-Tooth Disease Type 4c", *Human Molecular Genetics*, Vol. 19, No. 6, pp. 1009-1018.

Robinson, P.N., P. Krawitz, and S. Mundlos, 2011, "Strategies for Exome and Genome Sequence Data Analysis in Disease-gene Discovery Projects", *Clinical Genetics*, Vol. 80, No. 2, pp. 127-132.

Rozen, S., and H. Skaletsky, 2000, "Primer3 on the www for General Users and for Biologist Programmers", *Methods in Molecular Biology*, Vol. 132, pp. 365-386.

Safka Brozkova, D., S. Nevsimalova, R. Mazanec, B. Rautenstrauss, and P. Seeman, 2012, "Charcot-Marie-Tooth Neuropathy Due to a Novel Egr2 Gene Mutation with Mild Phenotype - Usefulness of Human Mapping Chip Linkage Analysis in a Czech Family", *Neuromuscular Disorders*, Vol. 22, No. 8, pp. 742-746.

Sahenk, Z., 1999, "Abnormal Schwann Cell-axon interactions in Cmt Neuropathies. The Effects of Mutant Schwann Cells On the Axonal Cytoskeleton and Regeneration-

associated Myelination", *Annals of the New York Academy of Sciences*, Vol. 883, pp. 415-426.

Scherer, S.S., 1996, "Molecular Specializations at Nodes and Paranodes in Peripheral Nerve", *Microscopy Research and Technique*, Vol. 34, No. 5, pp. 452-461.

Senderek, J., B. Hermanns, C. Bergmann, B. Boroojerdi, M. Bajbouj, M. Hungs, V.T. Ramaekers, S. Quasthoff, D. Karch, and J.M. Schroder, 1999, "X-linked Dominant Charcot-Marie-Tooth Neuropathy: Clinical, Electrophysiological, and Morphological Phenotype in Four Families with Different Connexin32 Mutations(1)", *Journal of Neurological Sciences*, Vol. 167, No. 2, pp. 90-101.

Senderek, J., C. Bergmann, V.T. Ramaekers, E. Nelis, G. Bernert, A. Makowski, S. Zuchner, P. De Jonghe, S. Rudnik-Schoneborn, K. Zerres, and J.M. Schroder, 2003 (A), "Mutations in the Ganglioside-induced Differentiation-associated Protein-1 (Gdap1) Gene in Intermediate Type Autosomal Recessive Charcot-Marie-Tooth Neuropathy", *Brain*, Vol. 126, No. Pt 3, pp. 642-649.

Senderek, J., C. Bergmann, C. Stendel, J. Kirfel, N. Verpoorten, P. De Jonghe, V. Timmerman, R. Chrast, M.H. Verheijen, G. Lemke, E. Battaloglu, Y. Parman, S. Erdem, E. Tan, H. Topaloglu, A. Hahn, W. Muller-Felber, N. Rizzuto, G.M. Fabrizi, M. Stuhrmann, S. Rudnik-Schoneborn, S. Zuchner, J. Michael Schroder, E. Buchheim, V. Straub, J. Klepper, K. Huehne, B. Rautenstrauss, R. Buttner, E. Nelis, and K. Zerres, 2003 (B), "Mutations in a Gene Encoding a Novel Sh3/Tpr Domain Protein Cause Autosomal Recessive Charcot-Marie-Tooth Type 4c Neuropathy", *The American Journal of Human Genetics*, Vol. 73, No. 5, pp. 1106-1119.

Sivakumar, K., T. Kyriakides, I. Puls, G.A. Nicholson, B. Funalot, A. Antonellis, N. Sambuughin, K. Christodoulou, J.L. Beggs, E. Zamba-Papanicolaou, V. Ionasescu, M.C. Dalakas, E.D. Green, K.H. Fischbeck, and L.G. Goldfarb, 2005, "Phenotypic Spectrum of Disorders associated with Glycyl-Trna Synthetase Mutations", *Brain*, Vol. 128, No. 10, pp. 2304-2314.

Snipes, G.J., U. Suter, A.A. Welcher, and E.M. Shooter, 1992, "Characterization of a Novel Peripheral Nervous System Myelin Protein (Pmp-22/Sr13)", T*he Journal of Cell Biology*, Vol. 117, No. 1, pp. 225-238.

Sorour, E., and M. Upadhyaya, 1995, "Identification of 7 Novel Mutations in Peripheral Myelin Genes", T*he American Journal of Human Genetics*, Vol. 57, No. 4, pp. 1322-1322.

Stauffer, K.A., 1995, "The Gap Junction Proteins Beta 1-Connexin (Connexin-32) and Beta 2-Connexin (Connexin-26) Can Form Heteromeric Hemichannels", *The Journal of Biological Chemistry*, Vol. 270, No. 12, pp. 6768-6772.

Suter, U., and S.S. Scherer, 2003, "Disease Mechanisms in Inherited Neuropathies", *Nature Reviews Neuroscience*, Vol. 4, No. 9, pp. 714-726.

Szigeti, K., and J.R. Lupski, 2009, "Charcot-Marie-Tooth Disease", *European Journal of Human Genetics*, Vol. 17, No. 6, pp. 703-710.

Taira, M., T. Iizasa, K. Yamada, H. Shimada, and M. Tatibana, 1989, "Tissue-differential Expression of Two Distinct Genes for Phosphoribosyl Pyrophosphate Synthetase and Existence of the Testis-Specific Transcript", *Biochimica Et Biophysica Acta*, Vol. 1007, No. 2, pp. 203-208.

Thomas, P.K., and D.B. Calne, 1974, "Motor Nerve Conduction Velocity in Peroneal Muscular Atrophy: Evidence for Genetic Heterogeneity", *Journal of Neurology, Neurosurgery and Psychiatry*, Vol. 37, No. 1, pp. 68-75.

Timmerman, V., E. Nelis, W. Van Hul, B.W. Nieuwenhuijsen, K.L. Chen, S. Wang, K. Ben Othman, B. Cullen, R.J. Leach, C.O. Hanemann, P. De Jonghe, P. Raeymaekers, G.J.B. van Ommen, J.J. Martin, H.W. Müller, J.M. Vance, K.H. Fischbeck and C. Van Broeckhoven, 1992, "The Peripheral Myelin Protein Gene Pmp-22 Is Contained within the Charcot-Marie-Tooth Disease Type 1a Duplication", *Nature Genetics*, Vol. 1, No. 3, pp. 171-175.

Tooth, H. H., 1886, "The Peroneal Type of Progressive Muscular Atrophy", Ph.D Thesis, H. K. Lewis, London.

Travis, J., and G.S. Salvesen, 1983, "Human Plasma Proteinase Inhibitors", *Annual Review of Biochemistry*, Vol. 52, pp. 655-709.

Valentijn, L.J., P.A. Bolhuis, I. Zorn, J.E. Hoogendijk, N. van den Bosch, G.W. Hensels, V.P. Stanton Jr., D.E. Housman, K.H. Fischbeck, D.A. Ross, G.A. Nicholson, E.J. Meershoek, H.G. Dauwerse, G.J.B. van Ommen and F. Bass, 1992 (A), "The Peripheral Myelin Gene Pmp-22/Gas-3 Is Duplicated in Charcot-Marie-Tooth Disease Type 1a", *Nature Genetics*, Vol. 1, No. 3, pp. 166-170.

Valentijn, L.J., F. Baas, R.A. Wolterman, J.E. Hoogendijk, N.H. van den Bosch, I. Zorn, A.W. Gabreels-Festen, M. de Visser, and P.A. Bolhuis, 1992 (B), "Identical Point Mutations of Pmp-22 in Trembler-J Mouse and Charcot-Marie-Tooth Disease Type 1a", *Nature Genetics*, Vol. 2, No. 4, pp. 288-291.

VIB-Department of Molecular Genetics, *Inherited Peripheral Neuropathies Mutation Database*, 2007, http://www.molgen.vib-ua.be/cmtmutations/, August 2012.

Wang, H.L., W.T. Chang, T.H. Yeh, T. Wu, M.S. Chen, and C.Y. Wu, 2004, "Functional Analysis of Connexin-32 Mutants Associated with X-linked Dominant Charcot-Marie-Tooth Disease", *Neurobiology of Disease*, Vol. 15, No. 2, pp. 361-370.

Wang, H.L., T. Wu, W.T. Chang, A.H. Li, M.S. Chen, C.Y. Wu, and W. Fang, 2000, "Point Mutation Associated with X-linked Dominant Charcot-Marie-Tooth Disease Impairs the P2 Promoter Activity of Human Connexin-32 Gene", *Molecular Brain Research*, Vol. 78, No. 1-2, pp. 146-153.

Weedon, M.N., R. Hastings, R. Caswell, W. Xie, K. Paszkiewicz, T. Antoniadi, M. Williams, C. King, L. Greenhalgh, R. Newbury-Ecob, and S. Ellard, 2011, "Exome Sequencing Identifies a Dync1h1 Mutation in a Large Pedigree with Dominant Axonal Charcot-Marie-Tooth Disease", *The American Journal of Human Genetics*, Vol. 89, No. 2, pp. 308-312.

Weil, D., S. Blanchard, J. Kaplan, P. Guilford, F. Gibson, J. Walsh, P. Mburu, A. Varela, J. Levilliers, M.D. Weston, P.M. Kelley, W.J. Kimberling, M. Wagenaar, F. Levi-Acobas, D. Larget-Piet, A. Munnich, K.P. Steel, S.D.M. Brown and C. Petit, 1995, "Defective Myosin Viia Gene Responsible for Usher Syndrome Type 1b", *Nature*, Vol. 374, No. 6517, pp. 60-61.

Wise, C.A., C.A. Garcia, S.N. Davis, Z. Heju, L. Pentao, P.I. Patel, and J.R. Lupski, 1993, "Molecular Analyses of Unrelated Charcot-Marie-Tooth (Cmt) Disease Patients Suggest a High Frequency of the Cmtia Duplication", *The American Journal of Human Genetics*, Vol. 53, No. 4, pp. 853-863.

Yoon, H.Y., J.S. Lee, and P.A. Randazzo, 2008, "Arap1 Regulates Endocytosis of Egfr", *Traffic*, Vol. 9, No. 12, pp. 2236-2252.

Young, P., and U. Suter, 2003, "The Causes of Charcot-Marie-Tooth Disease", *Cellular and Molecular Life Sciences*, Vol. 60, No. 12, pp. 2547-2560.

Zuchner, S., M. Noureddine, M. Kennerson, K. Verhoeven, K. Claeys, P. De Jonghe, J. Merory, S.A. Oliveira, M.C. Speer, J.E. Stenger, G. Walizada, D. Zhu, M.A. Pericak-Vance, G. Nicholson, V. Timmerman, and J.M. Vance, 2005, "Mutations in the Pleckstrin Homology Domain of Dynamin 2 Cause Dominant Intermediate Charcot-Marie-Tooth Disease", *Nature Genetics*, Vol. 37, No. 3, pp. 289-294.